2012

Physical processes and drivers on landscapes in coastal Louisiana and Cape Cod, Massachusetts

Mandy Michelle Green
Louisiana State University and Agricultural and Mechanical College

PHYSICAL PROCESSES AND DRIVERS ON LANDSCAPES IN COASTAL LOUISIANA AND CAPE COD, MASSACHUSETTS

A Dissertation

Submitted to the Graduate Faculty of the
Louisiana State University and
Agricultural and Mechanical College
in partial fulfillment of the
requirements for the degree of
Doctor of Philosophy

in

The Department of Geography and Anthropology

by
Mandy Green
B.S., University of Louisiana at Lafayette, 2002
M.S., Louisiana State University, 2004
December 2012

To the One who makes the impossible possible.

ACKNOWLEDGMENTS

I would like to express my gratitude to Dr. Patrick Hesp for serving as my advisor and committee chair. He has been extremely understanding in working with and around my work schedule, and his guidance and advice through this process are greatly appreciated. I would like to thank Dr. Barry Keim, Dr. Lei Wang, Mr. DeWitt Braud, and Dr. Cornelis De Hoop for their input in serving as members of my dissertation committee.

Sincere appreciation is extended to the leadership of the Coastal Protection and Restoration Authority of Louisiana for allowing me to continue my education while in their employment. The support of my immediate supervisors, Mr. William Rhinehart and Mr. Karim Belhadjali, was invaluable.

I would like to thank my family and friends for their support, encouragement, and understanding throughout this journey. Without their words of encouragement, shared laughter, and jokes about how much of my life I have spent in school, I would never have reached this point.

I would like to acknowledge my late grandmothers, Betty and Donna, for their contributions of love and support to my upbringing. I would like to also acknowledge the late Dr. Lora Lana Goodeaux for serving as a mentor and encouraging me to pursue higher education.

TABLE OF CONTENTS

ABSTRACT

This dissertation comprises an analysis of wind frequency and magnitude data and resulting sand transport for Cape Cod, Massachusetts; wind speed and wave height data for coastal Louisiana; and habitat classification and elevation data for a retrogradational barrier island in coastal Louisiana.

Chapter 2 presents an analysis of wind data for Cape Cod, Massachusetts in which annual, seasonal, niño, and storm-related wind patterns were investigated to analyze the potential for aeolian sand transport in a blowout dune located on Cape Cod. Results indicate that wind patterns, drift potential, and drift direction are seasonal. Sand drift potential varies at specific locations within the blowout dune based on the mean grain size for each morphological feature (i.e., deflation basin, depositional lobe, etc.). Winds above the threshold for sediment velocity occur during every season and topographic alteration and acceleration of winds can drive sand movement in a direction that is distinctly different from blowout orientation.

Chapter 3 discusses several techniques (Gumbel and Beta-P probability distributions; Southern Regional Climate Center and Huff-Angel regression methods) used to derive quantile estimates (return period and event magnitude) for extreme wind speed and wave height events resulting from tropical, frontal, and airmass thunderstorm weather events in coastal Louisiana. Results indicate that the Huff Angel regression method provides the best fit distribution for the majority of wind speed and wave height data sets analyzed. The methods described here to derive wind speed and wave height quantile estimates should be considered when determining the impact of wind and wave processes on restoration projects in coastal Louisiana.

Chapter 4 provides a classification of the habitats on Whiskey Island, a retrogradational barrier island along the Louisiana coast, as well as a comparison of habitat change over time and

the elevation at which vegetated habitats occur. Specific attention is paid to the emergent and woody vegetation present on the back barrier marsh of the island. The analyses indicate that without continued restoration and maintenance of the island, the effects of sea level rise, subsidence, storms, and other physical processes may render the island incapable of supporting the vegetation that currently colonizes the island.

CHAPTER 1: INTRODUCTION

1.1 Introduction

Sea level rise, subsidence, shoreline retreat, winds, waves, storm frequency, storm intensity, and other physical processes result in significant changes to coastal landscapes. The landscape of dynamic coastal environments, whether glacial or deltaic, tropical storm-dominated or frontal system-dominated, cannot be expected to remain unchanged throughout time. Those charged with maintaining, restoring, or protecting the landscape, communities and services that it provides should be informed of the consequences of their management actions and the costs of inaction. While the beaches, dunes, and barrier islands of Cape Cod may seem, at first glance, to have few similarities to the muddy, deltaic coast of Louisiana, both are regularly subjected to the processes mentioned above.

1.2 Shoreline Change

The United States Geological Survey, through the national assessment of shoreline change project, has produced a series of reports that map and analyze shoreline movement over both short and long-term time periods. The Southeast Atlantic Coast report, released in 2005, includes documentation of the geomorphology of the New England coast as well as the average, short-term, and long-term rates of shoreline change (Hapke *et al*., 2010). The area of Cape Cod, Massachusetts from Provincetown to Truro (northern end of Cape Cod) was classified as a mainland beach, from Truro to near Maroni Beach (north to central) as bluff with a linear beach with a minimal area of mainland beach near the center, and from Maroni Beach to Monomoy Island (central to south) as barrier beach. The average short-term rate of shoreline change (last 25-30 years) for Cape Cod is 0.3 meters/year (m/yr); the average long-term rate (last ~200 years) is -0.4 m/yr; and approximately 75 percent of the coastline of Cape Cod is eroding (Hapke *et al*.,

2010). Long-term shoreline change rates from Provincetown to Truro range from +/- 2.0 m/yr, while short-term rates range from -1.0/+4.0 m/yr for the same area.

Coastal Louisiana is made up of modern and relict delta lobes composed primarily of mud, and the barrier islands are low, narrow areas of sand reworked by wave and tidal processes and frequently overwashed by storm events (Morton, Miller, and Moore, 2004). Approximately 90% of the Louisiana coastline is eroding. The long-term average rate of shoreline change is approximately -8.2 m/yr, and the average short-term rate of change is -12.0 m/yr (Morton, Miller, and Moore, 2004). The highest rates of erosion in Louisiana are occurring on the barrier islands and headlands, including the Isles Dernieres barrier island chain.

1.3 Sea Level Rise

The IPCC (2007) predicted range of sea level rise through the end of the century is 0.18-0.59 meters (m), and does not include rapid dynamic changes in ice flow. Vermeer and Rahmstorf (2009) predict sea level rise of 0.75-1.8 m by 2100. Sea level rise near Woods Hole, Massachusetts has been documented at 2.6 millimeters/year (mm/yr) from 1930 to 2010 (Hapke *et al*., 2010), and sea level rise from 1950-2005 at Grand Isle, Louisiana has been documented at 9.39 mm/yr (Gonzales and Tornqvist, 2006). In late 2011, the US Army Corps of Engineers released an updated to their sea level rise guidance which indicates that development of water resources projects should incorporate eustatic sea level rise scenarios of 0.2 m (low), 0.5 m (intermediate), and 1.5 m (high) into every aspect of the project life cycle (USACE, 2011).

1.4 Subsidence

In addition to sea level rise, high rates of subsidence (downward displacement of the surface with respect to a datum) are occurring in many areas of coastal Louisiana. Subsidence in Louisiana has been attributed to six primary processes: tectonic subsidence, holocene sediment

compaction, sediment loading, glacial isostatic adjustment, fluid withdrawal, and surface water drainage and management (Reed and Yuill, 2009). The *Coast 2050* report indicates subsidence rates of 0-3.5 feet/century (ft/century; 0-10.7 mm/yr in coastal Louisiana (LCWCRTF, 1999), and a 2005 report by USGS indicates subsidence rates as high as 18.2 mm/yr for some areas of coastal Louisiana. Subsidence rates for Isles Dernieres range from 2.1-3.5 ft/century (6.4-10.7 mm/yr) (Kulp 2000; LCWCRTF, 1999). Although subsidence on Cape Cod is not as significant as subsidence in coastal Louisiana, Redfield (1967) documented rates near 2 mm/yr from 4000-2000 years ago and rates of 0.3 mm/yr from that time to present.

1.5 Storm Frequency and Intensity

The active 1995 Atlantic hurricane season and the relatively active seasons since then have focused attention on the possibility of a link between global climate change and more frequent and intense hurricanes. The devastation wrought by hurricanes affecting the United States in 2004, 2005, and 2008 have underscored the need to understand the cause(s) of these extreme events and the likelihood of future similar or greater events. Although sea surface temperatures (SSTs) have risen since 1905, there is no consensus among climatology experts on whether the high level of hurricane activity that has recently occurred in the Atlantic basin can be attributed to human-induced global warming. Additionally, there is ongoing debate regarding the effects of global warming on the frequency and magnitude of hurricanes (e.g., Emanuel, 2005; Pielke *et al.*, 2005; Shepherd and Knutson, 2007). Pielke *et al.* (2005) states the following about the potential link between global warming and hurricane impacts:

> No connection has been established between greenhouse gas emissions and the observed behavior of hurricanes…..the peer-reviewed literature reflects that a scientific consensus exists that any future changes in hurricane intensities will likely be small in the context of observed variability…..under the assumptions of the IPCC, expected future damages to society of its projected changes in the behavior of hurricanes are dwarfed by the influence of its own projections of growing wealth and population ….. (page 1574).

In contrast, Emanuel (2005) states that "the current levels of tropical storminess are unprecedented in the historical record and a global warming signal is now emerging in the records of hurricane activity (page E13)." Shepherd and Knutson (2007) state that "significantly more research – from observations, theory, and modeling – is needed to resolve the current debate around global warming and hurricanes (page 20)." The statements above illustrate the conflicting opinions of climate experts on the link between global warming and hurricanes. Further evidence of this is given in Pielke (2007), in which the author queried ten leading scholars on hurricanes and climate change about the values that should be used to describe the change in hurricane frequency and magnitude between 2006 and 2050 and 2100. For 2050, the range was 0-18% for intensity and -20% to +20% for frequency. For 2100, the range was 0-36% for intensity and -40% to +40% for frequency (Pielke, 2007).

The following environmental factors increase Atlantic hurricane activity: La Niña (El Niño Southern Oscillation [ENSO]), wet (African) Sahel rainfall, weak vertical wind shear, low Caribbean pressures, warm Atlantic SSTs, and westerly Quasi-Biennial Oscillation (QBO) (Kim, Webster, and Curry 2009; Landsea *et al*., 1999). For hurricane formations in the eastern North Atlantic, Atlantic SSTs are the dominant mechanism, but SSTs are not as important interannually on the basin scale or for intense hurricanes (Landsea *et al*., 1999). There is a strong correlation between decades with high hurricane activity and warm SSTs, as decades of warm SSTs show an 80% increase in intense (category 3-5) hurricane activity compared to decades of cold SSTs (Landsea *et al.*, 1999).

Webster *et al.* (2005) determined that category 4 and 5 hurricanes nearly doubled in number and proportion between 1975-1989 and 1990-2004 in all ocean basins, while the trend for category 1 hurricanes remained nearly constant and that for category 2 and 3 hurricanes slightly increased. An ensemble of global climate change model projections indicated a near

doubling in category 4 and 5 tropical storms globally, an 81% increase in category 4 and 5 hurricanes in the Atlantic basin, and an overall 28% decrease in the frequency of tropical storms and hurricanes by the end of the century (Bender *et al.*, 2010). In essence, fewer but more intense storms overall. The average number of storms in the Atlantic Basin has increased since 1995 (Henderson-Sellers *et al*., 1998); however, hurricane records support an interannual and multidecadal trend in hurricane activity.

Keim, Muller, and Stone (2007) analyzed 105 years of tropical cyclone strikes from Texas to Maine to document the return periods for tropical events. The authors determined that the average return periods for tropical storms and hurricanes, all hurricanes, and severe hurricanes (category 3-5) was 7, 35, and 105+ years, respectively for Chatham, Massachusetts on the southern end of Cape Cod (Keim, Muller, and Stone, 2007). The average return period for tropical storms and hurricanes at three Louisiana locations was 3 years, while the return period for all hurricanes ranged from 7 years at Boothville to 10 years at Morgan City and 15 years at Cameron. The return period for category 3 or greater hurricanes was 26 years at Boothville and Morgan City and 52 years at Cameron (Keim, Muller, and Stone 2007).

1.6 Winds and Waves

Winds on Cape Cod are seasonal, with winds from the south during summer and fall, from the west and north during the winter, and from the north and south during the spring (Forman *et al*., 2008). Average wind speeds off the coast of Cape Cod are approximately 6.5 meters/second (m/s; NDBC station 44018). Wind speeds for Hurricane Noel were measured as high as 45.0 m/s, and winds from frontal systems have been measured at similar speeds (NDBC station 44018).

The mean deep water wave conditions off the Louisiana coast are characterized by wave heights of 1 m, wave periods of 5-6 seconds, and dominant wave approach from the southeast (Penland, Boyd, and Suter, 1988). Local average wave heights are approximately 60 centimeters (cm), and wave heights associated with frontal systems may reach 2-3 m (Ritchie and Penland, 1988). Hurricanes in the Gulf of Mexico can produce wave heights greater than 17.9 m (Stone *et al*., 2005). During average weather conditions and before the passage of cold fronts, southerly winds impact the coastal Louisiana landscape, while following the passage of cold fronts or extratropical storms, waves produced by northerly winds impact the bay side of barriers and other landscape features. The passage of cold fronts occurs approximately 10-30 times per year, while tropical events occur approximately every 3-4 years (Keim, Muller, and Stone, 2007; Ritchie and Penland, 1988). Wind speeds for Hurricane Katrina were measured as high as 34.41 m/s in Terrebonne Bay, Louisiana, while wind speeds from cold fronts were measured as high as 23.1 m/s in Grand Isle, Louisiana.

1.7 Dissertation Structure

The development of blowout dune formations on Cape Cod may begin with destabilization of a dunefield resulting from climate change, and physical processes including wind velocity and direction, sand grain size, vegetation, and precipitation contribute to the evolution of blowout dunes. Blowout dunes occur across a wide spectrum of coastal and desert environments and may be the most common aeolian dune landform associated with wind erosion in partial to semi-vegetated terrains. Chapter 2 discusses the effects of wind direction and magnitude on the development and evolution of dunes within the Cape Cod National Seashore, including the seasonality of the winds and the resulting magnitude and direction of sand movement.

Barrier island and other types of coastal restoration projects provide protection for communities, infrastructure, and wetland ecosystems in Louisiana. Part of the process of designing restoration projects requires an understanding of the coastal processes (particularly, wave heights and wind speeds from storm events) that affect restoration projects and the return periods at which destructive events may occur. Chapter 3 discusses wind speed and wave height quantile estimates for coastal Louisiana and considerations for planning and design of coastal restoration projects.

Due to relative sea level rise, lack of sediment supply, hurricane impacts, and other factors, if left to natural deltaic and coastal processes, Whiskey Island in coastal Louisiana is not sustainable. Without regular maintenance (sediment addition), the island will continue to degrade. Because barrier islands serve as Louisiana's first line of defense against hurricane storm surge and provide a diverse array of habitats to support the abundant natural resources of Louisiana, it may be advisable to continue to invest in the restoration of these features. Chapter 4 discusses habitat classification and post-classification change detection on Whiskey Island from 1998-2009 to relate temporal and spatial changes to either short-term (hurricanes) or long-term (natural process) developments.

1.8 References

Bender, M.A.; Knutson, T.R.; Tuleya, R.E.; Sirutis, J.J.; Vecchi, G.A.; Garner, S.T.; and Held, I.M., 2010. Modeled impact of anthropogenic warming on the frequency of intense Atlantic hurricanes. *Science,* 327, 454-458.

Emanuel, K., 2005. Emanuel replies. *Nature,* 438, E13.

Forman, S. L.; Sagintayev, Z.; Sultan, M.; Smith, S.; Becker, R.; Kendall, M.; and Marin, L., 2008. The twentieth-century migration of parabolic dunes and wetland formation at Cape Cod National Seashore, Massachusetts, USA: landscape response to a legacy of environmental disturbance. *The Holocene*, 18(5), 765-774.

Gonzales, J.L. and Tornqvist, T.E. 2006. Coastal Louisiana in crisis: subsidence or sea level rise? *EOS, Transactions, American Geophysical Union,* 87(45), 493-498.

Hapke, C.J.; Himmelstoss, E.A.; Kratzmann, M.; List, J.H.; and Thieler, E.R., 2010. National Assessment of Shoreline Change: Historical Shoreline Change along the New England and Mid-Atlantic Coasts. *U.S. Geological Survey Open-File Report 2010-1118*, 57p.

Henderson-Sellers, A.; Zhang, H.; Berz, G.; Emanuel, K.; Gray, W.; Landsea, C.; Holland, G.; Lighthill, J.; Shieh, S-L.; Webster, P.; and McGuffie, K., 1998. Tropical cyclones and global climate change: A post-IPCC assessment. *Bulletin of the American Meteorological Society*, 79(1), 19-38.

Intergovernmental Panel on Climate Change (IPCC), 2007: *Climate Change 2007: Synthesis Report. Contribution of Working Groups I, II and III to the Fourth Assessment Report of the Intergovernmental Panel on Climate Change* Core Writing Team, Pachauri, R.K and Reisinger, A. (eds.). Geneva, Switzerland: IPCC, 104 pp.

Keim, B.D.; Muller, R.A.; and Stone, G.W. 2007. Spatiotemporal patterns and return periods of tropical storm and hurricane strikes from Texas to Maine. *Journal of Climate*, 20, 3498-3509.

Kim, H-M.; Webster, P.J.; Curry, J.A., 2009. Impact of shifting patterns of Pacific Ocean warming on North Atlantic tropical cyclones. *Science*, 325, 77-80.

Kulp, M., 2000. Holocene Stratigraphy, History, and Subsidence: Mississippi Delta Region, North-central Gulf of Mexico. Lexington, Kentucky: University of Kentucky, Ph.D. thesis, 336 p.

Landsea, C.W.; Pielke, R.A.; Jr., Mestas-Nuñez, A.M.; and Knaff, J.A., 1999. Atlantic basin hurricanes: Indices of climatic changes. *Climatic Change*, 42, 89-129.

Louisiana Coastal Wetlands Conservation and Restoration Task Force and the Wetlands Conservation and Restoration Authority (LCWCRTF). 1999. Coast 2050: Toward a Sustainable Coastal Louisiana, The Appendices. *Appendix B— Technical Methods*. Baton Rouge, Louisiana: Louisiana Department of Natural Resources, 50p.

Morton, R.A.; Miller, T.L., and Moore, L.J., 2004. National Assessment of Shoreline Change: Part 1: Historical Shoreline Changes and Associated Coastal Land Loss along the U.S. Gulf of Mexico. *U.S. Geological Survey Open-file Report 2004-1043*, 45p.

Penland, S.; Boyd, R.; and Suter, J.R., 1988. Transgressive depositional systems of the Mississippi Delta Plain: A model for barrier shoreline and shelf sand development. *Journal of Sedimentary Petrology*, 58, 932-949.

Ritchie, W. and Penland, S. 1988. Rapid dune changes associated with overwash processes on the deltaic coast of south Louisiana. *Marine Geology*, 81, 97-122.

Pielke, R.A.; Jr., Landsea, C.; Mayfield, M.; Laver, J.; and Pasch, R., 2005. Hurricanes and global warming. *American Meteorological Society*, 86(11), 1571-1575.

Pielke, R.A., Jr., 2007. Future economic damage from tropical cyclones: Sensitivities to societal and climate changes. *Philosophical Transactions of the Royal Society A,* 365, 2717-29.

Redfield, A.C., 1967. Postglacial change in sea level in western north Atlantic Ocean. *Science,* 157(3789), 687-691.

Reed, D. J. and Yuill, B., 2009. Understanding Subsidence in Coastal Louisiana. New Orleans, Louisiana: Pontchartrain Institute for Environmental Sciences, University of New Orleans, 69 p.

Shepherd, J.A. and Knutson, T., 2007. The current debate on the linkage between global warming and hurricanes. *Geography Compass,* 1(1), 1-24.

Stone, G.W.; Walker, N.D.; Hsu, S.A., Babin, A.; Liu, B.; Keim, B.D.; Teague, W.; Mitchell, D.; and Leben, R., 2005. Hurricane Ivan's impacts along the northern Gulf of Mexico. *EOS Transactions, American Geophysical Union,* 86(48), 500-501.

U.S. Army Corps of Engineers (USACE). 2011. Sea-level Change Considerations for Civil Works Programs. *USACE EC 1165-2-212,* 32 p.

Vermeer, M. and Rahmstorf, S., 2009. Global sea level linked to global temperature. *Proceedings of the National Academies of Sciences of the United States of America,* 106(51), 21527-21532.

Webster, P.J.; Holland, G.J.; Curry, J.A.; and Chang, H.R., 2005. Changes in tropical cyclone number, duration, and intensity in a warming environment. *Science,* 309, 1844-1846.

CHAPTER 2: A COMPARATIVE STUDY OF THE ANNUAL, SEASONAL, AND STORM WINDS AND RELATIONSHIPS TO BLOWOUTS IN THE CAPE COD REGION

2.1 Introduction

The northern end of Cape Cod in the Provincetown region is characterized by large overlapping parabolic dunes. Within these dunes there are very significant numbers of relict, stabilizing, incipient and active blowouts, with saucer and bowl types being the most common. Many bowl blowouts are quite deep and large (10+ meters deep, 10's meters across). Observations indicate that the blowouts develop very rapidly in this roaring 40's wind environment (area between the 40^{th} and 50^{th} parallel north characterized by strong winds) (e.g., Hesp, 2011; Hesp and Walker, 2012a). As a first step towards studying the morphodynamics and evolution of the blowouts in this region, the wind record was examined to gain an understanding of how winds might drive blowout development and the relationships between blowout morphology and sediment patterns and aeolian activity.

This paper examines wind characteristics from the Cape Cod region to determine how wind has driven the development of dunes in the area, with a major focus on modern blowouts. Specifically, the study seeks to determine whether annual, seasonal and storm winds have driven the development of blowouts in the Cape Cod region; whether the geomorphology of the region can be explained by the available wind data; whether there is seasonality in the wind records analyzed, and if so, how it has affected, and/or, how it might affect dune dynamics and blowout evolution; how grain size variations across blowouts affects potential sediment transport; and whether the length of the data record is sufficient to explain the geomorphology of the Cape Cod region.

2.2 The Cape Cod Region

The Cape Cod National Seashore (CCNS), legislatively established as a national park by President John F. Kennedy in 1961, is located along the outer portion of Cape Cod, Massachusetts and comprises approximately 44,600 acres. The National Park Service is responsible for management of the CCNS. A portion of the CCNS near Provincetown, Massachusetts on the northern end of Cape Cod is the site for this study (Figure 2.1).

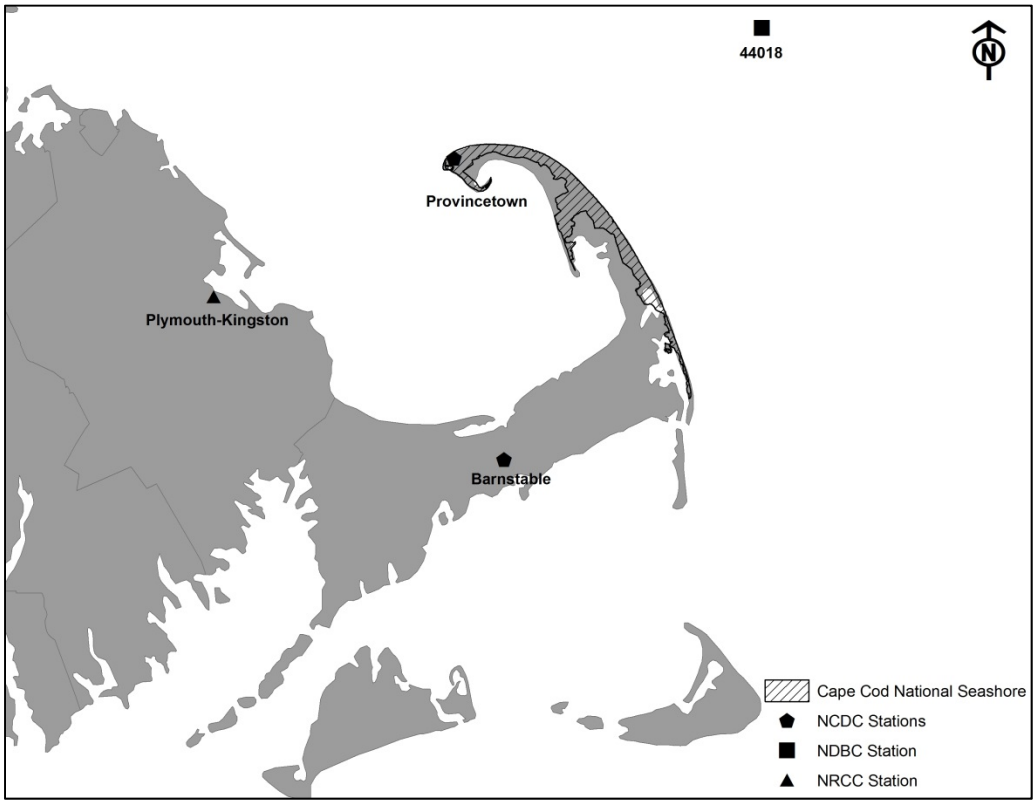

Figure 2.1. The map shows the Cape Cod region as well as the study area of Provincetown, Massachusetts. The location of both wind speed/direction and precipitation monitoring station is also depicted.

Mean monthly average temperatures near Provincetown range from a low of 30.1^0 F in February to a high of 70.8^0 F in July with a mean annual temperature of 49.7^0 F (NOAA, 2002a). From 1971-2000, mean annual precipitation was determined to be 41.95 inches with monthly means ranging from 2.75 inches in July to 4.38 inches in November (NOAA, 2002a). Mean annual temperature and precipitation data from 1961-1990 are similar to data from 1971-2000

referenced above with a mean temperature of 50^0 F and mean precipitation of 40.0 inches (NOAA, 2002b). Forman *et al*. (2008) documented that summer and fall winds are predominantly from the south, while spring and winter winds are bi-directional with spring winds coming from the north and south (with weak west winds) and winter winds coming from the west and north.

Keim, Muller, and Stone (2007) analyzed 105 years of tropical cyclone strikes from Texas to Maine to document the return periods for tropical events, and determined that the average return periods for tropical storms and hurricanes, all hurricanes, and severe hurricanes (category 3-5) was 7, 35, and 105+ years, respectively for Chatham, Massachusetts on the southern end of Cape Cod. Extratropical winter storms, also known as northeasters, occur more frequently in the Cape Cod region than tropical storms and are usually larger, slower moving storms that last for several days (Dolan, Lins, and Hayden, 1988). Colucci (1976) noted that the maximum number of extratropical storms between 1964 and 1973 occurred along a band extending from Cape Hatteras, North Carolina across Cape Cod and into the Gulf of Maine. In a reanalysis of East Coast winter storms from 1948 and 1951-1997, Hirsch, DeGaetano, and Colluci (2001) found that an average of twelve storms occurred per winter season, with a minimum of five storms in 1984-1985 and a maximum of nineteen storms in 1962-1963 and 1995-1996. Additionally, they found that about three strong northeasters with winds greater than 23.2 m/s occur each season. The maximum number of northeasters occurs between December and April, with the strongest occurring between October and March (Dolan and Davis, 1992). The monthly storm distribution shows a maximum in January and a minimum in October (Hirsch, DeGaetano, and Colluci 2001). There is a significant increase in the number of storms during December-February during El Niño periods (Hirsch, DeGaetano, and Colluci 2001).

According to Giese *et al*. (2011), the morphology of the outer coast of Cape Cod consists of eroding bluffs of glacial outwash deposits at the center, and dunes, barrier beaches, and estuaries on either end. Their study determined that the majority of the outer coast of Cape Cod, from Chatham to near Provincetown, is eroding but that accretion is occurring on the northern end of Cape Cod near an area known as Provincetown Hook (Giese *et al*., 2011). The greatest erosion (~40 m^3/m/yr) has occurred along the bluffs near the center of the Cape, and the greatest accretion (~62 m^3/m/yr) has occurred near Race Point Light on the northern end of the Cape (Giese *et al*., 2011). The net annual sediment change along the outer coast is 1.1 million m^3 (Giese *et al*., 2011). Due to greater erosion at the southern end of the bluffs compared to the northern end, Giese and Adams (2007) noted a clockwise shift in coastal orientation of Cape Cod and attributed it to an increase in wave energy from the southeast as a result of the submergence of George's Bank off the outer continental shelf southeast of Cape Cod (cf. Davis, 1895).

WM Davis wrote a seminal paper on Cape Cod in 1895 and showed that the Cape had originally formed at a significantly greater seawards arc than the present coastline. There are many accounts of how early colonists changed a fully forested land into a semi-desert by cutting down the forest, and that the origin of the large-scale parabolic dunes along the cape relate to that colonial period (e.g. Kucinski and Eisenmenger, 1943). This is highly unlikely given the size of the parabolic dunes present on the Cape, the presence of multiple paleosols throughout the dunes, and the history of other barrier systems in this portion of the United States. Rather, it is likely that the early colonists destabilized an existing dunescape.

Forman *et al*. (2008) utilized aerial photography from 1938-2003 to monitor movement of eleven parabolic dunes on the northern end of Cape Cod and determined that over 75% of dune movement occurred between 1938-1977 for ten of the eleven monitored dunes and less than

12% of the movement occurred since 1987. Total movement of the dunes ranged from 130-221 m with a 4 m/yr average during the peak period of movement and a 1 m/yr average since 1987 (Forman *et al*., 2008). The peak period of movement corresponds to a period of drier conditions (generally negative Palmer Drought Severity Index (PDSI)), while the period of reduced movement corresponds to a wetter period (generally positive annual PDSI) (Forman *et al*., 2008). The parabolic dunes are migrating in a southeasterly direction.

There is a huge number of modern and relict blowouts on the dunes at Cape Cod, particularly in the Provincetown region where they principally occur on the crestal regions of the large parabolics. They may also be found in almost every location except generally in the stabilized deflation plains and basins of the parabolics. The principal blowout types are saucer and bowl blowouts. Saucer blowouts are semi-circular and shallow, while bowl blowouts tend to be deeper and semi-circular to circular (Hesp, 2002; Hesp and Walker, 2012b).

2.3 Methods

2.3.1 Wind Data

Wind speed and direction data were collected from the National Data Buoy Center (NDBC) station 44018 (latitude: 42.126^0; longitude: -69.63^0; elevation: sea level) and from the National Climatic Data Center (NCDC) stations at Barnstable Municipal Airport (latitude: 41.669^0; longitude: -70.28^0; elevation: 15.8 meters) and Provincetown Municipal Airport (latitude: 42.072^0; longitude: -70.221^0; elevation: 2.8 meters) on Cape Cod. The NDBC station is located approximately 43 kilometers (km) east of Provincetown, Massachusetts at sea level and reports wind speed data averaged over an eight-minute period. The NCDC stations report wind speed data averaged over a one-hour period. The Barnstable station is located approximately 35 km southwest of Provincetown. At the 44018 station, wind speed data are

provided in m/s, and wind direction data are provided based on the direction the wind is coming from in degrees clockwise from true north. The period of record available for station 44018 was from 2002-2011. Wind speed data from the NCDC stations are provided hourly in knots, and wind direction data at these stations are also provided based on the direction the wind is blowing from in degrees clockwise from true north. The period of record was 1973-2008 for the Barnstable station and 1991-2008 for the Provincetown station.

2.3.2 Precipitation Data

Precipitation data were obtained from the Northeast Regional Climate Center for the Plymouth-Kingston station (latitude: 41.98 degrees; longitude: -70.70 degrees) located west of Provincetown, Massachusetts near Plymouth Bay. Daily data were available from 1893-2012.

2.3.3 Sand Samples and Analyses

Sand samples were taken along transects running both north-south and east-west across a bowl blowout (named *Jinx*) near Provincetown (Figure 2.2). The depositional lobe is located on the north end of the dune with a scarp on the south. Twelve fifty-gram surface samples were taken from the deflation basin, the depositional lobe, along the west slope, at points along the north, south, east, and west rims of the blowout, and in the scarp. Each sand sample was thoroughly rinsed to remove salts and detritus and dried in an oven to remove all moisture. Forty grams of dry sand was extracted from each sample and sieved at ½ phi intervals. All sand retained by each sieve was removed and weighed. The total weight of sand for each sieve size was entered into an excel spreadsheet that calculated the total sediment weight for each whole phi size (i.e., sample weight from phi size 0.50 and phi size 1.0 are combined into a total weight for phi size 1.0). The phi scale is commonly used for measuring particles size and requires conversion of particle size in millimeters to the negative of its logarithm in base 2 to yield simple

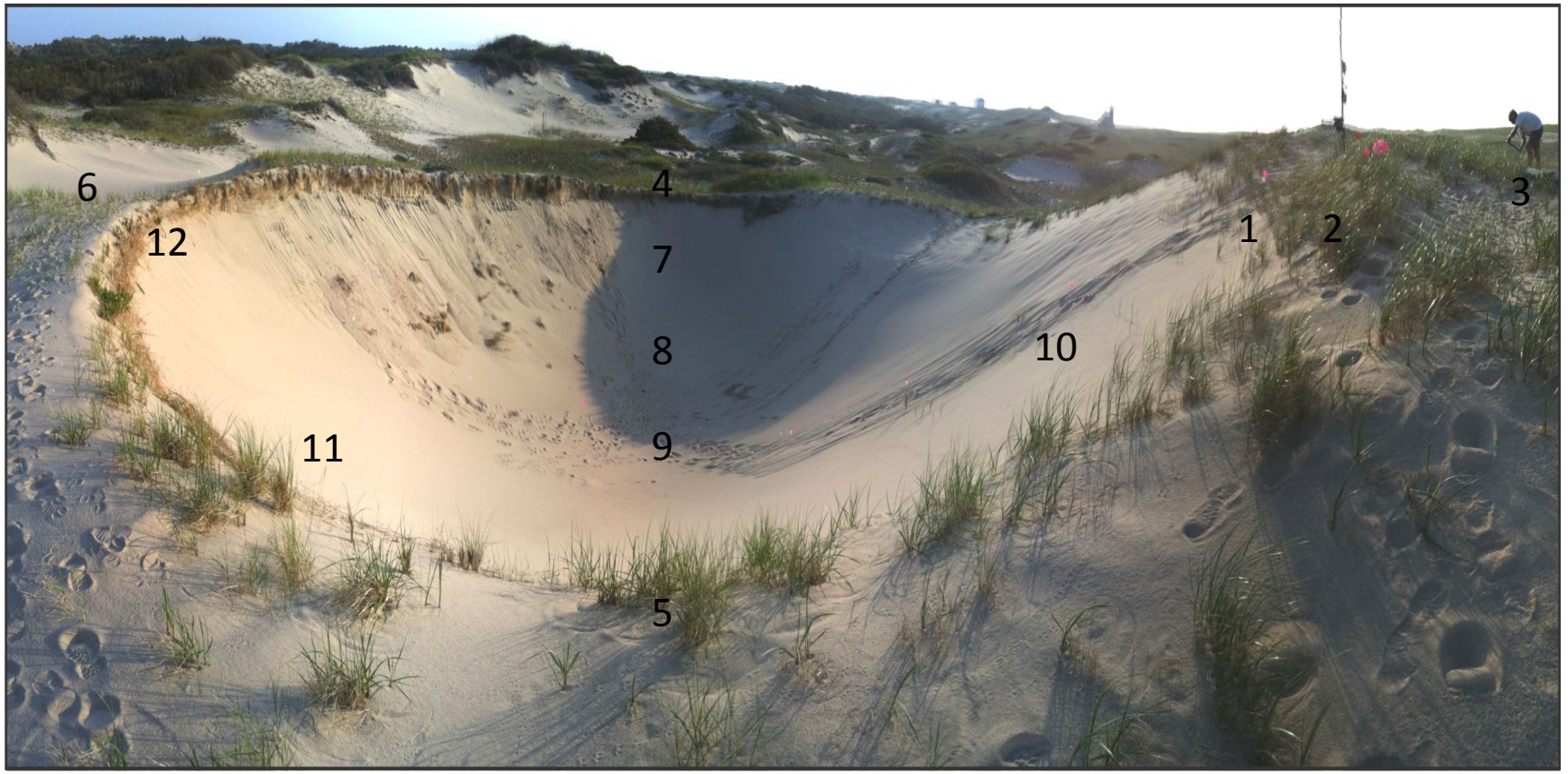

Figure 2.2. Digital photograph of the *Jinx* blowout with the twelve locations from which sand samples were collected. The depositional lobe of the blowout dune is located on the right side of the photograph (north) near sample locations 1-3, the deflation basin near the center of the photograph at sample location 9, the scarp of the blowout on the left side of the photograph (south) between sample locations 6 and 12, the west rim of the blowout near sample location 4, and the east rim of the blowout near sample location 5.

whole numbers. These data were then entered into the GSSTAT software package (Poppe, Eliason, and Hastings, 2004) to determine the mean, median, standard deviation, skewness and other statistical parameters of the sand sample.

2.3.4 Wind Roses and Fryberger and Dean Resultant Drift Potentials

Wind roses were constructed for the full length of the data set, seasonal time periods, El Niño Southern Oscillation (ENSO) events, and selected large storm events. Wind roses were constructed using WRPLOT software available from Lakes Environmental (http://www.web lakes.com/products/ wrplot/index.html). The wind speed classes used for wind rose creation were modified from Pearce and Walker (2005) and based on Miot da Silva and Hesp (2010). The wind speed classes used were 0.1-3.0 m/s, 3.0-5.6 m/s, 5.6-7.0 m/s, 7.0-8.7 m/s, 8.7-11.3 m/s, 11.3-14.3 m/s, 14.3-17.4 m/s, 17.4-20.6 m/s, and greater than 20.6 m/s.

A sand rose is defined by Fryberger and Dean (1979, p. 147) as ‘a circular histogram which represents potential sand drift from the 16 directions of the compass. The arms of a sand rose are proportional in length to the potential sand drift from a given direction as computed in vector units. Thus, a sand rose expresses graphically both the amount of potential sand drift (drift potential) and its directional variability.’ The method used to construct sand roses in Fryberger and Dean (1979) was used to determine drift potential (DP), resultant drift potential (RDP), resultant drift direction (RDD), and directional variability (RDP/DP) at each of the sample locations identified in Figure 2.2. Fryberger and Dean (1979), Bullard (1997), and Pearce and Walker (2005) discuss potential errors associated with sand rose creation using this methodology. The Fryberger and Dean (1979) method uses a “standard” mean grain size of 0.25-0.30 mm, which results in a threshold velocity of approximately 5.96 m/s for any dune anywhere on earth. The use of a standard grain size commonly results in a minor to considerable

underestimation or overestimation of potential sand transport. Thus, due to the much larger grain sizes observed at the Cape Cod study sites, sand roses for this study were generated by estimating threshold velocities using the calculated mean grain size at each site. Aeolian threshold velocities for the mean grain size of each sand sample taken from *Jinx* were calculated using the methods in Zingg (1953) and Belly (1964) (e.g., Hesp *et al*., 2007; Miot da Silva and Hesp, 2010).

2.3.5 El Niño, La Niña, and ENSO Neutral Wind Roses

Data from the NOAA Oceanic Niño Index (ONI) were used to determine time periods during which either El Niño, La Niña, or ENSO Neutral events occurred over the available data record for station 44018 (http://www.cpc.ncep.noaa.gov/products/analysis_monitoring/enso stuff/ensoyears.shtml). Once these events were identified, the event of the shortest duration in months was determined and wind data for this duration was extracted from the available data. For example, if the identified El Niño event had a duration of twelve months (e.g., January-December), data were extracted for this event period as well as for a La Niña event and an ENSO Neutral event that also had a twelve month duration. Ensuring that the data extracted for each event encompassed the same months (even if different years) theoretically removed or lessened the effects of wind seasonality for the period of record. In addition, seasonal and monthly data were extracted from time periods during which each of the three types of events occurred to determine if there were noticeable differences in wind direction and magnitude between types of events during different seasons or months.

2.3.6 Storm Event Wind Roses

The five storms that produced the highest recorded wind speeds at station 44018 were identified from the wind records, and the wind data record for the duration of the storm event

was extracted. Four of the five identified storms were northeasters, and one was a tropical event. The storms occurred during the months of November, December, or January.

2.4 Results

2.4.1 Long-Term Wind Data

Wind roses were constructed for the Barnstable, Provincetown, and 44018 stations for their entire records (Figures 2.3-2.5). The resultant wind direction is from the west-northwest for the Barnstable station, from the west for the Provincetown station, and from the west-southwest for the 44018 station. The wind roses for all three stations indicate a higher percentage of winds from the south and southwest; however, high velocity winds from the north and west are only observed for the Provincetown and 44018 stations. Average wind speeds are highest for the 44018 station and lowest for the Barnstable station. The Provincetown station is missing the complete year of data for 1997, 1998, and 2001. The Fryberger and Dean RDP, RDD, and RDP/DP for each station are shown in Table 2.1. The RDP for the 44018 station is higher than the RDP for the Barnstable and Provincetown stations, but the RDD and RDP/DP for 44018 and Provincetown are similar to each other when compared to the same statistics for the Barnstable station.

Wind roses were constructed for the Barnstable, Provincetown, and 44018 stations for a five-year period which these stations had in common (2003-2007) to select one station to use for the more detailed investigation. The axes of the larger scale parabolic dunes and their net migration is consistent with winter winds which blow from the west-northwest (cf. Forman *et al*., 2008). Therefore, it was important to ensure that the wind data selected for use in the more detailed analysis of wind magnitude and direction and thus potential sand movement indicated that winds of the greatest magnitude occurred during the winter season and were from the northwest. Because all three stations showed similar resultant wind directions for the winter

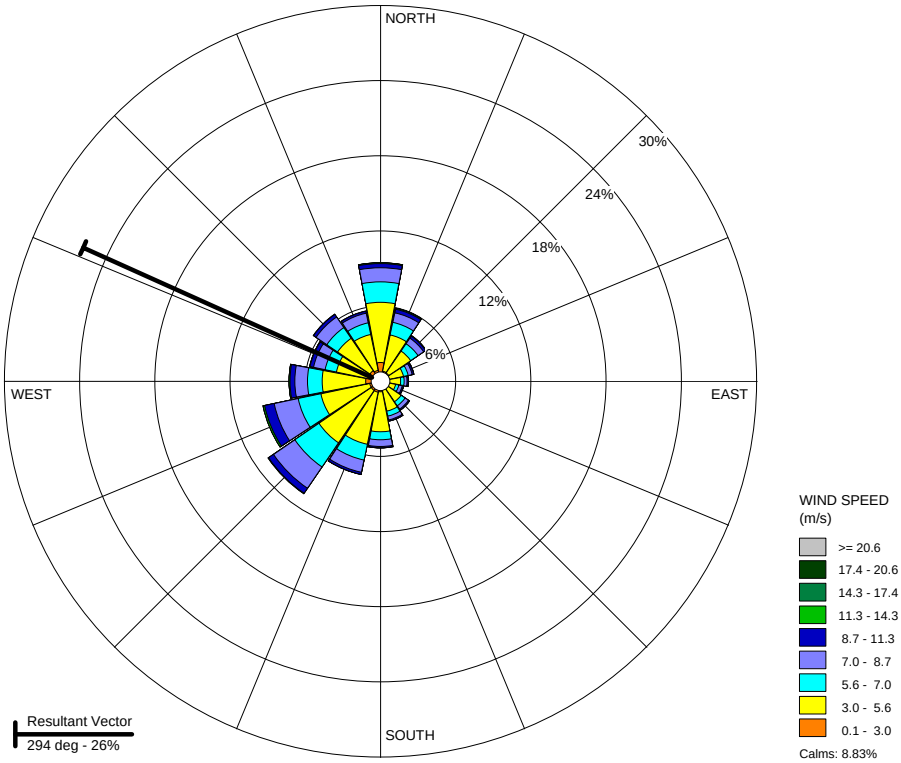

Figure 2.3. Wind rose indicating the frequency, magnitude, and resultant direction of winds for the full data record (1973-2011) for the Barnstable station.

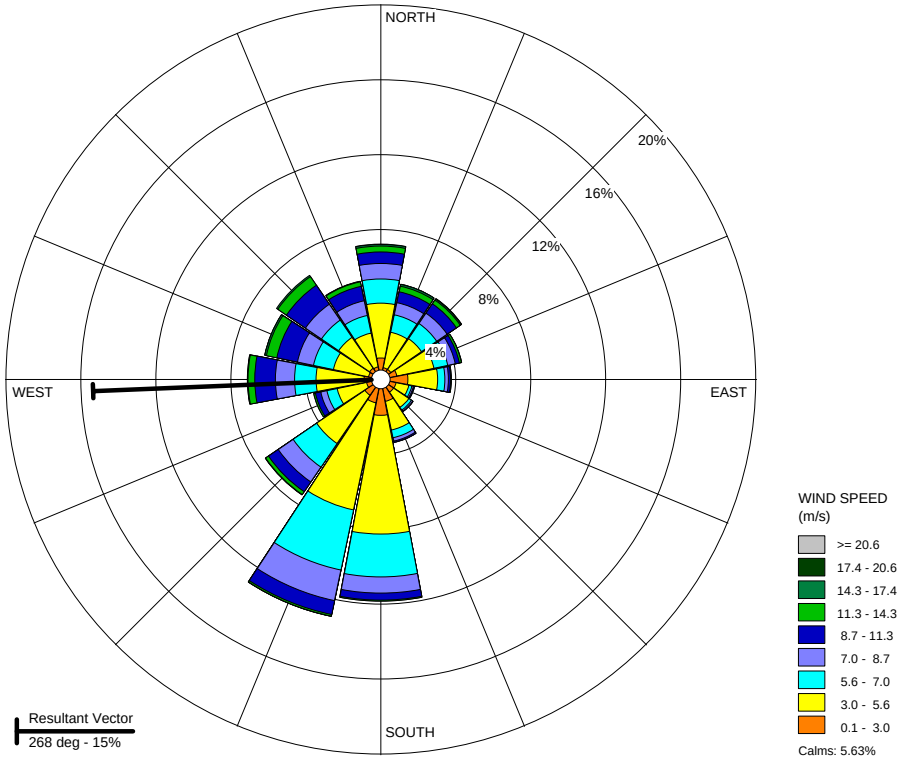

Figure 2.4. Wind rose indicating the frequency, magnitude, and resultant direction of winds for the full data record (1991-2008) for the Provincetown station.

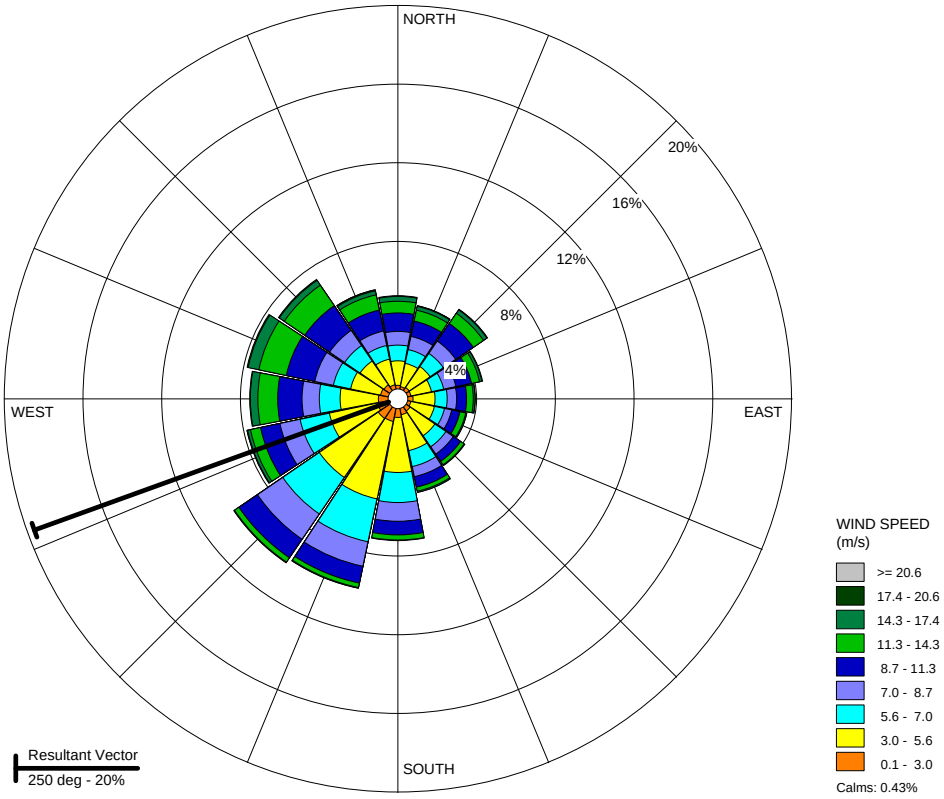

Figure 2.5. Wind rose indicating the frequency, magnitude, and resultant direction of winds for the full data record (2002-2011) for station 44018.

Table 2.1. Resultant drift potential, resultant drift direction, and directional variability (RDP/DP) for the Barnstable, Provincetown, and 44018 stations for the full data record as well as the five year period (2003-2007) which the stations had in common.

Time Period	RDP	RDD	RDP/DP
Barnstable Full Record	0.12	280.66	0.16
Barnstable 2003-2007	0.35	180.48	0.53
Provincetown Full Record	2.73	179.50	0.59
Provincetown 2003-2007	1.75	147.92	0.61
44018 Full Record	11.09	145.83	0.48
44018 2003-2007	0.09	136.16	0.45

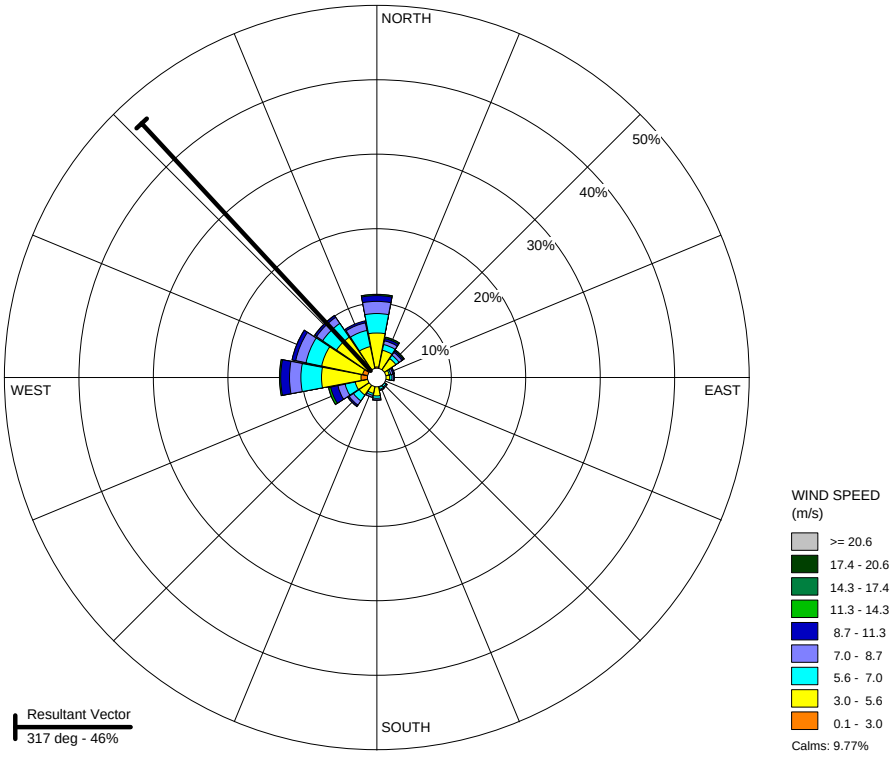

Figure 2.6 Winter wind rose indicating the frequency, magnitude, and resultant direction of winds for the Barnstable station from 2003-2007.

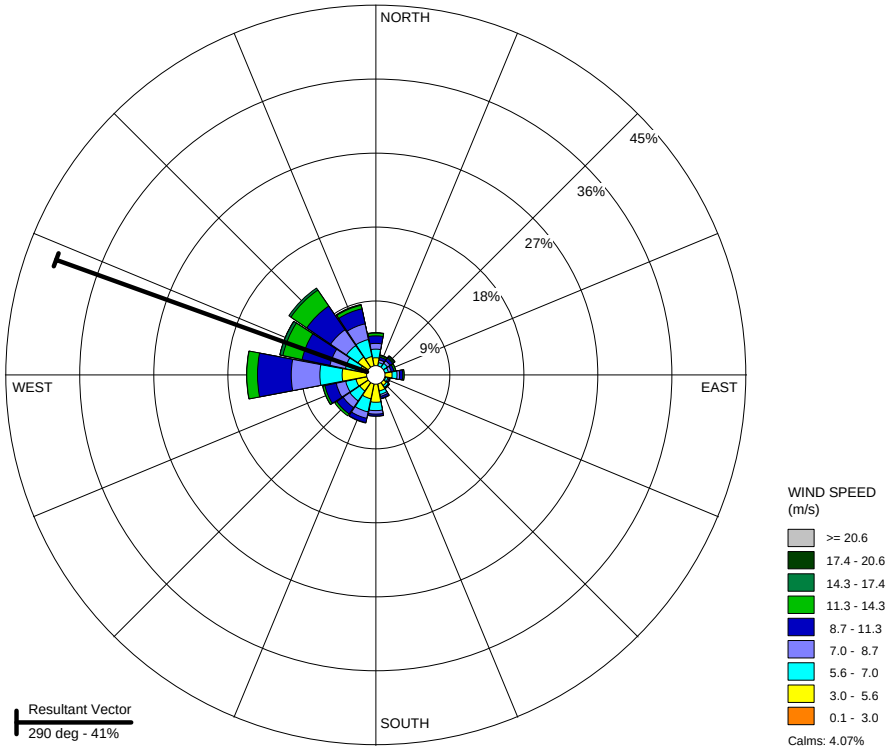

Figure 2.7. Winter wind rose indicating the frequency, magnitude, and resultant direction of winds for the Provincetown station from 2003-2007.

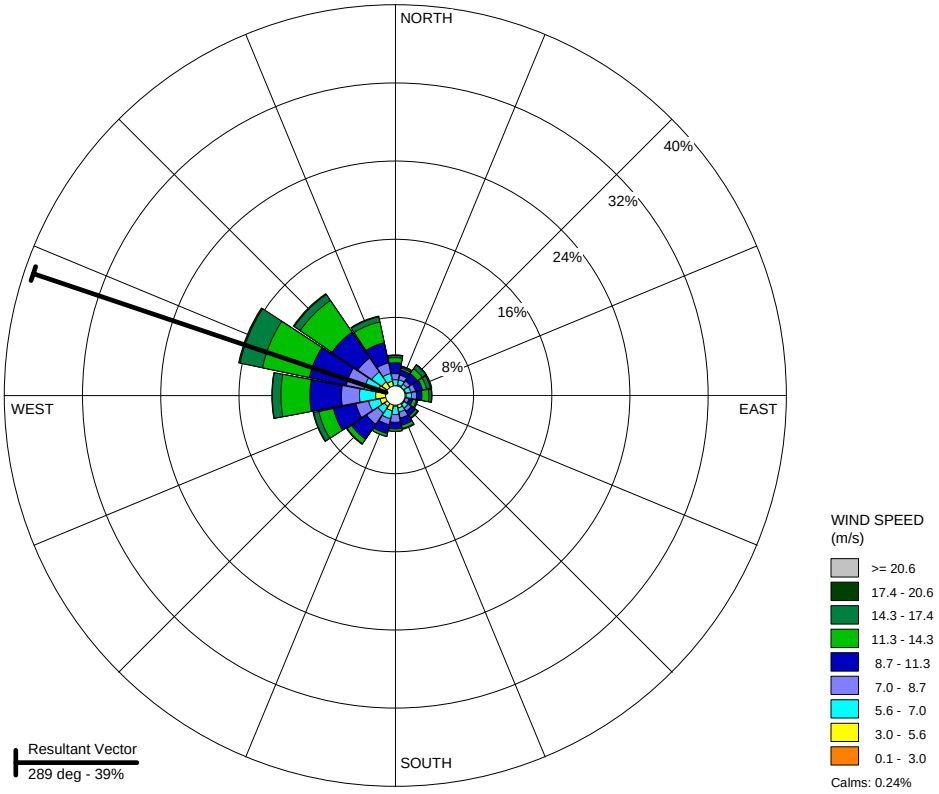

Figure 2.8. Winter wind rose indicating the frequency, magnitude, and resultant direction of winds for station 44018 from 2003-2007.

period during which wind speeds are greatest (Figures 2.6-2.8), station 44018 was selected for use in this study. Although the Barnstable station has a longer data record, the annual wind patterns from 2003-2007 are similar to that of station 44018. Additionally, the Barnstable station had the lowest average wind speed of the three stations suggesting that perhaps wind speeds at that location could be influenced by, or diminished by, landscape features. Station 44018 is approximately 43 km offshore of Cape Cod and is not subject to influences by landscape features which could alter wind direction or velocity.

2.4.2 Seasonal Wind Analyses

Data from 2002-2011 for station 44018 indicate that the mean annual wind direction is from the west-southwest with a higher percentage of winds coming from the southwest, but with winds of greater magnitude coming from the west and northwest (Figure 2.9). However, there is

great seasonality in wind direction with spring winds blowing from the north and the west (Figure 2.10), summer winds blowing mainly from the south (Figure 2.11), fall winds blowing from northeast and southwest (Figure 2.12), and winter winds blowing mostly from the northwest (Figure 2.13). Winds of the highest magnitude occur during the winter season, and winds of the lowest magnitude occur during the summer season. The season in which winds of the greatest magnitude occur, lines up well with the direction of parabolic dune movement measured by Forman *et al*. (2008), in which they noted that dune migration was to the southeast and corresponded with winter winds blowing from the northwest.

Blowouts at Cape Cod are spread across the landscape and face virtually every direction. They thus, have depositional lobes that extend in almost every direction. For example, *Jinx* is located on a south facing dune slope, and is roughly aligned south-north with a principal depositional lobe that extends to the north (Figure 2.2). However, it also has rim dunes which surround the edges of the bowl, and it is clear that at times winds from directions other than from the southerly quadrant erode sand from the blowout and deposit it on and near the east, west or south rim. A large bowl blowout (named *Vixen*) is located adjacent to *Jinx*, but faces into the northwest and the principal depositional lobe extends to the southeast. The long-term and seasonal analyses of the wind records (Figures 2.9-2.13) shows that winds are multidirectional in the region, and this explains why blowouts can develop from simple, poorly vegetated sand patches a meter or less in diameter to large blowouts anywhere in the landscape.

In addition, the seasonal analysis shows that winds from the southwest in summer could be the initiating winds for blowouts on slopes oriented in a northwest-southeast direction. Although the resultant direction of spring winds is from the west, winds are multidirectional over this period. Spring winds blowing from the north and west tend to have the highest magnitudes

and greatest frequency of occurrence. However, because of the multidirectional nature of the spring winds, it is possible that blowouts could be initiated on any dune slope due to topographic alteration of the wind flow at a specific location. Fall winds are similarly multidirectional and because winds of the greatest magnitude occur from the north and west quadrants, blowouts could be initiated on northeast-southwest facing dune slopes during this season. The analysis also shows that winter winds from the northwest direction are the strongest and that there should be more blowouts with their longer axis aligned northwest-southeast in similarity to the larger parabolic dunes. However, winter is also accompanied by snow, and field observations in January demonstrate that the blowout slopes and base are frozen, so in mid-winter there may be considerably less transport and blowout development despite this being the period of strongest winds.

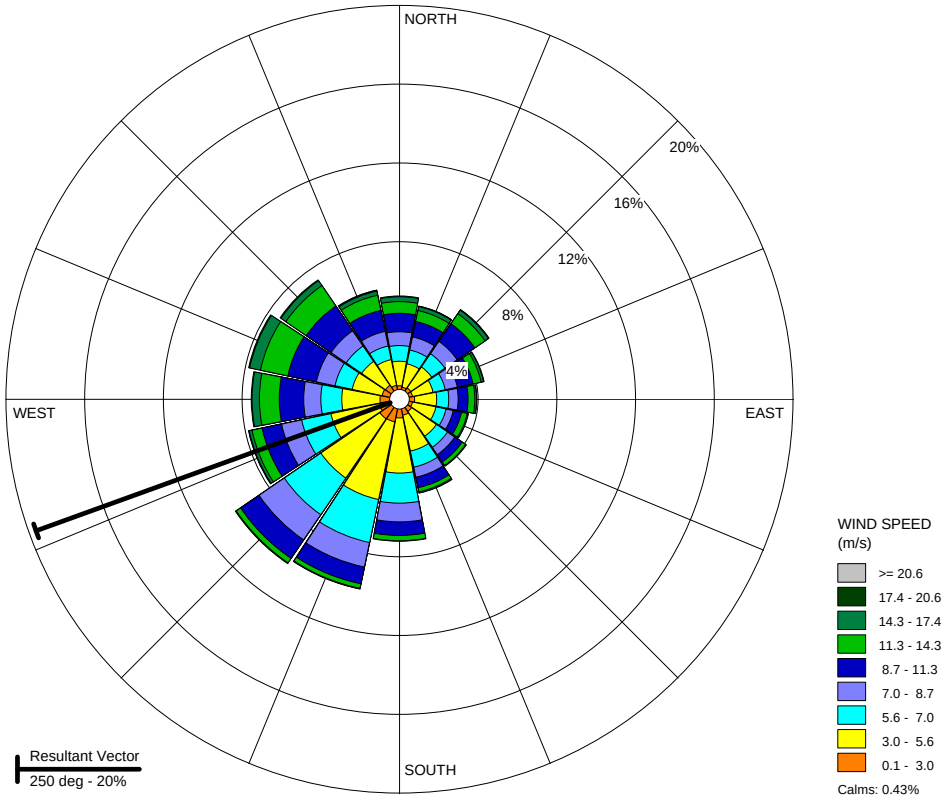

Figure 2.9. Wind rose indicating the frequency, magnitude, and resultant direction of winds for station 44018 for the full length of the data record (2002-2011).

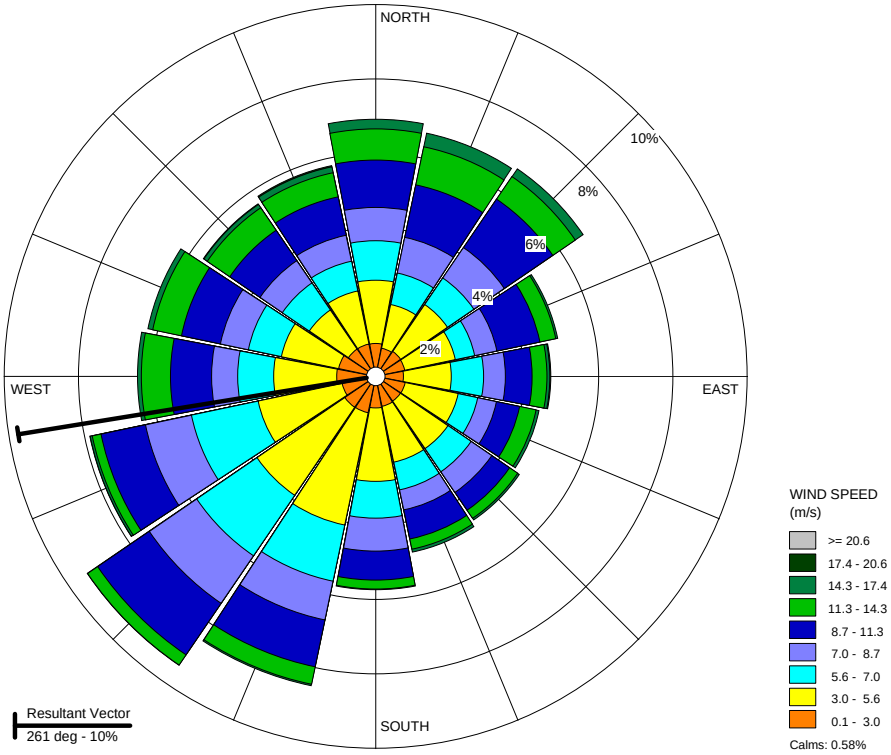

Figure 2.10. Spring wind rose indicating the frequency, magnitude, and resultant direction of winds for station 44018 for the full length of the data record (2002-20111).

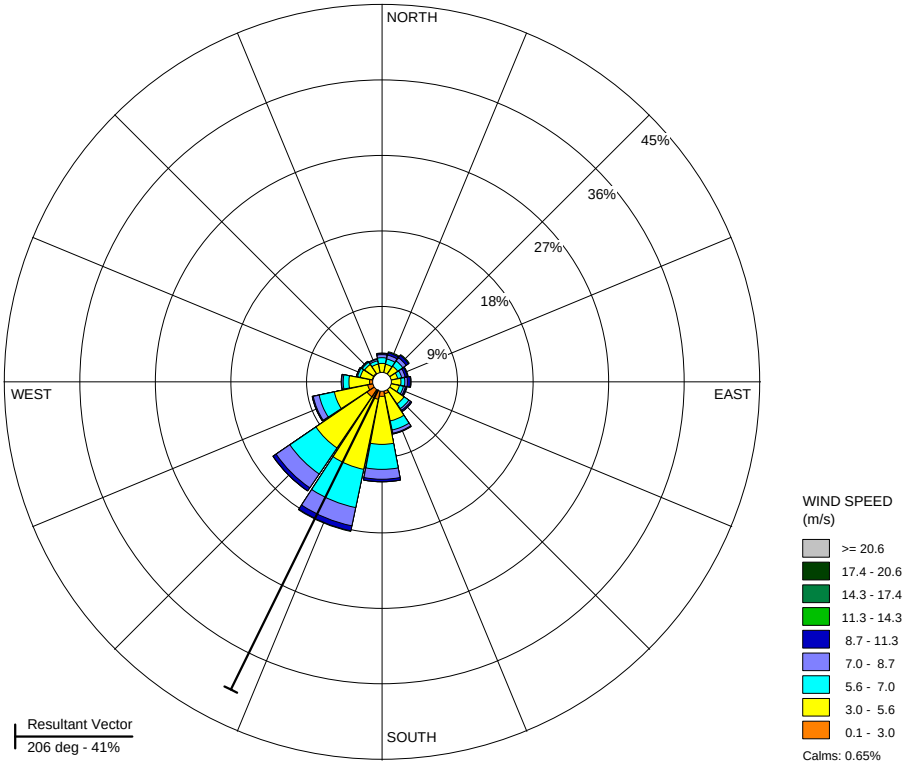

Figure 2.11. Summer wind rose indicating the frequency, magnitude, and resultant direction of winds for station 44018 for the full length of the data record (2002-2011).

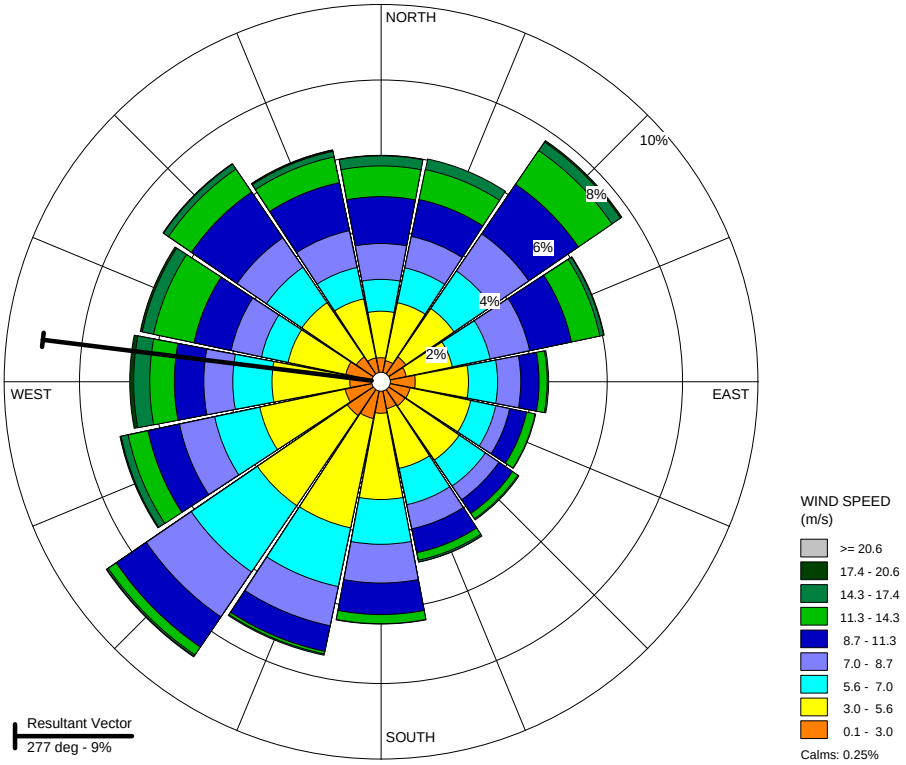

Figure 2.12. Fall wind rose indicating the frequency, magnitude, and resultant direction of winds for station 44018 for the full length of the data record (2002-2011).

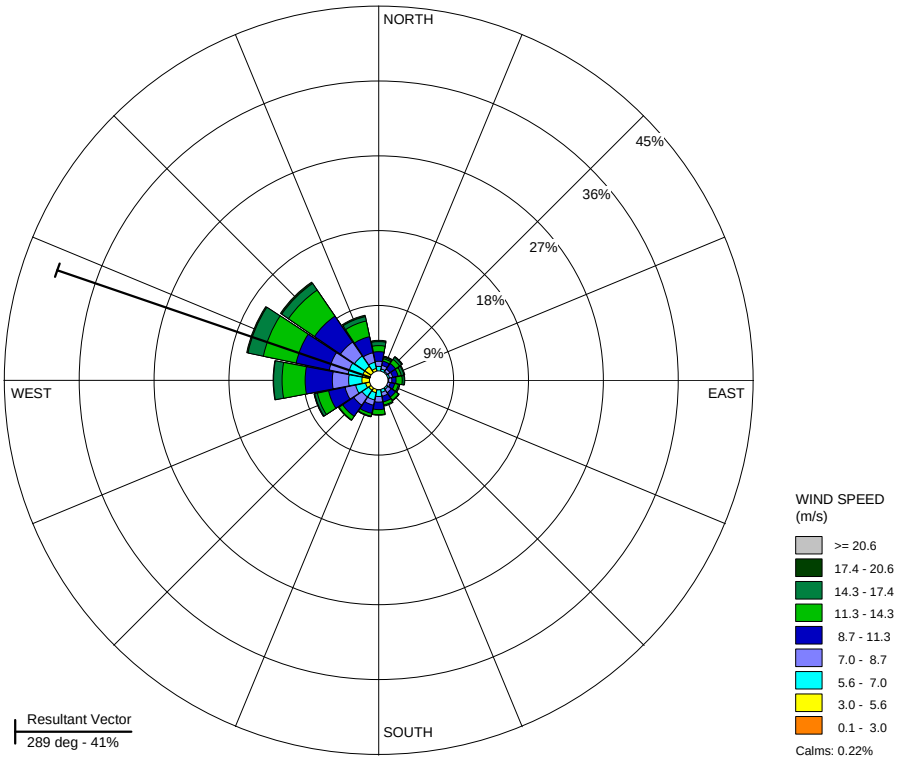

Figure 2.13. Winter wind rose indicating the frequency, magnitude, and resultant direction of winds for station 44018 for the full length of the data record (2002-2011).

2.4.3 Resultant Drift Potential, Direction, and Variability within the *Jinx* Blowout

Twelve sand samples were taken from various points within a deep bowl blowout (*Jinx*) near Provincetown (Figure 2.2). This sampling was undertaken to gain an understanding of how the surface sediment varied in size across a typical bowl blowout, and then how this might affect potential sediment transport within the blowout. The samples predominantly comprised coarse sand, with all samples including at least 74% coarse sand and at least 82% coarse and very coarse sand (Table 2.2). None of the samples contained measurable fine or very fine sand. Sand collected from the middle of the deflation basin (sample location 9) had the highest mean grain size (0.801 mm), likely due to the fact that this zone is the deepest portion of the blowout, has lost the largest amount of the finer grains, and coarse grains are concentrated here as a lag. This zone thus has the highest threshold velocity for sand movement (14.51 m/s). Sand collected from the west rim of the dune (sample location 4) had the lowest mean grain size (0.642 mm) and therefore the lowest threshold velocity for sand movement (12.52 m/s), and sand collected from the middle of the depositional lobe (sample location 2) had a mean grain size of (0.732 mm) and a threshold velocity of (13.66 m/s) (Table 2.3).

Table 2.2. Sand size classification for each of the twelve sample locations within the *Jinx* blowout as indicated on Figure 2.2.

Sand Classification	1	2	3	4	5	6	7	8	9	10	11	12
% very coarse	16%	10%	10%	1%	3%	3%	5%	1%	22%	16%	14%	6%
% coarse	81%	85%	82%	84%	83%	91%	77%	90%	74%	78%	80%	86%
% medium	4%	5%	7%	15%	14%	6%	17%	10%	4%	5%	7%	9%
% fine	0%	0%	0%	0%	0%	0%	0%	0%	0%	0%	0%	0%
% very fine	0%	0%	0%	0%	0%	0%	0%	0%	0%	0%	0%	0%

As a result of differences in wind magnitude and frequency during various times of the year as well as differences in mean sand grain size at specific locations within the dune, the resultant drift potential varies both temporally and spatially within the *Jinx* blowout (Table 2.4). Resultant drift potential is given in vector units as described in Fryberger and Dean (1979). The resultant drift potential at sample location 2 (median grain size of the twelve samples) is 5.47 in the spring, 0.03 in the summer, 9.43 in the fall, and 32.65 in the winter. By comparison, the RDPs for sample location 9 (greatest mean grain size of the twelve samples) are 3.50, 0.02, 6.58, and 22.85 for spring, summer, fall, and winter, respectively; and for sample location 4 (lowest mean grain size of the twelve samples), the RDP is 9.10 for spring, 0.15 for summer, 14.51 for fall, and 50.13 for winter. Because the grain size at the bottom of the deflation basin (sample location 9) is the coarsest of the sampled locations, the threshold velocity for moving sand is the highest and therefore the resultant drift potential is lowest at that location. The seasonal sand roses for sample locations 4, 2, and 9 are shown in Figures 2.14, 2.15, and 2.16, respectively. The sand roses represent the combined wind events for each season for the available data record.

Table 2.3. Mean grain size and threshold velocity for each of the twelve sample locations within the *Jinx* blowout as indicated on Figure 2.2.

Sample Number	Mean Grain Size (mm)	Threshold Velocity (m/s)
1	0.768	14.105
2	0.732	13.659
3	0.722	13.535
4	0.642	12.524
5	0.651	12.639
6	0.688	13.108
7	0.646	12.575
8	0.664	12.804
9	0.801	14.511
10	0.758	13.982
11	0.742	13.784
12	0.693	13.171

Examination of the available wind data above (in combination with grain size and threshold velocity) proves that there are sufficient wind velocities on Cape Cod to erode sand. However, as a blowout deepens, the finest sediments are removed first by the lower but above threshold winds. Coarse sand is concentrated in the deflation basin. As the blowout continues to evolve, increasingly stronger winds are required to erode sand from the deflation basin, and with time this trend must be intensified. As deposition occurs up the inner depositional lobe slope, onto the depositional lobe crest, and over the rims, the spatial variation in sediment sizes is increased. Thus, wind from one particular direction may be able to move only certain portions of the blowout slopes and basin; for example, a light summer wind may only move sand from the depositional lobe crest, while a very strong winter wind may be the only wind that can excavate the basin, once a blowout has a significant depth. Presumably, there will come a point where no deflation is possible within the basin area, and this may perhaps signal a beginning of the stabilization process.

Table 2.4. Resultant drift potential (RDP) for each of the twelve sample locations within the *Jinx* blowout as indicated on Figure 2.2.

Time Period	1	2	3	4	5	6	7	8	9	10	11	12
Full Record	9.32	11.09	11.59	17.18	16.07	13.29	16.69	14.5	7.71	9.81	10.6	13.04
Spring	4.44	5.47	5.76	9.1	8.41	6.75	8.79	7.45	3.5	4.73	5.19	6.6
Summer	0.02	0.03	0.03	0.15	0.09	0.03	0.12	0.04	0.02	0.02	0.02	0.03
Fall	7.94	9.43	9.85	14.51	13.59	11.28	14.1	12.29	6.58	8.35	9.01	11.07
Winter	27.5	32.65	34.09	50.13	46.98	39.02	48.73	42.54	22.85	28.93	31.21	38.29

2.4.4 El Niño, La Niña, and ENSO Neutral Sand Roses

The RDP, RDD, and RDP/DP statistics were also calculated for El Niño, La Niña, and ENSO Neutral climate events for the full record of the climate event, for each season, and for the

month with the highest RDP (January) for the period 2002 to 2011 (Table 2.5). Although variability exists between the sand rose statistics for these three types of climatic events, a clear pattern does not exist that would allow any conclusions to be drawn. Unfortunately, the relatively short period of available wind data at this station does not allow for comparison between multiple events of the same type (e.g., comparison of one El Niño to another El Niño).

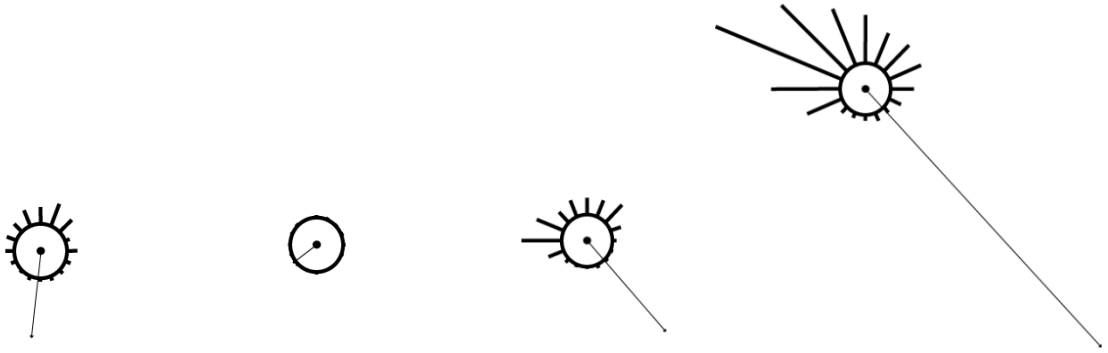

Figure 2.14. Spring, summer, fall, and winter sand roses (from left to right) for sample location 4 as indicated on Figure 2.2. Sample location 4 had the lowest mean grain size and threshold velocity of the twelve samples taken at the *Jinx* blowout.

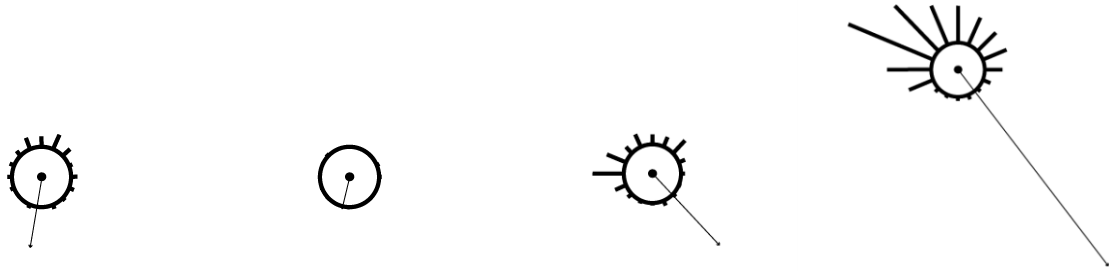

Figure 2.15. Spring, summer, fall, and winter sand roses (from left to right) for sample location 2 as indicated on Figure 2.2. Sample location 2 had the median grain size and threshold velocity of the twelve samples taken at the *Jinx* blowout.

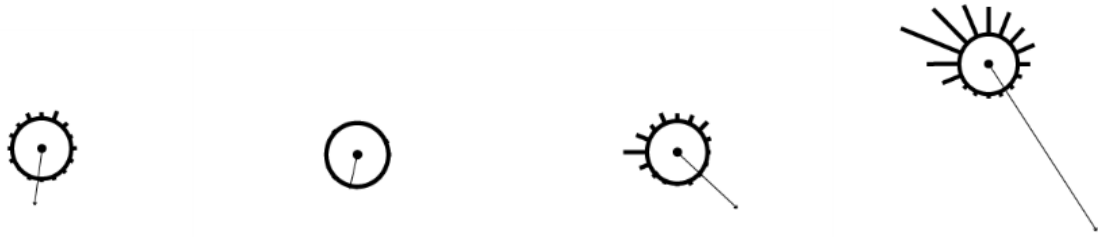

Figure 2.16. Spring, summer, fall, and winter sand roses (from left to right) for sample location 9 as indicated on Figure 2.2. Sample 9 had the highest mean grain size and threshold velocity of the twelve samples taken at the *Jinx* blowout.

2.4.5 Annual Sand Roses

Sand rose statistics were developed for each individual year within the data record that contained a full twelve months of data (2003-2010), and the RDP, RDD, and RDP/DP for each year are shown in Table 2.6. Although there appears to be a general trend that years with lower RDP/DP (greater directional variability) have lower RDP, this does not hold true in all cases; however, it would seem intuitive that years with greater directional variability in sand movement, would produce a lower RDP. Years in which the direction of sand movement is more unimodal (lower directional variability) should result in years with higher RPD when compared to years in which the direction of sand movement is shown to be bimodal or complex (higher directional variability). For the annual sand roses, RDD ranges from east-southeast to south, with the median direction being southeast.

Table 2.5. Resultant drift potential (RDP), resultant drift direction (RDD), and directional variability (RDP/DP) for the full record of the ENSO event, for each season within the ENSO event duration, and for January for El Niño, La Niña, and ENSO Neutral weather patterns.

Time Period	El Niño			La Niña			ENSO Neutral		
	RDP	RDD	RDP/DP	RDP	RDD	RDP/DP	RDP	RDD	RDP/DP
Full Record	0.23	177.57	0.58	0.20	146.78	0.55	0.10	120.72	0.54
Spring	0.33	206.30	0.71	0.03	354.40	0.35	0.07	187.80	0.95
Summer	-	-	-	0.01	258.75	0.98	-	-	-
Fall	0.13	184.09	0.56	0.14	166.47	0.58	0.05	185.40	0.32
Winter	0.47	162.08	0.59	0.56	142.07	0.61	0.32	104.60	0.70
January	0.33	137.06	0.54	0.33	111.27	0.56	0.34	111.89	0.80

Sand rose statistics were also developed for one year (2008), one season (winter; the season with highest RDP), one month (January; the month with the highest RDP), and one storm

(January 27-29, 2008) to provide greater clarity on how sand rose statistics can vary throughout a twelve month period and how seasons and storms can influence RDP. The sand rose statistics are shown in Table 2.7. In general, directional variability tends to decrease with shorter time periods. RDP is obviously highest for the storm event because the majority of the storm winds are above the threshold for sand movement and directional variability of the wind is lowest (i.e., storm winds are generally blowing from one direction or quadrant).

Table 2.6. Resultant drift potential (RDP), resultant drift direction (RDD), and directional variability (RDP/DP) for station 44018 for the full length of the data record (2002-2011) and for each year within the data record having a full twelve months of data.

Time Period	RDP	RDD	RDP/DP
Full Record	11.09	145.83	0.48
2003	0.15	117.74	0.49
2004	0.12	182.30	0.68
2005	0.04	185.81	0.32
2006	0.06	131.58	0.44
2007	0.12	121.63	0.53
2008	0.08	144.09	0.42
2009	0.14	149.78	0.61
2010	0.20	176.73	0.60

Table 2.7. Resultant drift potential (RDP), resultant drift direction (RDD), and directional variability (RDP/DP) for 2008 , the 2009-2009 winter season, January 2008 , and the January 27-29, 2008 storm event.

Time Period	RDP	RDD	RDP/DP
2008	0.08	144.09	0.42
Winter 2008	0.02	152.34	0.04
January 2008	0.51	203.19	0.84
January 27-29, 2008	5.35	199.47	0.94

Finally, sand rose statistics were developed for the storms producing the five highest wind speeds at station 44018 (Table 2.8). As previously mentioned, four of these storms were northeasters and one was tropical. The storms varied from two to six day events and occurred during the months of November through January. RDP ranged from 0.53-5.35, and RDD varied from north to southwest. Directional variability for storm events was intermediate to low indicating that the greatest wind magnitude was from one general direction. Storm events tend to produce high wind speeds over a relatively short duration. When the wind is above the threshold for sand movement and blowing from one general direction, relative sand movement and thus dune development and evolution can be substantial. A comparison of the RDP (0.08) for 2008 (high directional variability) to the RDP (5.35) for the January 27-29, 2008 storm event (low directional variability) elucidates this point.

Table 2.8. Resultant drift potential (RDP), resultant drift direction (RDD), and directional variability (RDP/DP) for the five storms that produced the highest recorded wind speed at station 44018 over the length of the available data record (2002-2011).

Time Period	RDP	RDD	RDP/DP
December 26-30, 2004	3.60	201.71	0.89
November 20-25, 2005	0.53	8.25	0.74
November 2-4, 2007	3.33	177.89	0.77
January 27-29, 2008	5.35	199.47	0.94
January 12-13, 2011	4.31	80.54	0.67

2.4.6 Wind Speeds, Resultant Drift Potential, and Precipitation

The full wind record for station 44018 was sorted by wind speed, and the number of hours for each wind speed was totaled (e.g., the total hours at which winds speeds were 0-0.99 m/s were determined, and so on for each wind speed). The total hours at each wind speed increases from 0-5 m/s, and declines from that point forward with increasing wind speeds. This

is shown graphically in Figure 2.17, and the wind hour curve is bell-shaped and skewed to the right. Because RDP is calculated from winds above threshold velocity, it is only at wind speeds greater than the threshold velocity that sand movement occurs. Of the 68,750 wind hours in the data record for station 44018, only 3,725 hours have winds sufficient to move sand. Values for RDP were calculated by multiplying the RDP for sample location 2 (threshold velocity of 13.659 m/s) by the number of wind hours at each wind speed above the threshold velocity. Even though the RDP is calculated by squaring the wind velocity, RDP reaches its maximum at the threshold velocity and declines with higher wind speeds because the RDP is strongly related to the percent frequency of winds in each class. Thus, Figure 2.17 shows that most sand movement occurs when the wind is just above threshold because these winds are the most frequent as shown in the wind hours curve.

A similar graph (Figure 2.18) constructed for a three-day northeaster weather event that occurred January 27-29, 2008 shows a somewhat different picture. Of the total wind hours for the storm, approximately 58% were at or greater than the threshold velocity, and rather than the relatively smooth wind hour curve for the full data record, the limited data for the storm results in a highly crenulate curve. The resulting transport is quite different to that shown in Figure 2.17. Rather than a smoothly declining curve there are peaks of transport at 15 m/s and 18 m/s, showing that at least this storm has significantly greater transport potential at high wind velocities which are sustained for some time. It is likely that storms of this kind have the capability of excavating deep bowl blowouts in the region.

Storms and other windy events may often be accompanied by high rainfall, and this will obviously reduce the actual aeolian transport. In order to assess the effect of precipitation on the calculated potential aeolian transport (as shown by the RDP), the rainfall record was examined.

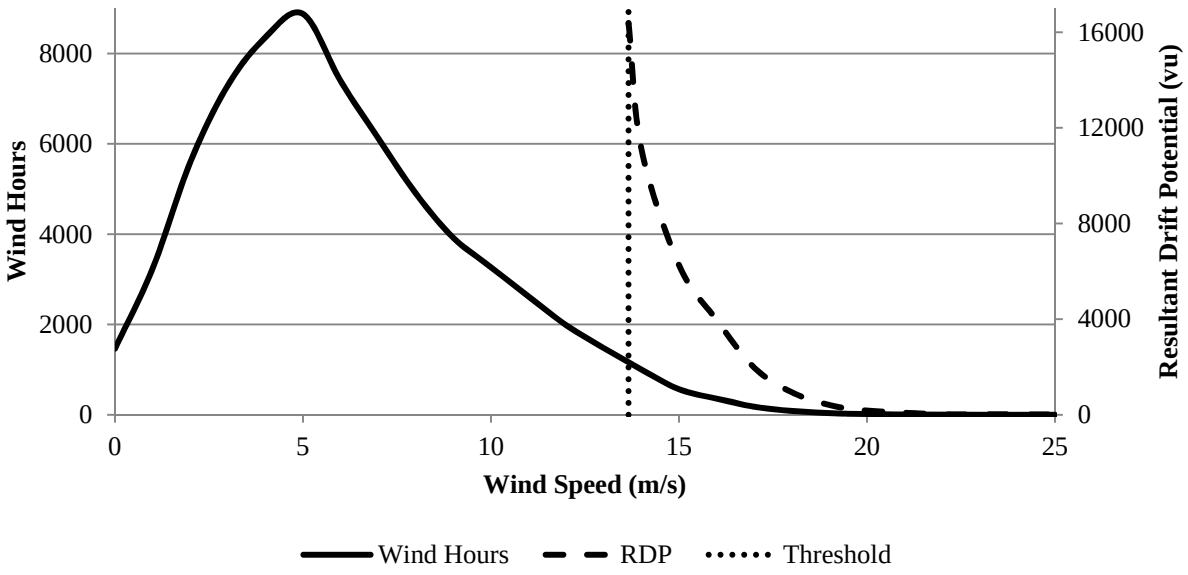

Figure 2.17. The solid black line depicts total wind hours at each given wind speed; the dotted vertical line depicts the threshold velocity at sample location 2 (as shown on Figure 2.2); and the dashed line depicts resultant drift potential at sample location 2.

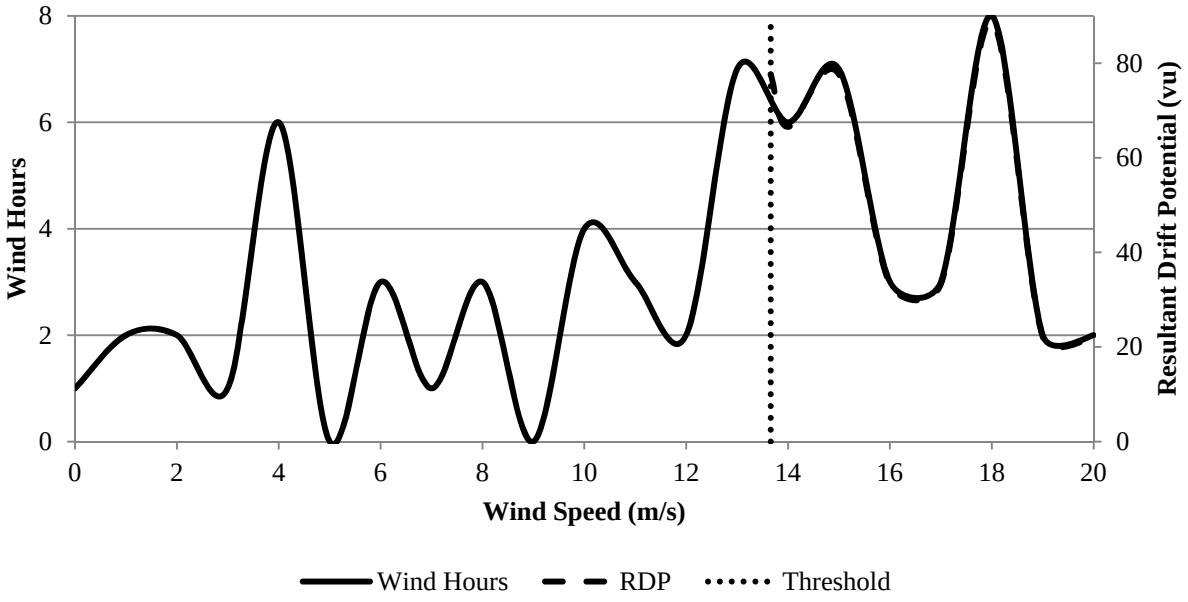

Figure 2.18. The solid line depicts total wind hours at a given wind speed; the dotted vertical line depicts the threshold velocity at sample location 2 (as shown on Figure 2.2); and the dashed black line depicts resultant drift potential at that location for a northeaster event occurring on January 27-29, 2008. The line depicting resultant drift potential follows the wind hours line exactly from the threshold wind speed through a wind speed of 20.0 m/s.

Over the 2002-2011 wind record for station 44018, 455.20 inches of precipitation occurred.

Similar to the calculation of wind hours for each wind speed, total precipitation was also

calculated for each wind speed. Though the curve for precipitation is not as smooth as that for wind hours (Figure 2.19), it is evident that greater precipitation occurs at lower wind speeds suggesting perhaps that heavier precipitation occurs before and after the highest storm winds rather than during them. Mather (1974) and Medlin, Kimball, and Blackwell (2007) indicate that wind can have a significant impact on the accuracy of rain gauge measurements, with inaccuracy increasing as wind speeds increase. Rainfall was also calculated by calendar year from 2002-2011 and by individual ten month periods that correspond to the period for which ENSO sand rose statistics were generated (see section 2.4.4). Table 2.9 indicates that total rainfall was lowest for the La Niña periods, while rainfall during El Niño and ENSO Neutral periods was not distinguishable. This suggests that RDP during drier La Niña periods could be greater than RDP during El Niño or ENSO Neutral periods, especially since RDP for the winter La Niña period was greater than RDP for the El Niño or ENSO Neutral winter periods (Table 2.5).

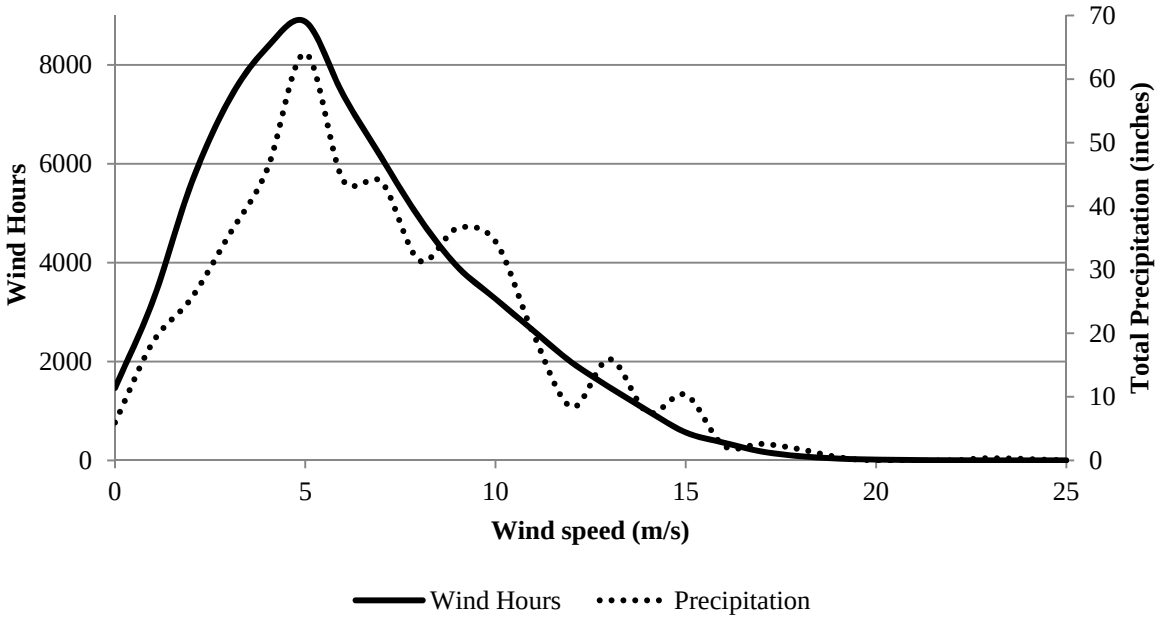

Figure 2.19. The solid line depicts the total wind hours at each given wind speed for the full length of the data record (2002-2011) at station 44018, and the dotted line depicts the total precipitation recorded over the same time period at each given wind speed.

Table 2.9. Rainfall by calendar year and by a ten month period (July-April) that corresponds to the period for which Niño sand rose statistics were generated (see section 2.4.4 for additional information).

Time Period	Rainfall (in)	Niño Event
2002	55.4	
July 2002-April 2003	51.54	El Niño
2003	68.62	
July 2003-April 2004	49.22	ENSO Neutral
2004	41.35	
July 2004-April 2005	44.57	El Niño
2005	54.8	
July 2005-April 2006	39.11	La Niña
2006	58.23	
July 2006-April 2007	42.5	El Niño
2007	44.7	
July 2007-April 2008	38.88	La Niña
2008	63.63	
July 2008-April 2009	54.56	ENSO Neutral
2009	56.13	
July 2009-April 2010	55.39	El Niño
2010	52.64	
July 2010-April 2011	40.82	La Niña
2011	57.97	

2.5 Discussion

Creating a sand rose with the mean grain size and resulting threshold velocity from one location within a blowout would not provide an accurate representation of the sand movement that could potentially occur at all locations within the blowout. The original Fryberger and Dean (1979) methodology used a mean grain size of 0.25-0.30 mm and a threshold velocity of approximately 5.96 m/s in all calculations. This grain size and threshold velocity is less than half of the grain size and threshold velocity for the *Jinx* sample location at the Provincetown study site with the smallest mean grain size (0.642 mm and 12.52 m/s threshold velocity).

Modifications of the original methodology to account for grain size at specific locations within the study site were necessary for the development of more accurate sand roses and the determination of RDP, RDD, and RDP/DP for each location.

The direction in which sand movement, and thus dune migration, occurs is in many cases a direct result of the direction from which winds at or above the threshold for sand movement occur. Based on the sand roses constructed from wind magnitudes, frequencies, and directions at station 44018, the greatest drift potential occurs over the winter months and transports sediment in the southeasterly direction. While this corresponds to the direction that the parabolic dunes near Provincetown are migrating toward (southeast), it is not the case for the *Jinx* blowout, or very many blowouts in the region. The orientation of the *Jinx* blowout, which lies on a north-south axis, does not line up with the predominant winter wind direction (from the northwest). The depositional lobe of the *Jinx* blowout is located on the north side and the erosional scarp wall on the south side. While the annual and summer wind roses for station 44018 (Figures 2.9 and 2.11, respectively) indicate that the resultant wind direction is to the east-northeast and north-northeast, respectively, the RDP resulting from these winds is minimal (i.e., winds are below the threshold velocity for sand movement) and not sufficient to result in significant blowout development and evolution. Therefore, it is likely that winds from other directions, and especially those from the west to northwest, actually promote deflation and blowout development. Hugenholtz and Wolfe (2009) and Hesp and Walker (2012b) show that winds within such bowl blowouts are characterized by complex, topographically steered, separated flows, so winds from multiple directions can affect transport and deflation within a bowl blowout despite the blowout orientation and geographical position on a slope.

2.6 Conclusion

- Wind direction and magnitude are seasonal, with winds of the greatest magnitude occurring during the winter months.
- As a result, resultant drift potential is highest during the winter period; although, RDPs discussed here do not directly take into account the effects of precipitation, temperature, vegetation, or other processes on sand movement.
- The mean grain size and resulting threshold velocity must be adjusted from that used in Fryberger and Dean (1979) so that these values are site specific. If the grain size and threshold velocity are not adjusted, the RDP has the potential to be significantly inaccurate.
- RDPs vary at specific locations within the *Jinx* blowout due to differences in grain size, with the lowest RDP being at the bottom of the deflation basin and the highest on the western rim of the blowout. This corresponds to higher grain size and threshold velocity at the bottom of the deflation basin and lower grain size and threshold velocity along the western rim of the blowout.
- The orientation of the relict and modern parabolic dunes near Provincetown appears to be explained by the predominant winter wind direction, as winter winds blow from the northwest and the dunes are migrating toward the southeast.
- Blowouts on Cape Cod are oriented in nearly every direction, consequently the orientation of the *Jinx* blowout and other blowouts on Cape Cod cannot be explained by the predominant winter wind direction; however, the wind roses for both annual and seasonal time periods clearly show the multidirectional nature of the wind. Winds above the threshold for sediment velocity occur during every season and topographic alteration and acceleration of winds can

drive sand movement in a direction that is distinctly different from the resultant wind direction at a particular time period and location.

2.7 References

Belly, P.Y., 1964. *Sand Movement by Wind*. Washington, DC: U.S. Army Corps of Engineers, Technical Memorandum 1, 38p.

Bullard, J.E., 1997. A note on the use of the Fryberger method for evaluating potential sand transport by wind. *Journal of Sediment Research*, 67(3A), 499-501.

Colucci, S.J., 1976. Winter cyclone frequencies over the eastern United States and adjacent western Atlantic, 1964-1973. *Bulletin of the American Meteorological Society*, 57, 548-553.

Davis, W.M., 1895. The outline of Cape Cod. *Proceedings of the American Academy of Arts and Sciences*, 13, 303-332.

Dolan, R. and Davis, R.E., 1992. An intensity scale for Atlantic Coast Northeast storms. *Journal of Coastal Research*, 8(4), 840-853.

Dolan, R.; Lins, H.; and Hayden, B., 1988. Mid-Atlantic coastal storms. *Journal of Coastal Research*, 4(3), 417-433.

Forman, S. L.; Sagintayev, Z.; Sultan, M.; Smith, S.; Becker, R.; Kendall, M.; and Marin, L., 2008. The twentieth-century migration of parabolic dunes and wetland formation at Cape Cod National Seashore, Massachusetts, USA: landscape response to a legacy of environmental disturbance. *The Holocene*, 18(5), 765-774.

Fryberger, S.G. and Dean, G., 1979. Dune forms and wind regime. *In*: McKee, E.D. (ed.), A *Study of Global Sand Seas: Geological Survey Professional Paper, 1025*. Washington, DC: U.S. Government Printing Office, pp. 137-150.

Giese, G.S.; Adams, M.B.; Rogers, S.S.; Dingman, S.L.; Borrelli, M.; and Smith, T.L., 2011. Coastal sediment transport on outer Cape Cod, Massachusetts: Observation and theory. *The Proceedings of the Coastal Sediments 2011* (Miami, Florida, World Scientific), pp. 2353-2365.

Giese, G.S. and Adams, M.B., 2007. Changing orientation of ocean-facing bluffs on a transgressive coast, Cape Cod, Massachusetts. *Proceedings of the Sixth International Symposium on Coastal Engineering and Science of Coastal Sediment Process* (New Orleans, Louisiana, ASCE), pp. 1142-1152.

Hesp, P.A., 2002. Foredunes and blowouts: Initiation, geomorphology and dynamics. *Geomorphology*, 48: 245-68.

Hesp, P.A., 2011. Dune Coasts. *In*: Wolanski, E. and McLusky, D.S. (eds.), *Treatise on Estuarine and Coastal Science, Volume 3*. Waltham: Academic Press, pp. 193–221.

Hesp, P.A.; Abreu de Castilhos, J.; Miot da Silva, G.; Dillenburg, S.; Martinho, C.T.; Aguia, D.; Fornari,; and M. Antunes, G., 2007. Regional wind fields and dunefield migration, southern Brazil. *Earth Surface Processes and Landforms*, 31, 561-573.

Hesp, P.A. and Walker, I.J., 2012a. Aeolian environments: Coastal dunes. *In*: Shroder, J. (Editor in Chief), Lancaster, N., Sherman, D.J., and Baas, A.C.W. (Eds.), *Treatise on Geomorphology, Volume 11, Aeolian Geomorphology*. San Diego, California: Academic Press.

Hesp, P.A. and Walker, I.J., 2012b. Three-dimensional aeolian dynamics within a bowl blowout during offshore winds: Greenwich Dunes, Prince Edward Island, Canada. *Aeolian Research*, 3, 389–399.

Hirsch, M.E.; DeGaetano, A.T.; and Colucci, S.J., 2001. An East Coast winter storm climatology. *Journal of Climate*, 14, 882-899.

Hugenholtz, C.H. and Wolfe, S.A., 2009. Form-flow interactions of an aeolian saucer blowout *Earth Surface Processes and Landforms* 34(7), 919-928.

Keim, B.D.; Muller, R.A.; and Stone, G.W. 2007. Spatiotemporal patterns and return periods of tropical storm and hurricane strikes from Texas to Maine. *Journal of Climate*, 20, 3498-3509.

Kucinski, K.J. and Eisenmenger, W.S., 1943. Sand dune stabilization on Cape Cod. *Economic Geography*, 19(2), 206-214.

Mather, J.R. 1974. Climatology: Fundamentals and Applications. New York: McGraw-Hill, 412p.

Medlin, J.M.; Kimball, S.K.; and Blackwell, K.G., 2007. Radar and rain gauge analysis of the extreme rainfall during hurricane Danny's (1997) landfall. *Monthly Weather Review*, 135,1869-1888.

Miot da Silva, G.M. and Hesp, P. 2010. Coastline orientation, aeolian sediment transport and foredune and dunefield dynamics of Mocambique Beach. *Southern Brazil. Geomorphology*, 120, 258-278.

National Oceanic and Atmospheric Administration (NOAA), 2002a. *Climatography of the United States No. 81, monthly normals of temperature, precipitation and heating and cooling days, 1971–2000, Massachusetts*. Asheville, NC: National Oceanic and Atmospheric Administration, National Climatic Data Center, 16 pp.

National Oceanic and Atmospheric Administration (NOAA), 2002b. Climatography of the U.S. No. 81 - Supplement # 3Maps of Annual 1961-1990 Normal Temperature, Precipitation and Degree Days. URL: http://www.ncdc.noaa.gov/oa/documentlibrary/clim81supp3/clim81 .html; accessed on September 9, 2012.

Pearce, K.I. and Walker, I.J., 2005. Frequency and magnitude biases in the "Fryberger" model, with implications for characterizing geomorphically effective winds. *Geomorphology*, 68, 39-55.

Poppe, L.J.; Eliason, A.H.; and Hastings, M.E., 2004. A visual basic program to generate sediment grain-size statistics and to extrapolate particle distributions. *Computers and Geosciences*, 30 (7), 791-795.

Sloss, C. R.; Shepherd, M.; and Hesp, P., 2012. Coastal dunes: Geomorphology. *Nature Education Knowledge*, 3(3):2.

Zingg, A.W., 1953. Wind tunnel studies of the movement of sedimentary material. Proceedings 5th Hydraulics Conference, Bulletin, volume 34. Institute of Hydraulics, Iowa City, pp. 111-135.

CHAPTER 3: TECHNIQUES TO DERIVE WIND SPEED AND WAVE HEIGHT QUANTILE ESTIMATES: CONSIDERATIONS FOR RESTORATION IN COASTAL LOUISIANA

3.1 Introduction

According to Penland, Boyd, and Suter (1988), the northern coast of the Gulf of Mexico is a storm-dominated environment i.e., tropical and extratropical events result in significant impacts to the system that otherwise experiences low energy levels resulting from wind and wave processes. However, during the passage of winter cold fronts (September through May), and hurricanes and tropical storms (June through November), conditions can change substantially. The mean deep water wave conditions off the Louisiana coast are characterized by wave heights of 1 m, wave periods of 5-6 seconds, and dominant wave approach from the southeast (Penland, Boyd, and Suter, 1988). Local average wave heights are approximately 60 cm, and wave heights associated with frontal systems may reach 2-3 m (Ritchie and Penland, 1988). Furthermore, hurricanes can produce wave heights in the Gulf of Mexico greater than 17.9 m (Stone *et al*., 2005).

During fair weather conditions and before the passage of cold fronts, southerly winds impact the Gulf side of the barrier islands, while following the passage of cold fronts (extratropical storms), waves produced by northerly winds impact the bay side of barriers causing erosion of the marsh platform. The passage of cold fronts occurs approximately 10-30 times per year, while hurricanes occur approximately every 4 years (Ritchie and Penland, 1988). More recent estimates indicate that hurricane return periods along coastal Louisiana range from 7 years at Boothville, LA to 15 years at Cameron, LA (Keim, Muller, and Stone, 2007). In the data sets analyzed, hurricane wind speeds were measured as high as 34.41 m/s (76.97 miles per hour (mph); measured for Hurricane Katrina at CSI5; CSI5 is located on a platform in Terrebonne

Bay), while wind speeds from cold fronts were measured as high as 23.1 m/s (51.67 mph; measured on Grand Isle at GDIL1 on March 13, 1993; measurement taken 9.4 m above site elevation).

The design of coastal restoration projects is often based on analyses of regional and local coastal processes, including wave heights and wind speeds generated by storm events. Wave heights are especially important in determining the necessary elevation to construct barrier island dune systems that should be high and wide enough to avoid or minimize breaching or overtopping of the barrier island due to tropical or extratropical storm events and associated storm surges (Stone and Liu, 2005; Stone *et al*., 1993; Williams, Penland, and Sallenger, 1992). They are also important in determining appropriate designs for other restoration projects that are built along the coastline, including hard protection features (e.g., rock breakwaters that due to their location would likely be subjected to extreme wave events). Wind speed is another important process to analyze as it contributes to wave setup before and during storms. Based on the desired design life of a restoration project, a 'design storm' is commonly determined (e.g., a 25-year design storm may be used to design a project that will have an expected 20-year life). Restoration projects are then designed to withstand the coastal processes that are expected to result from the occurrence of the design storm. Other factors that may be included in the design storm analysis are currents, water levels, tides, land loss, and sediment transport rates (T. Baker Smith and Moffatt & Nichol, 2007).

Various techniques have been used to determine quantile estimates for extreme events. Weather Bureau Technical Paper No. 40 used the Gumbel distribution to determine quantile estimates for heavy rainfall events in the United States (Hershfield, 1961). Wilks (1993) found that the Beta-P distribution best represented partial duration series precipitation data in the

northeastern and southeastern United States. Using a regional approach, Huff and Angel (1992) developed a regression method to determine quantile estimates for heavy rainfall events in the Midwestern United States, and Faiers, Keim, and Muller (1997) developed a similar method to do the same for the southcentral United States (the Southern Regional Climate Center regression method). Both regression methods use the Weibull plotting position formula; however, the Huff Angel regression is plotted on a log-log scale while the Southern Regional Climate Center regression is plotted on a log-linear scale.

The Gumbel, Beta-P, and Weibull (or a variation thereof) methods have also been used to model annual extreme gust wind speeds across the United States (Cheng and Yeung, 2002), to estimate 50-year extreme wave heights in the German Bight (Emeis and Turk, 2009), to predict extreme waves in Kuwaiti territorial waters (Neelamani, Al-Salem, and Rakha, 2007), and to model extreme wind speeds in the Netherlands (Escalante-Sandoval, 2008). Therefore, the application of these techniques seems appropriate for deriving quantile estimates for wind speed and wave heights in coastal Louisiana.

The focus of this paper is to derive and compare wind speed and wave height quantile estimates for coastal Louisiana using the Gumbel, Beta-P, Huff Angel, and Southern Regional Climate Center methods, and to then establish the best fit distribution for the data sets. To accomplish this, wind speed and wave height data were collected from monitoring stations across coastal Louisiana and processed based upon the procedures outlined below.

3.2 Methods

The study area for this paper is coastal Louisiana from south of Cameron Parish in western Louisiana to the Chandeleur Islands in the east (Figure 3.1). Many coastal restoration projects have been constructed across this region of coastal Louisiana, and many more projects

are in various stages of planning, engineering and design, construction, and operation, maintenance, and monitoring (CPRA, 2012a; CPRA, 2012b). Restoration project types include barrier island restoration, shoreline protection, bankline stabilization, marsh creation, ridge creation, diversions, and others.

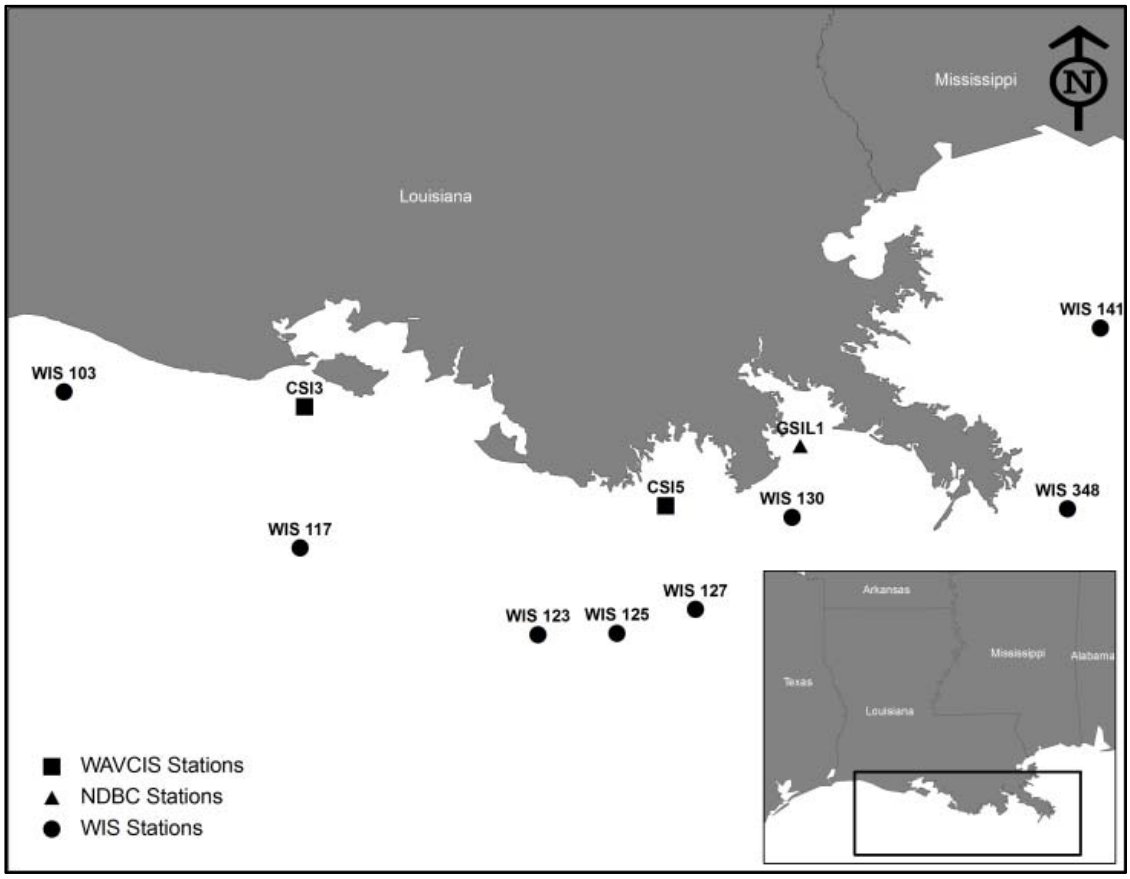

Figure 3.1. Coastal Louisiana study location showing the wind speed and wave height monitoring station locations.

3.2.1 Wind Speed and Wave Height Data

Wind speed and wave height data were collected from three station types in the study area: National Data Buoy Center (NDBC), Wave Information System (WIS), and Wave and Current Information System (WAVCIS). The National Data Buoy Center (NDBC) designs, develops, operates, and maintains a network of data collecting buoys and coastal stations (NDBC, 2009). Wind speed data are available from these stations and are measured in m/s

averaged over a two-minute period and reported hourly. The US Army Corps of Engineers Research and Development Center performed a hindcast of waves and winds for 1956-1976, 1976-1994, and 1990-1999 for locations along the Louisiana coast (USACE-WIS, 2003). Hourly averaged wind speed in m/s and significant wave height in meters are available from 1980-1999 for these WIS stations. The Coastal Studies Institute at Louisiana State University operates eight WAVCIS stations to provide real-time meteorological conditions across the Louisiana coast (LSU-WAVCIS, 2009). Hourly averaged wind speed and wave height data are available for these stations.

Wind speed data were collected from two NDBC stations on Grand Isle, GDIL1 and GISL1. GISL1 replaced GDIL1 following Hurricane Katrina in 2005. The combined data record for these stations was 26 years (1984-2010). Wind speed and wave height data were collected from eight WIS stations, from south of Cameron to east of the Chandeleur Islands. The record length for all WIS stations was 20 years, from 1980-1999. Wind speed and wave height data were also collected from two WAVCIS stations, one south of Marsh Island (CSI3) and one southeast of Whiskey Island (CSI5). The record length was 10 years for CSI3 wind data and 8 years for wave data and 10 years for CSI5 wind and wave data. The location of each of the twelve stations is shown in Figure 3.1.

3.2.2 Partial Duration Series

For each wind and wave data set analyzed, the most extreme one hour wind speed and wave height events were extracted from the available data record. The number of events extracted was equal to the length of the record (in years); this type of data set is known as a partial duration series (PDS) and is recommended by Dunne and Leopold (1978) for this type of research. Each extreme event record in the PDS was independent, meaning that only one record

(the largest) was extracted for each storm event. To statistically test whether there was a significant difference in the magnitudes of extreme events by weather type, each record in the PDS was assigned to one of three weather types – tropical (TR), frontal (FR), or airmass thunderstorm (AT) as utilized in Faiers, Keim, and Hirschboeck (1994) and Keim and Faiers (1996). The Kruskal-Wallace (K-W) test (a one-way nonparametric analysis of variance) was run to determine whether a mixed distribution existed for each individual data set. Mixed distributions were defined by Hirschboeck (1988, page 43) as 'multiple populations in a hydrologic time series.' The majority of wind speed data sets documented above were determined to have mixed distributions resulting from significant differences between the magnitudes of tropical events as compared to airmass thunderstorm events (WIS 141; K-W statistic = 0.28; p. = 0.009) and between the magnitudes of airmass thunderstorm events as compared to frontal events (WIS 141; K-W statistic = 0.59; p. = 0.009). As such, rather than deriving one quantile estimate for the data from each station, partial duration series of events for each weather type were compiled for each station, and quantile estimates were derived for each of the three weather types independently.

3.2.3 Probability and Regression Methods

Quantile estimates were derived for each extreme wind speed and wave height PDS using four distributions: the Gumbel and Beta-P probability distributions and the Huff Angel and Southern Regional Climate Center (SRCC) regression methods. After determining the wind speed and wave height quantile estimates for each of the stations, the Kolmogorov-Smirnov (K-S) association test was used to determine which of the distributions produced the best fit for each data set. The K-S test compares the expected number of events for each return period to the number of events estimated for each return period by the four distributions discussed. The

expected number of events was determined by dividing the length of the data record by the return period (i.e., for a record length of 25 years and a return period of 5 years, the expected number of events would be 5). The non-parametric K-S test does not account for the magnitude of each event.

3.3 Results

3.3.1 Identification of Best Fit Method

Using the procedure described in Keim and Faiers (2000), tables similar to Tables 3.1 and 3.2 below were generated for each return period to provide a method for ranking the 'fit' of each of the techniques used to derive quantile estimates for each station and weather type. A smaller K-S statistic indicates a distribution with a better fit for the data set. The highest ranked distribution is the one with the best fit (smallest K-S statistic) of the expected number of events compared to the number of events that occurred based on the quantile estimates from each of the four distributions. Of the distributions analyzed, no one distribution provided the best fit for all of the data sets. Results of the K-S test indicate that the Huff Angel regression method provides the best fit distribution for the wind data sets analyzed, as well as for the FR and AT wave data sets. The Huff Angel and Gumbel methods provide the best fit for the TR wave data sets. The SRCC regression distribution and the Beta-P probability distribution did not provide the best fit distribution for any of the data sets. For wind speed quantile estimates for AT, FR, and TR weather types and wave height quantile estimates for AT and FR, the Huff Angel method produced the lowest sum of rankings and the highest undisputed number one rankings and number one rankings including ties. For the wave quantile estimates for TR, the SRCC provided the lowest sum of rankings; while, Huff Angel and Gumbel tied with the highest undisputed number one rankings and number one rankings including ties.

Table 3.1. Ranking of airmass thunderstorm (wind speed) quantile estimate-producing techniques for coastal Louisiana stations. Shading indicates the highest ranked or best fit distribution(s) for each station. For stations with tied rankings, the mid-point of the rank order was used. If the tie was for first place, the tied rankings are highlighted.

Location	H-A	SRCC	Gumbel	Beta-P
WIS 103	2.5	2.5	4	1
WIS117	1	2	3	4
WIS 123	1	2	4	3
WIS 125	1	3	4	2
WIS 127	1	2	4	3
WIS 130	1	2	4	3
WIS 348	1	2	4	3
WIS 141	1	2	4	3
CSI3	3	3	1	3
CSI5	2.5	2.5	2.5	2.5
GDIL1/GISL 1	1	2	4	3
Sum	16	25	38.5	30.5
Undisputed No. 1s	8	0	1	1
No. 1s including ties	9	1	1	1

Table 3.2. Ranking of airmass thunderstorm (wave height) quantile estimate-producing techniques for coastal Louisiana stations. Shading indicates the highest ranked or best fit distribution(s) for each station. For stations with tied rankings, the mid-point of the rank order was used. If the tie was for first place, the tied rankings are highlighted.

Location	H-A	SRCC	Gumbel	Beta-P
WIS 103	1	2	4	3
WIS117	2	1	4	3
WIS 123	1.5	1.5	4	3
WIS 125	3	2	4	1
WIS 127	1.5	1.5	3	4
WIS 130	1	4	3	2
WIS 348	1	2.5	4	2.5
WIS 141	2	2	4	2
CSI3	3.5	3.5	1	2
CSI5	3.5	3.5	2	1
Sum	20	23.5	33	23.5
Undisputed No. 1s	3	1	1	2
No. 1s including ties	6	4	1	3

3.3.2 Quantile Estimates for Wind Speed and Wave Height

Quantile estimates for wind speed and wave height were determined for the 2, 5, 10, 25, 50, and 100-year return periods. The highest five-year quantile estimates for wind speed derived in this study are 18.6 m/s, 20.5 m/s, and 30.0 m/s for AT, FR, and TR events, respectively. Similarly, the highest twenty-five year wind speed estimates are 21.0 m/s for AT events, 24.0 m/s for FR events and 50.0 m/s for TR events. The highest five-year quantile estimates for wave height are 4.7 m, 5.2 m, and 7.0 m for AT, FR, and TR events, respectively. The highest twenty-five year wave height estimates are 5.5 m for AT events, 6.9 m for FR events and 16 m for TR events. Wind speed and wave height quantile estimates are similar for all events at the two and five-year return periods, but wind speeds and wave heights between storm types begin to diverge at the ten-year return period. They are much higher for TR events at twenty-five year return periods than they are for AT and FR events and this trend continues for 50 and 100-year return periods. Tables 3.3 and 3.4 report the wind speed and wave height quantile estimates for 2, 5, 10, 25, 50, and 100-year return periods for all data sets used in this study. Figure 3.2 shows the variation in wind speed, and Figure 3.3 shows the variation in wave height quantile estimates by distribution for WIS 141. Quantile estimates for both wind speed and wave height are similar for all four distributions for the 2, 5, and 10-year return periods but begin to separate for the 25, 50, and 100-year return periods.

3.4 Discussion

It should be noted that 50 and 100-year return periods for all stations should be regarded as highly uncertain due to the limited data record from which they were determined. Additionally, only 8-10 years of data have been collected at the CSI stations. Examination of wind speed graphs for each return period indicate a noticeable increase in wind speed magnitude

Table 3.3. Wind speed quantile estimates including the return period and magnitude for airmass thunderstorm, frontal, and tropical weather events.

Wind Speed Quantile Estimates for Airmass Thunderstorm Events											
Return Period	WIS 103	WIS 117	CSI 3	WIS 123	WIS 125	CSI 5	WIS 127	WIS 130	GDIL	WIS 348	WIS 141
2 year	16.8	16.2	15.1	15.7	15.8	17.2	15.8	15.5	17.0	15.6	16.0
5 year	18.5	17.4	15.7	17.0	17.0	18.6	17.5	16.6	18.0	17.3	17.5
10 year	19.5	19.0	17.0	18.2	18.2	19.0	18.5	18.0	20.0	18.2	19.0
25 year	21.0	20.0	18.0	20.0	20.0	20.5	20.0	20.0	22.0	20.0	21.0
50 year	22.5	21.5	19.0	21.5	21.5	22.0	21.5	21.5	23.0	22.0	22.5
100 year	23.5	22.5	19.7	23.0	22.5	23.0	23.0	23.0	25.0	23.0	24.0
Wind Speed Quantile Estimates for Frontal Events											
Return Period	WIS 103	WIS 117	CSI 3	WIS 123	WIS 125	CSI 5	WIS 127	WIS 130	GDIL	WIS 348	WIS 141
2 year	18.0	17.1	17.6	16.5	16.4	19.5	16.3	16.1	17.0	16.3	16.7
5 year	19.0	17.8	19.0	17.5	17.4	20.5	17.2	17.0	18.2	17.3	17.5
10 year	19.8	18.6	20.0	18.0	17.8	21.0	17.8	17.8	19.6	18.2	18.6
25 year	21.5	19.2	21.5	19.5	18.6	24.0	18.6	19.0	21.0	19.0	19.6
50 year	22.5	20.0	24.0	19.5	19.5	25.0	19.8	19.5	21.5	20.0	20.5
100 year	24.0	21.0	25.0	20.0	20.5	26.5	20.5	20.1	23.0	21.0	22.0
Wind Speed Quantile Estimates for Tropical Events											
Return Period	WIS 103	WIS 117	CSI 3	WIS 123	WIS 125	CSI 5	WIS 127	WIS 130	GDIL	WIS 348	WIS 141
2 year	16.0	14.3	20.0	13.6	15.0	22.0	14.0	13.3	15.6	15.0	13.6
5 year	19.5	18.5	28.5	19.0	20.0	30.0	19.5	20.0	21.5	20.0	20.0
10 year	23.0	22.0	35.0	24.5	25.0	39.0	25.5	26.3	27.5	26.8	26.0
25 year	30.0	27.5	48.5	31.5	35.0	50.0	35.0	37.5	39.0	38.0	37.5
50 year	36.5	32.5	60.0	40.0	46.0	60.5	45.0	51.0	50.0	50.0	50.0
100 year	45.0	39.5	77.0	50.0	59.8	78.0	57.0	69.5	63.0	65.0	65.0

Table 3.4. Wave height quantile estimates including the return period and magnitude for airmass thunderstorm, frontal, and tropical weather events.

Wave Height Quantile Estimates for Airmass Thunderstorm Events										
Return Period	WIS 103	WIS 117	CSI 3	WIS 123	WIS 125	CSI 5	WIS 127	WIS 130	WIS 348	WIS 141
2 year	3.0	3.7	1.1	3.6	3.6	1.7	3.5	3.3	4.3	3.3
5 year	3.3	4.1	1.2	3.9	3.9	1.8	3.8	3.6	4.7	3.7
10 year	3.6	4.5	1.3	4.2	4.1	2.0	4.0	3.8	5.0	3.9
25 year	3.8	5.0	1.4	4.6	4.4	2.2	4.3	4.0	5.5	4.2
50 year	4.1	5.3	1.5	4.8	4.7	2.4	4.6	4.2	5.9	4.5
100 year	4.4	5.9	1.5	5.2	4.9	2.6	4.9	4.5	6.3	4.8
Wave Height Quantile Estimates for Frontal Events										
Return Period	WIS 103	WIS 117	CSI 3	WIS 123	WIS 125	CSI 5	WIS 127	WIS 130	WIS 348	WIS 141
2 year	3.4	3.8	1.3	3.9	4.0	1.9	4.0	3.8	4.6	4.0
5 year	3.9	4.3	1.6	4.3	4.5	2.1	4.3	4.1	5.2	4.5
10 year	4.2	4.7	1.8	4.8	4.9	2.3	4.7	4.4	6.0	4.9
25 year	4.9	5.1	2.0	5.1	5.2	2.4	5.1	4.8	6.9	5.5
50 year	5.3	5.5	2.2	5.7	5.8	2.6	5.5	5.1	7.8	6.0
100 year	5.9	5.9	2.5	6.0	6.1	2.8	5.9	5.5	8.5	6.5
Wave Height Quantile Estimates for Tropical Events										
Return Period	WIS 103	WIS 117	CSI 3	WIS 123	WIS 125	CSI 5	WIS 127	WIS 130	WIS 348	WIS 141
2 year	3.0	3.4	1.9	3.7	3.9	2.5	3.8	3.4	4.5	3.7
5 year	4.0	4.7	3.5	4.9	5.3	2.9	5.4	5.0	7.0	5.4
10 year	5.0	5.7	5.8	6.0	6.8	3.2	7.1	6.9	10.0	7.3
25 year	6.8	7.1	12.0	7.9	9.1	3.7	11.0	10.0	16.0	12.0
50 year	8.5	8.9	19.0	9.9	12.5	4.1	14.0	14.0	23.0	16.0
100 year	10.5	10.5	30.0	12.5	16.0	4.5	18.0	18.0	32.0	20.0

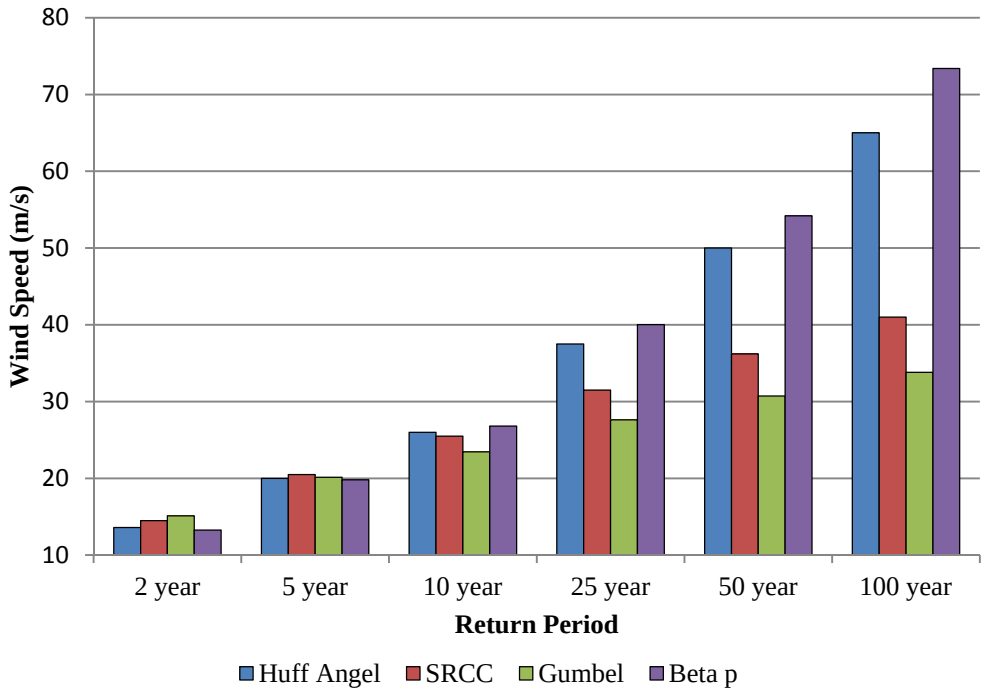

Figure 3.2. Comparison of quantile estimates (return period and magnitude) for tropical events for the Huff Angel, SRCC, Gumbel, and Beta P distributions for wind speeds for the WIS 141 station.

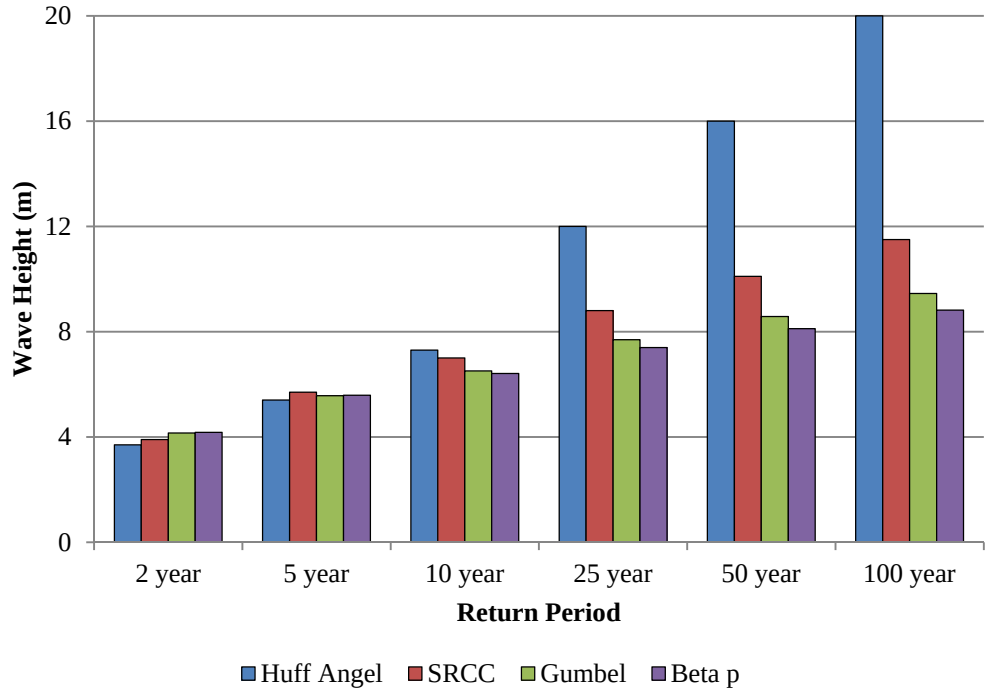

Figure 3.3. Comparison of quantile estimates (return period and magnitude) for tropical events for the Huff Angel, SRCC, Gumbel, and Beta P distributions for wave heights for the WIS 141 station.

for the two CSI stations compared to other stations (Figures 3.4 and 3.5). The likely reason for this is the occurrence of hurricanes Katrina, Rita, Gustav, and Ike within the data record that would be smoothed out with a longer record as appears to be the case with other stations analyzed (Figures 3.4 and 3.6). When only WIS stations are graphed (Figures 3.5 and 3.7), it appears that there is an increasing linear/geographical trend in TR quantile estimates from station WIS 117 (south of Marsh Island) to station WIS 130 (south of Grand Isle), which may be related to increasing tropical storm and hurricane strikes along this section of coast (see Keim *et al*., 2007). The same does not hold true for FR and AT quantile estimates. Graphs of wave height quantile estimates also show noticeable differences in magnitude for the CSI stations compared to other stations, although these differences do not show the same pattern as those for wind speed (Figures 3.8 and 3.10). The wave height graphs both for all stations and for WIS stations only indicate increasing linear trends for TR, FR, and AT quantile estimates from west to east (Figures 3.9-3.11).

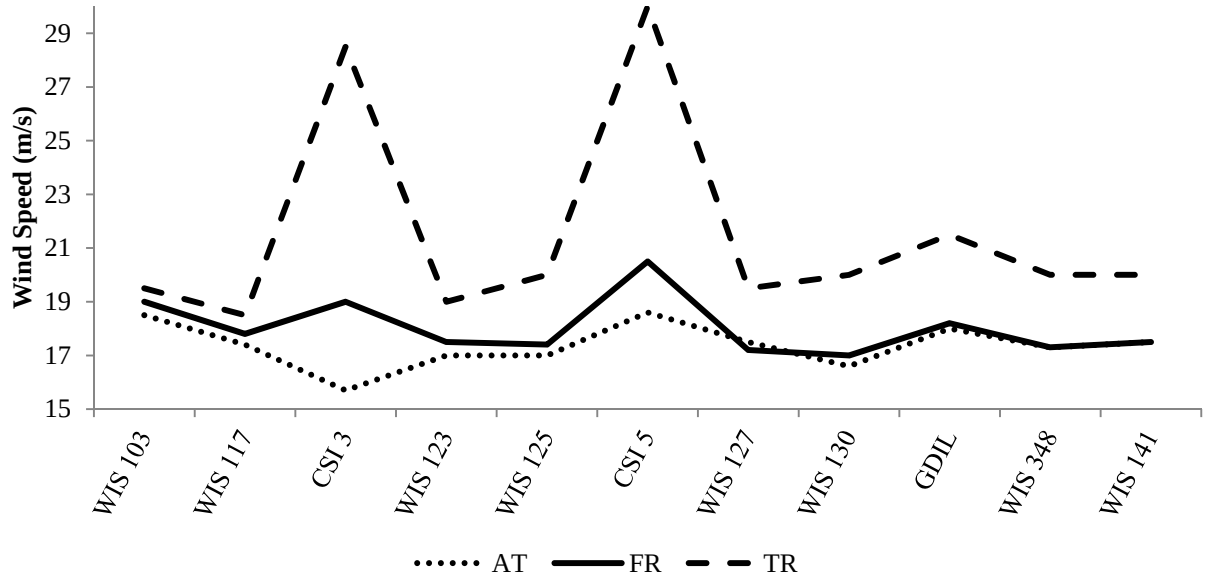

Figure 3.4. Five year wind speed quantile estimates for airmass thunderstorm (AT), frontal (FR), and tropical (TR) weather events for all stations. Stations are arranged from west to east.

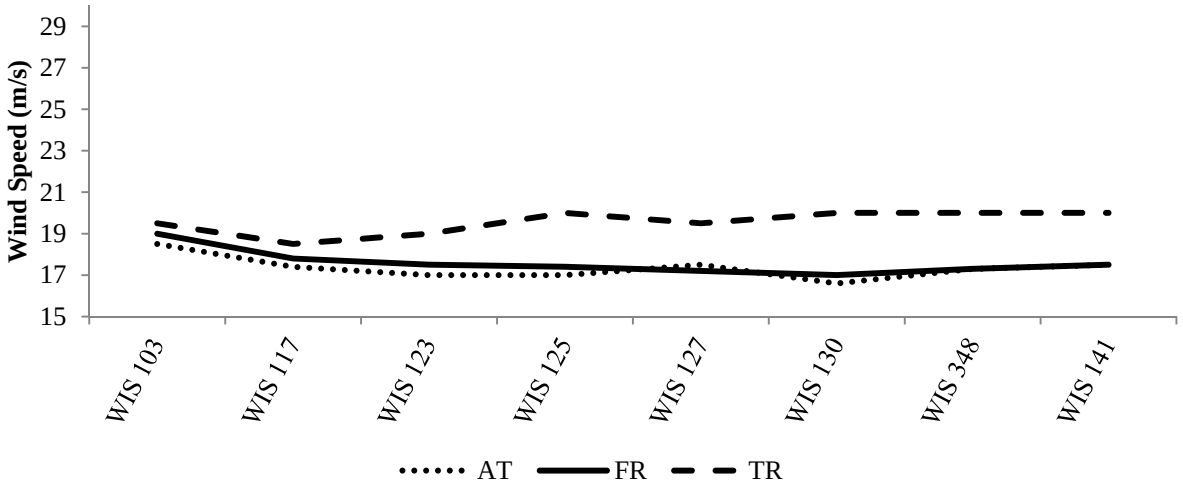

Figure 3.5. Five year wind speed quantile estimates for airmass thunderstorm (AT), frontal (FR), and tropical (TR) weather events for WIS stations only. Stations are arranged from west to east.

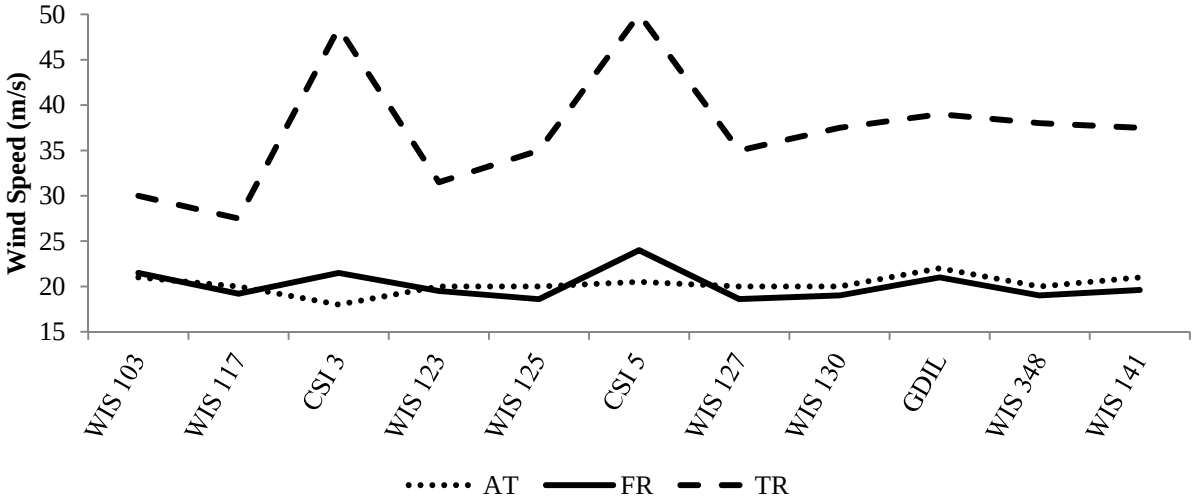

Figure 3.6. Twenty-five year wind speed quantile estimates for airmass thunderstorm (AT), frontal (FR), and tropical (TR) weather events for all stations. Stations are arranged from west to east.

Due to the length of the data records analyzed for this paper, it is not possible to say whether the 50 and 100-year return period estimates produced by the methods discussed are under or overestimations; however, this remains a possibility. Wilks (1993) noted that the Gumbel distribution underestimated magnitudes associated with larger precipitation amounts (the right tail of the distribution) in the northeastern United States, and this seemed to be the case

with the analysis presented here as well. Keim and Faiers (2000) found that the Gumbel distribution produced the smallest estimates for 20, 50, and 100-year return periods for heavy rainfall in arid and mountainous environments. For the analysis completed here, either the Gumbel or Beta-P distribution produced the smallest estimates for 25, 50, and 100-year return periods for all three storm types for both wind speed and wave height data sets (with the exception of CSI 3 for wind speed during AT storm events).

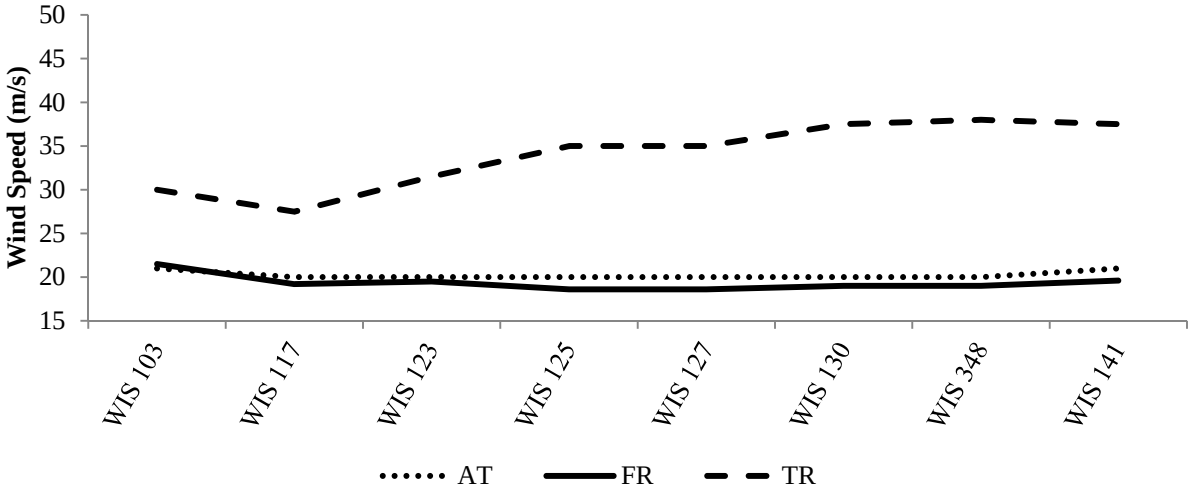

Figure 3.7. Twenty-five year wind speed quantile estimates for airmass thunderstorm (AT), frontal (FR), and tropical (TR) weather events for WIS stations only. Stations are arranged from west to east.

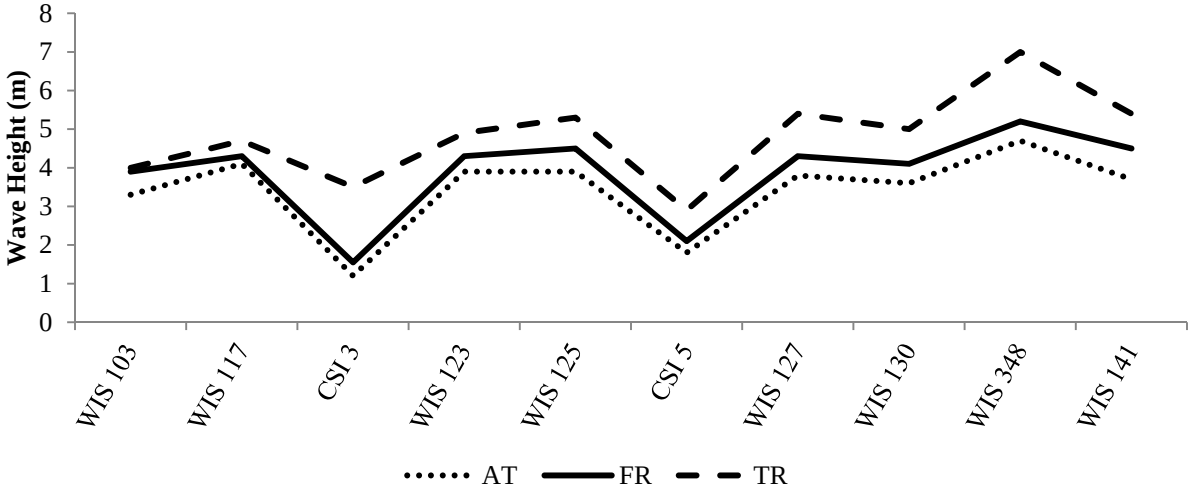

Figure 3.8. Five year wave height quantile estimates for airmass thunderstorm (AT), frontal (FR), and tropical (TR) weather events for all stations. Stations are arranged from west to east.

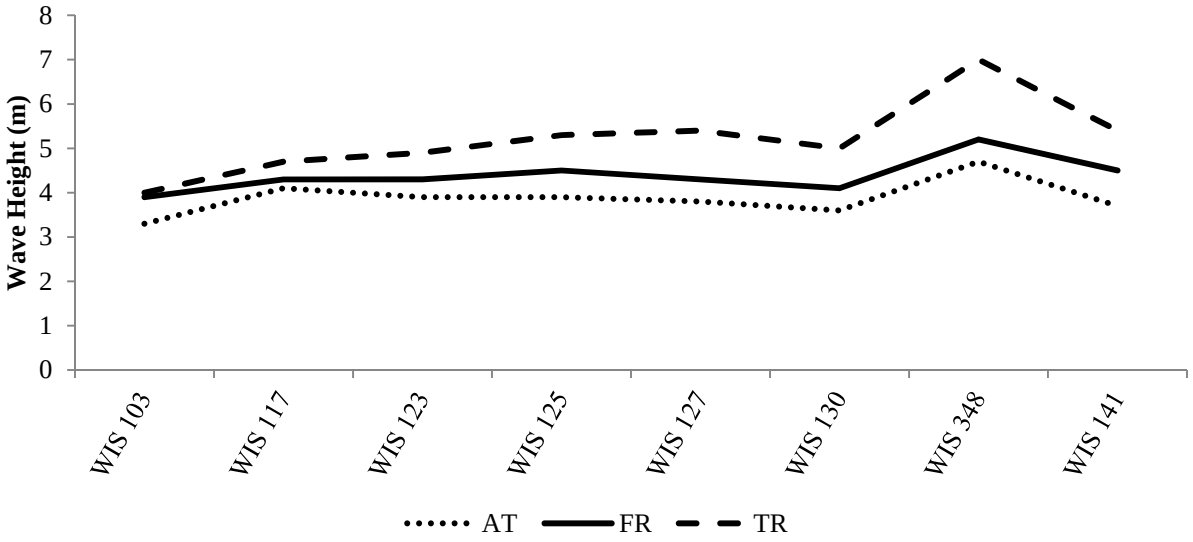

Figure 3.9. Five year wave height quantile estimates for airmass thunderstorm (AT), frontal (FR), and tropical (TR) weather events for WIS stations only. Stations are arranged from west to east.

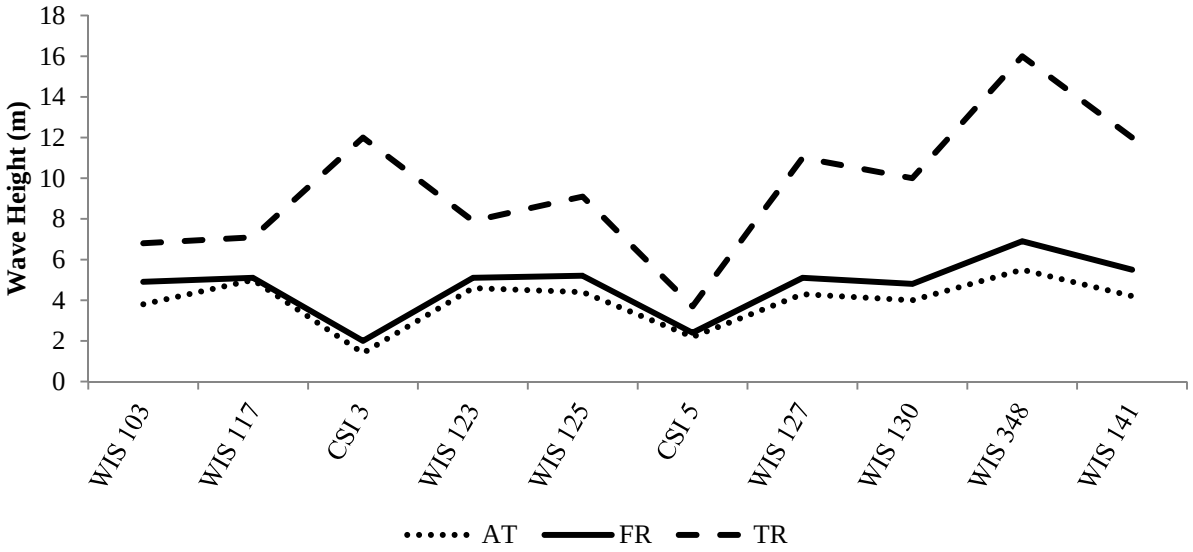

Figure 3.10. Twenty-five year wave height quantile estimates for airmass thunderstorm (AT), frontal (FR), and tropical (TR) weather events for all stations. Stations are arranged from west to east.

The majority of stations from which these wind speed and wave height quantile estimates were derived are in the nearshore and offshore environments. Engineering and design of restoration projects that are nearest to the coast, as opposed to those further inland and away from the direct effects of the open Gulf of Mexico, would benefit the most from this analysis.

Louisiana's Comprehensive Master Plan for a Sustainable Coast (CPRA, 2012a) lists a significant number of barrier island restoration, ridge restoration, marsh creation, shoreline protection, and oyster barrier reef creation projects that are on or just adjacent to Louisiana's coastline. While engineering and design of the majority of these projects has not begun, ensuring the successful creation and sustainability of these projects will depend in part on the magnitude and frequency of wind speeds and wave heights that they are able to withstand. Additional coastal processes such as sea level rise, subsidence, storm intensity, and sediment availability (Campbell, Benedet, and Thompson, 2005; Georgiou, FitzGerald, and Stone, 2005) also need to be carefully considered as these projects move beyond the planning phase.

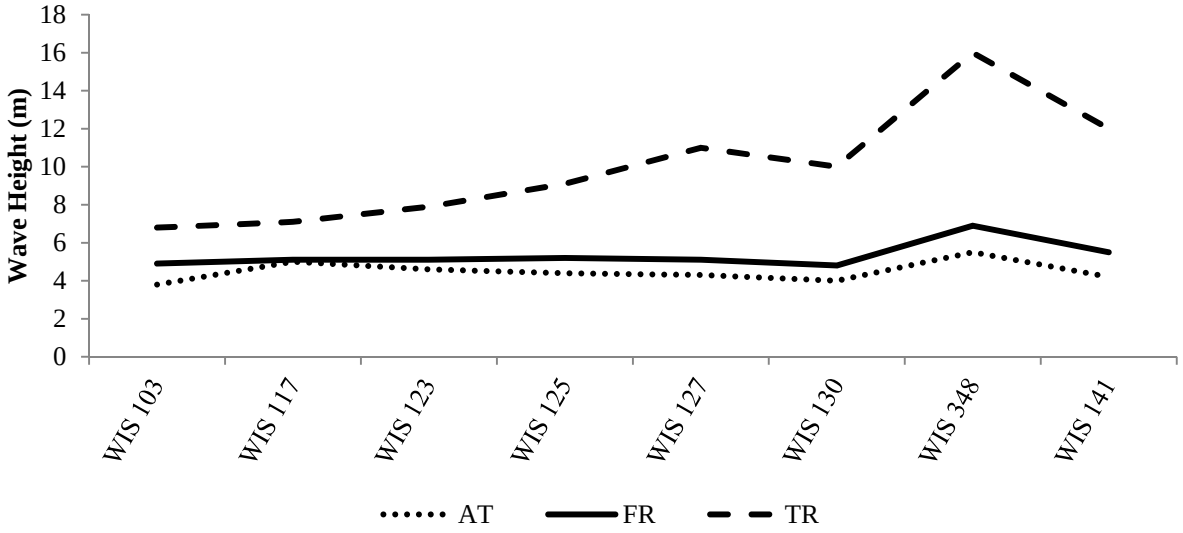

Figure 3.11. Twenty-five year wave height quantile estimates for airmass thunderstorm (AT), frontal (FR), and tropical (TR) weather events for WIS stations only. Stations are arranged from west to east.

3.5 Conclusion

The majority of restoration projects in coastal Louisiana have been designed for a 20-year project life; however, as large-scale restoration planning efforts for coastal Louisiana intensify, projects are being designed to remain on the landscape for 50 years or more. The intent of project design is to understand the processes that occur as a result of tropical, frontal, and airmass

thunderstorm weather events and accurately estimate the impacts of these weather events on the project. As such, this paper provides a baseline for determining the potential return periods of high wind and wave events. One limitation of these quantile estimates is the short records on which they are based, but the estimates can be updated as more data become available.

Various types of probability distributions are commonly used to determine the characteristics (i.e., wind speeds, wave heights, etc.) of a design storm for engineering and design of coastal restoration projects. This study provides a first attempt at estimating the magnitude and return period of wind speed and wave heights resulting from tropical, frontal, and airmass thunderstorm events across coastal Louisiana. Estimated wind speeds for AT events range from 18.0-22.0 m/s for the twenty-five year return period to 19.0-23.0 m/s for the fifty year return period. Wind speed estimates for these return periods are similar for FR events, with a range of 18.6-24.0 m/s for the twenty-five year return period and 19.5-25.0 m/s for the fifty year return period. Estimated wind speeds for TR events are much greater than those for AT and FR events, with a wind speed range of 30.0-50.0 m/s for the twenty-five year return period and a range of 32.5-60.5 m/s for the fifty year return period. For the twenty-five year return period, wave heights ranged from 1.4-5.5 m for AT events to 2.0-6.9 m for FR events to 3.7-16.0 m for TR events. By contrast, wave height estimates for the fifty year return period ranged from 1.5-5.9 m for AT events to 2.2-7.8 m for FR events to 4.1-23.0 m for TR events.

Future research for deriving quantile estimates for restoration project planning and design might consider the following:

- analysis of wave height and wind speed data for future coastal restoration projects should include use of other methods besides the Gumbel and Beta-P distributions for deriving quantile estimates;

- although the Huff Angel regression method produced the best fit for the majority of the data sets analyzed for coastal Louisiana, to apply this same methodology to other areas in the United States or the world, it may be best to examine multiple types of distributions for the specific application before deciding on which to use for a project in a particular location;
- quantile estimates derived from tropical events (not airmass thunderstorm or frontal events) should be considered for use in determining the optimal design of a restoration project built along the Louisiana coastline, as the effects of winds and waves (generated by tropical events) on coastal landscapes should be accounted for in the design of restoration projects;
- because wind speed and wave height quantile estimates are shown to vary based on location within coastal Louisiana as well as the length of the data record, care should be taken in selecting the data from which quantile estimates are derived.

3.6 References

Campbell, T.; Benedet, L.; and Thomson, G., 2005. Design considerations for barrier island nourishments and coastal structures for coastal restoration in Louisiana. *Journal of Coastal Research*, 44, 186-202.

Cheng, E. and Yeung, C., 2002. Generalized extreme gust wind speeds distributions. *Journal of Wind Engineering and Industrial Aerodynamics*, 90, 1657-1669.

Coastal Protection and Restoration Authority (CPRA), 2012a. *Fiscal Year 2013 Annual Plan: Integrated Ecosystem Restoration and Hurricane Protection in Coastal Louisiana*. Baton Rouge, Louisiana: Coastal Protection and Restoration Authority, 212p.

Coastal Protection and Restoration Authority of Louisiana (CPRA), 2012b. *Louisiana's Comprehensive Master Plan for a Sustainable Coast*. Baton Rouge, Louisiana: Coastal Protection and Restoration Authority of Louisiana, 188p.

Dunne, T. and Leopold, L.B., 1978. *Water in Environmental Planning.* San Francisco, California: W.H. Freeman and Company, 818p.

Emeis, S. and Turk, M., 2009. Wind-driven wave heights in the German Bight. *Ocean Dynamics*, 59, 463-475.

Escalante-Sandoval, C., 2008. Bivariate distribution with two-component extreme value marginals to model extreme wind speeds. *Atmosfera*, 21(4), 373-387.

Faiers, G.E.; Keim, B.D.; and Hirschboeck, K.K., 1994. Synoptic evaluation of frequencies and intensities of extreme three- and twenty-four-hour rainfall in Louisiana. *The Professional Geographer*, 46(2), 156-163.

Faiers, G.E.; Keim, B.D.; and Muller, R.A., 1997. Rainfall Frequency/Magnitude Atlas for the South-Central United States. Baton Rouge, Louisiana: Geoscience Publications, *Southern Regional Climate Center Technical Report 97-1*, 40 p.

Georgiou, I.Y.; FitzGerald, D.M.; and Stone, G.W., 2005. The impact of physical processes along the Louisiana coast. *Journal of Coastal Research*, 44, 72-89.

Hershfield, D.M., 1961. Rainfall Frequency Atlas of the United States. Washington, DC: U.S. Department of Commerce, *Weather Bureau Technical Paper No. 40*, 115 p.

Hirschboeck, K.K., 1988. Flood hydroclimatology. *In*: Baker, V.R., Kochel, R.C., and Patton, P.C., (eds.), Flood Geomorphology. New York, New York: John Wiley & Sons, pp. 27-49.

Huff, F.A. and Angel, J.R., 1992. Rainfall Frequency Analysis of the Midwest. Champaign, Illinois: *Midwestern Climate Center and Illinois Water Survey Bulletin 71*, 141 p.

Keim, B.D. and Faiers, G.E., 1996. Heavy rainfall distributions by season in Louisiana: Synoptic interpretations and quantile estimates. *Water Resources Bulletin*, 32(1), 117-124.

Keim, B.D. and Faiers, G.E., 2000. A comparison of techniques to produce quantile estimates of heavy rainfall in arid and mountainous environments: a test case in western Texas. *Journal of Arid Environments*, 44, 267-275.

Keim, B.D.; Muller, R.A.; Stone, G.W., 2007. Spatiotemporal patterns and return periods of tropical storm and hurricane strikes from Texas to Maine. *Journal of Climate*, 20, 3498-3509.

T. Baker Smith and Moffatt & Nichol Staff. 2002. *Whiskey Island Back Barrier Marsh Creation Project No. TE-50 95% Design Report*. Houma, Louisiana: T. Baker Smith, Inc. and Moffatt & Nichol, 53 p.

Neelamani, S.; Al-Salem, K.; and Rakha, K., 2007. Extreme waves for Kuwaiti territorial waters. *Ocean Engineering*, 34, 1496-1504.

Penland, S.; Boyd, R.; and Suter, J.R., 1988. Transgressive depositional systems of the Mississippi Delta Plain: A model for barrier shoreline and shelf sand development. *Journal of Sedimentary Petrology*, 58, 932-949.

Ritchie, W. and Penland, S., 1988. Rapid dune changes associated with overwash processes on the deltaic coast of south Louisiana. *Marine Geology*, 81, 97-122.

Stone, G.W.; Grymes, J.M.; Robbins, K.D.; Underwood, S.G.; Steyer, G.D.; and Muller, R.A., 1993. A chronologic overview of climatological and hydrological aspects associated with Hurricane Andrew and its morphological effects along the Louisiana coast, U.S.A. *Shore and Beach*, 61(2), 2-12.

Stone, G.W. and Liu, B., 2005. Offshore hydrodynamics and geological impacts of Hurricane Ivan along the northeastern Gulf of Mexico. *Transactions - Gulf Coast Association of Geological Societies*, 55, 809-810.

Stone, G.W.; Walker, N.D.; Hsu, S.A., Babin, A.; Liu, B.; Keim, B.D.; Teague, W.; Mitchell, D.; and Leben, R., 2005. Hurricane Ivan's impacts along the northern Gulf of Mexico. *EOS Transactions, American Geophysical Union*, 86(48), 500-501.

Wilks, D.S., 1993. Comparison of three-parameter probability distributions for representing annual extreme and partial duration precipitation series. *Water Resources Research*, 29, 3543-3549.

Williams, S.J.; Penland, S.; and Sallenger, A., 1992. Louisiana Barrier Island Erosion Study: Atlas of Shoreline Changes from 1853 to 1989. *U.S. Geological Survey Miscellaneous Investigations Series Map I-2150-A*, 108 p.

CHAPTER 4: EFFECT OF PHYSICAL PROCESSES AND RESTORATION ON HABITAT DYNAMICS ON WHISKEY ISLAND, A RETROGRADATIONAL LOUISIANA BARRIER ISLAND

4.1 Introduction

Louisiana's barrier islands serve as the first line of defense against hurricane-generated storm surge. The barrier islands provide a buffer that protects landward marshes and ecosystems, communities, and infrastructure. Barrier islands also serve as important habitat for various marine organisms and avian species. A number of important commercial (e.g., white and brown shrimp and blue crab) and recreational (e.g., red drum and spotted seatrout) fishery species make use of the back barrier marsh for nursery habitat, foraging, and predator refugia (NRCS, 2005). Neotropical migratory avian species use the island as feeding and resting habitat during their annual migration, and colonial waterbirds use the island for nesting habitat (NRCS, 2005). The threatened piping plover and the recently de-listed brown pelican also make use of barrier islands for feeding and/or nesting (NRCS, 2005).

Marsh vegetation, both emergent and woody, serves as important wildlife habitat on barrier islands, and the different vegetation types present on the island provide some indication of the natural conditions, such as inundation extent and duration, occurring at that location. In general, woody vegetative species inhabit areas of higher elevation which are less frequently inundated when compared to emergent vegetative species which inhabit areas of lower elevation. Comparing the change in extent of specific marsh vegetation types aids in understanding the impact of both short-term (hurricanes) and long-term (natural evolution) processes on the vegetation species.

In 1993, a near-term strategy for large-scale restoration of the Isles Dernieres barrier islands was developed between the State of Louisiana and five federal agencies (Khalil and Lee,

2006) working together under the Coastal Wetlands Planning, Protection and Restoration Act (CWPPRA) program. Through CWPPRA, a number of barrier island restoration projects have been completed including projects on the Isles Dernieres islands, and many others are in the planning or engineering and design phase. The primary method of restoration of these islands was through the placement of dredged material on the islands to increase their height and width (Khalil and Lee, 2006). Barrier island restoration projects are also a significant component of *Louisiana's Comprehensive Master Plan for a Sustainable Coast* (CPRA, 2012a). The plan allocates $1.75 billion for restoration of barrier islands in the Terrebonne and Barataria basins, including the Isles Dernieres island chain. The $50 billion plan is not funded; however, there are several sources of funding that are expected to be available over the next several years (e.g., Natural Resource Damage Assessment and Clean Water Act fines from the Deepwater Horizon oil spill, Gulf of Mexico Energy Security Act, etc.).

The Whiskey Island Restoration (TE-27) project was completed in 1998, and resulted in emplacement of approximately 2.85 million cubic yards of material dredged from passes and lakes near the islands (Khalil and Lee, 2006). The material was used to construct back barrier marsh habitat, and sand fences and vegetation plantings were used to stabilize the newly placed sediments and to capture sediment being transported by aeolian processes (Khalil and Lee, 2006). Post-construction monitoring reports for this project indicate that the use of dredged material, sand fencing, and vegetative plantings are credible ways to provide 'quasi-stabilization' of barrier islands and further prolong their life expectancies (West and Dearmond, 2004 a and b). Additional restoration of Whiskey Island was completed in the fall of 2009. The Whiskey Island Back Barrier Marsh Creation (TE-50) project resulted in the construction of a 300-acre back barrier marsh platform with pre-excavated tidal creeks and ponds and vegetation plantings and

an enhanced 13,000 linear foot dune along which sand fences were constructed and vegetation was planted (T. Baker Smith/Moffatt & Nichol, 2007).

Quantification of the spatial pattern of vegetation and elevation change on Whiskey Island was necessary to evaluate the influence of restoration projects and the effects of tropical events, such as overwash. Additionally, the relationship between elevation change and change in vegetation habitat type has not been quantified for the island. Therefore, this paper intends to provide a comparison of the extent of two marsh vegetation types, emergent and woody, on Whiskey Island from 1998-2009 and to relate temporal and spatial changes to either short-term (hurricanes) or long-term (natural process) developments; to compare the elevation change over eight transects across the east and west lobes of Whiskey Island to determine if changes in elevation are associated with changes in marsh vegetation types; and to use modeled predictions of elevations 25 and 50 years in the future to discuss the likely impact on the marsh vegetation habitats that currently exist on Whiskey Island.

4.2 Study Area

The Isles Dernieres barrier island chain is located in Terrebonne Parish in southcentral Louisiana approximately 20 miles southwest of Cocodrie. Although once a continuous island stretching approximately 20 miles in length, the island fragmented into five islands (from west to east): Raccoon, Whiskey, East, Trinity, and Wine (Figure 4.1). Whiskey Island is located within the Isles Dernieres Barrier Island Refuge managed by the Louisiana Department of Wildlife and Fisheries (Figure 4.1). It is surrounded by Coupe Colin on the west, Lake Pelto, Caillou Boca, and Caillou Bay on the north, and Whiskey Pass on the east. The island is approximately 4 miles long and 0.7 miles wide at its greatest extent.

Louisiana contains about 40% of the coastal wetlands in the United States and is experiencing about 80% of the coastal wetland erosion, and the Isles Dernieres barrier island chain is one of the most rapidly deteriorating barrier island systems in Louisiana (Penland *et al*., 1990b). According to Stone *et al*. (2004), there are six main factors that are responsible for the deterioration of the Isles Dernieres barrier island chain. These factors include: eustatic sea level rise, compactional and geological subsidence, wave erosion, wind deflation, reduction in sediment supply, and anthropogenic activity (Stone *et al*., 2004).

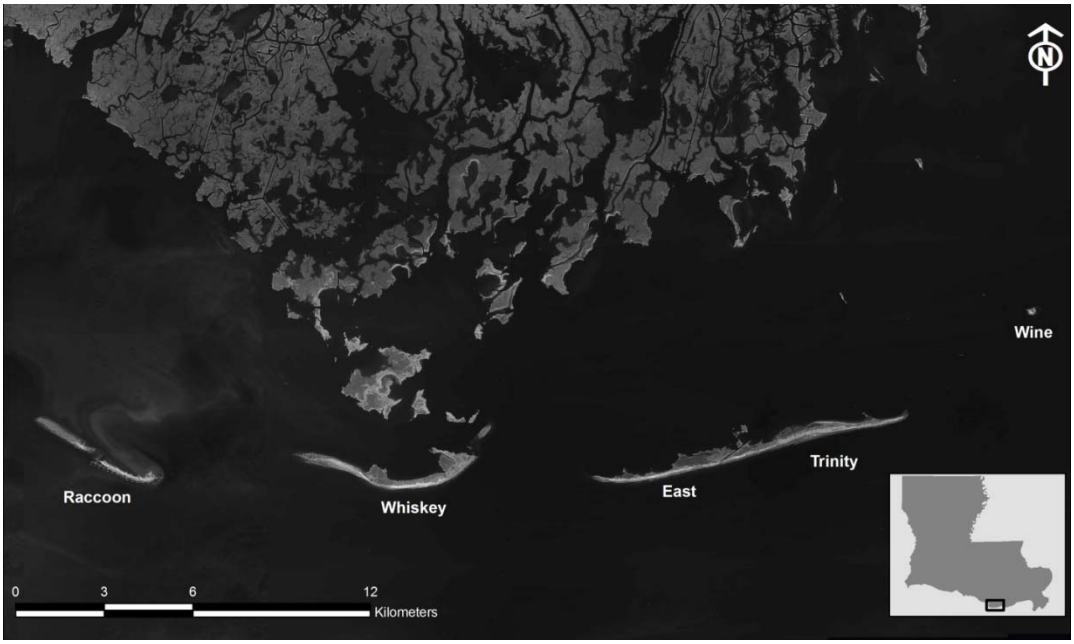

Figure 4.1. The fragmented Isles Dernieres barrier island chain, including from west to east, Raccoon, Whiskey, East, Trinity, and Wine islands (2008 Digital Orthophoto Quarter Quadrangle imagery).

According to Stone *et al*. (1997), washover processes related to storm events have played a significant role in the evolution of the barrier islands of Louisiana. Erosion, reduced elevation, fragmentation, and migration of barriers due to hurricanes and to a lesser extent tropical storms may be the dominant reason for landward translation of the barriers (Ritchie and Penland, 1988; Stone *et al*., 1997). Post-storm barrier island recovery is dependent on the degree of storm damage and the supply of sediment to the system (Stone *et al*., 1997). However, due to factors

mentioned above such as subsidence, relative sea level rise, and declining sediment supply, the barrier islands of Louisiana are prone to long-term land loss (Stone *et al*., 1997). Sallenger, Penland, and Krabill (2003) found that wave runup resulting from Tropical Storm Isidore (landfall on September 26, 2002) and Hurricane Lili (landfall on October 3, 2002) was greater than dune elevations on the Isles Dernieres and lead to the inland migration of sand bodies by several hundred meters, and Stone *et al*. (1997) indicates that episodic landward translation of barrier island beaches resulting from stronger hurricanes routinely approaches 100 meters.

According to Penland *et al*. (1990a), Louisiana is experiencing some of the highest rates of coastal erosion and land loss in the United States and is the hot spot for coastal erosion in the Gulf of Mexico. Based on more recent rates of land loss and including the restoration efforts that have been completed, the long-term (1887-2002) disappearance date for the complete Isles Dernieres barrier system was 2034 and the short-term (1988-2002) disappearance date was 2075 according to Penland *et al*., (2005). Long-term erosion rates (1887- 2002) on Whiskey Island ranged from 46-78 ft along the gulf shoreline (Penland and Campbell, 2004). From 1988-2002, Whiskey Island experienced average erosion rates of 86 ft/year (Penland and Campbell, 2004). Between November 2002 and 2004, total erosion on the eastern flank of the island was about 200 ft (Moffatt &Nichol, 2007). Shoreline erosion rates following the 2005 hurricane season (from 2004 to November 2005) were determined to be approximately 120 ft near the center of the island and 400 ft on the eastern flank of the island (Moffatt & Nichol, 2007).

Vegetation types present on the back barrier marsh areas of Whiskey Island include *Spartina alterniflora, Distichlis spicata, Sporobolus virginicus, Spartina patens, Baccharis halimifolia, Panicum amarum, Eustoma exaltatum, Strophostyles helvula, Sesuvium portulacastrum, Salicornia bigelovii, and Avicennia germinans* (Curole, 2007; Rodrigue *et al*.,

2008). According to Curole (2007), the back barrier marsh was mapped as a *Spartina alterniflora* (smooth cordgrass) saline marsh. Campbell *et al*. (2004) identifies *Spartina alterniflora* as the dominant plant species in back barrier marsh habitats and further states that *Avicennia germinans* (black mangrove) can also be found in this habitat type but at slightly higher elevations than *Spartina alterniflora*. Black mangrove is a freeze-intolerant species that is highly valued for the nesting and roosting habitat that it provides for shore birds (Campbell *et al*., 2004). Lewis (2005) notes that mangroves are largely found above mean sea level in areas that are inundated 30% of the time or less. Reduced survival, growth, and productivity of coastal wetland plants result from increases in submergence and salinity and lead to changes in species composition, distribution, and successional patterns of plant communities (DeLaune, Pezeshki, and Patrick, 1987).

4.3 Methods

4.3.1 Habitat Classification

Supervised maximum likelihood classification of digital orthophoto quarter quadrangles (DOQQs) from 1998, 2004, 2005, 2008, and post-construction aerial imagery from 2009 was completed using ERDAS IMAGINE software (version 9.3). The DOQQ images have a 1.0-m resolution, and the 2009 aerial imagery has a 0.5-meter resolution. The images were clipped to a created polygon outline that encompassed the entire island throughout the eleven years of imagery coverage. Five of the eight categories of habitat discussed in Penland *et al*. (2004) were used for classification. The categories were water, intertidal, barrier vegetation, beach, and bare land. The beach and bare land classes were combined for this study. The marsh category identified in Penland *et al*. (2004) was divided into two separate categories: emergent marsh vegetation (e.g., *Spartina alterniflora*) and woody marsh vegetation (e.g., *Avicennia germinans*). Once the classifications were completed, the images were cleaned by using mathematical

morphology operations (Soille, 2002). A final manual cleaning was completed to correct the areas that remained inaccurately classified.

4.3.2 Post-classification Change Detection

Post-classification change detection was completed on a pixel-by-pixel basis and was used to determine the location and extent of vegetation habitat change that occurred between the first and last years of photography analyzed, between the 1998 and 2004 imagery, between the 2004 and 2005 imagery, and between the 2008 and 2009 imagery. The 1998-2004 comparison was indicative of gradual change including the impact of two hurricanes (Lili and Isidore) and multiple tropical storm strikes over the six year period. The 2004-2005 comparison provided insight into the vegetation habitat dynamics that occurred as a result of the significant hurricane events that occurred in 2005, while the 2008-2009 comparison indicated the habitat class differences resulting from the 2009 restoration of the island. The 1998-2009 comparison specified changes that occurred over the eleven year study period, including those from tropical and frontal events, restoration activities, and day-to-day coastal processes.

4.3.3 Elevation Transects

LiDAR (Light Detection And Ranging) data for 2001 and 2011 were obtained from the United States Geological Survey; 2006 LiDAR data generated for the Barrier Island Comprehensive Monitoring (BICM) program were obtained from the Coastal Protection and Restoration Authority of Louisiana (CPRA); and DEMs (Digital Elevation Models) for 2010, 2035, and 2060, generated through the morphology modeling effort used to predict the effects of restoration and protection projects for *Louisiana's Comprehensive Master Plan for a Sustainable Coast*, were obtained from the CPRA (CPRA, 2012b). The LiDAR data had a resolution of 5 m, while the DEMs had a resolution of 30 m. The 2010 DEM was compiled from elevation datasets

available in 2010 and represents the restoration projects that had been constructed at that time as well as projects that were funded for construction. The DEMs for 2035 and 2060 represent modeled predictions of elevation based upon a specified set of prescribed environmental conditions for sea level rise (0.27 meters over 50 years; CPRA 2012a), subsidence (8.8 mm/year; CPRA 2012a), and other environmental factors. The coarse resolution, planning level model used to produce the DEMs was developed to complete a large number of model runs within a relatively short time period. Because of this limitation, the models relied more on empirical data from historical trends in land change than on processes, such as dune overwash and barrier breaching following storm events, which are known to result in significant elevation change. Four transects were created across each of the marsh lobes on Whiskey Island, three in a north-south direction and one in an east-west direction (Figure 4.2). Elevation data were extracted at equally spaced points every 25 m along each transect from the above data sets.

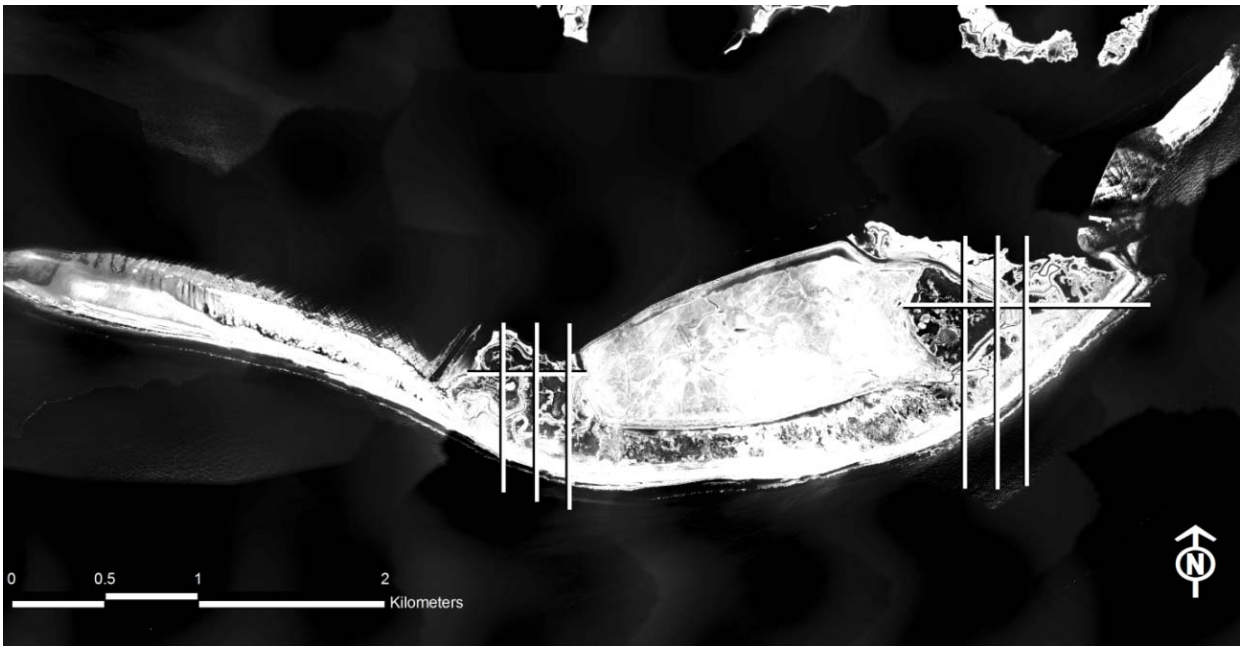

Figure 4.2. Aerial imagery from 2009 showing transect locations across marsh lobes. Elevation data were taken at evenly spaced points every 25 meters along each transect to determine the average elevation of emergent and woody vegetation habitats.

4.3.4 Water Level Elevation and Variability

Gage height data were retrieved for the USGS Caillou Bay SW of Cocodrie monitoring station to derive some measure of water level elevation and variability near Whiskey Island. The data are provided in feet and recorded once daily. Data were available from 1999 to present.

4.4 Results

4.4.1 Classification Accuracy

Error matrices were constructed for each year to determine the overall accuracy, producer's accuracy, and user's accuracy of each habitat for each of the images. Producer's accuracy is a measure of how accurately the analyst classified the image data by category and quantifies whether a particular pixel is omitted from its correct class. User's accuracy is a measure of how well the classification performed in the field and quantifies whether a pixel is committed to an incorrect class (http://www.csc.noaa.gov/crs/lca/faq_tech.html#q4). The reference for field performance was visual inspection of the imagery. The error matrices allow for a quantitative comparison of the classifications. An example error matrix generated for the 2009 classification is shown in Table 4.1. Table 4.2 shows the accuracy for each of the classifications by habitat class. It should be noted that the overall accuracy is heavily dominated by the water habitat class as the accuracy assessment was based upon random points generated over the entire classified surface rather random points generated by a stratified random sampling scheme. Overall accuracy of the five habitat classifications ranged from 88%-97%, and the water class had the highest accuracy for all classifications. The intertidal class had the lowest user's accuracy for all classifications except 2009. A likely reason for this is the similarity in spectral signatures between the transition zones of the intertidal, beach/bare, water, and emergent vegetation classes depending on which year of photography is being considered. The user's

accuracy for the emergent vegetation class ranged from 87%-92% and for the woody vegetation class ranged from 72%-90%.

Table 4.1. Error matrix for 2009 habitat classification showing the accuracy of the classification for each of the habitat types. The overall accuracy for this classification was 97%.

	Beach/Bare	Emergent Vegetation	Woody Vegetation	Water	Intertidal	Total	User's Accuracy
Beach/Bare	34	1	0	0	1	36	94%
Emergent Vegetation	0	26	2	0	2	30	87%
Woody Vegetation	0	0	9	0	1	10	90%
Water	0	0	0	232	0	232	100%
Intertidal	2	2	0	2	85	91	93%
Total	36	29	11	234	89	399	
Producer's Accuracy	94%	90%	82%	99%	96%		

The first large-scale restoration of Whiskey Island was completed in August 1998 and resulted in closure of the breach along the gulf shoreline as well as creation of a back barrier platform. The 1998 DOQQ used in this study was taken prior to restoration and shows the result of decades of barrier island degradation (natural and anthropogenic) (Figure 4.3). Figure 4.4 shows the habitat classification results for the 1998 DOQQ. A comparison of the percent of woody vegetation to emergent vegetation shows that emergent vegetation covered approximately 2% more of the study area in 1998. Between 1998 and 2004, the extent of woody vegetation increased by 1%, while the extent of emergent vegetation declined by 1%.

Table 4.2. Producer's accuracy, user's accuracy, and overall accuracy for each habitat type for the five images classified.

Habitat Type	1998			2004		
	Producer's Accuracy	User's Accuracy	Overall Accuracy	Producer's Accuracy	User's Accuracy	Overall Accuracy
Water	98%	97%	91%	93%	99%	88%
Intertidal	79%	77%		88%	54%	
Beach/Bare	94%	85%		74%	88%	
Emergent Vegetation	80%	88%		68%	92%	
Woody Vegetation	73%	83%		86%	76%	

Habitat Type	2005			2008		
	Producer's Accuracy	User's Accuracy	Overall Accuracy	Producer's Accuracy	User's Accuracy	Overall Accuracy
Water	97%	98%	91%	100%	100%	95%
Intertidal	78%	38%		85%	71%	
Beach/Bare	75%	97%		89%	93%	
Emergent Vegetation	68%	87%		74%	87%	
Woody Vegetation	84%	80%		81%	72%	

Habitat Type	2009		
	Producer's Accuracy	User's Accuracy	Overall Accuracy
Water	99%	100%	97%
Intertidal	96%	93%	
Beach/Bare	94%	94%	
Emergent Vegetation	90%	87%	
Woody Vegetation	82%	90%	

The extent of woody vegetation remained lower than the extent of emergent vegetation throughout the study period. The area of emergent vegetation declined between 1998 and 2009, and after a small increase in the area of woody marsh from 1998-2004, the extent of this habitat declined from 2004-2009. The total vegetated area declined from approximately 8% of the study area in 1998 to 6% in 2009. While part of this decline is due to vegetation being covered by sediment pumped onto the island for the 2009 back barrier and dune restoration, it may also be a result of continued island shrinkage. The total water area within the study area increased from

1998-2008, then declined following the 2009 island restoration. The extent of intertidal habitat increased from 1998-2004 and again between 2008 and 2009, likely a result of the restoration events that occurred in 1998 and 2009. Figure 4.5 graphically depicts the percent change in habitat classes over the study period.

Figure 4.3. Whiskey Island as depicted in the 1998 Digital Orthophoto Quarter Quadrangle imagery.

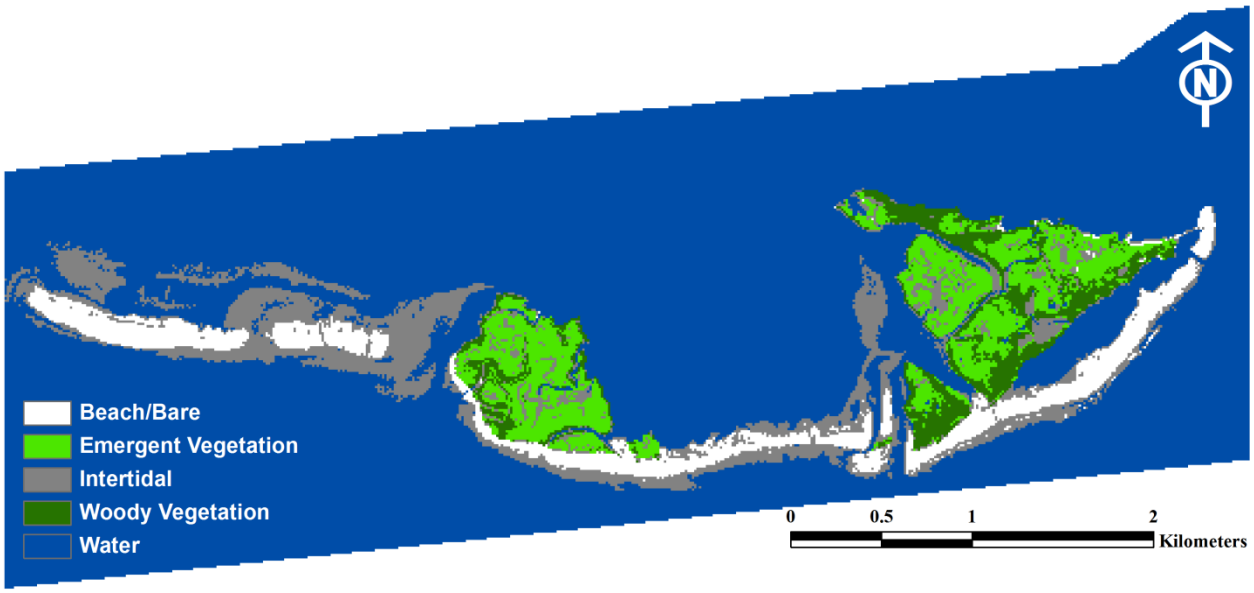

Figure 4.4. Habitat classification of Whiskey Island using the 1998 Digital Orthophoto Quarter Quadrangle imagery showing beach/bare, emergent vegetation, intertidal, woody vegetation, and water habitats.

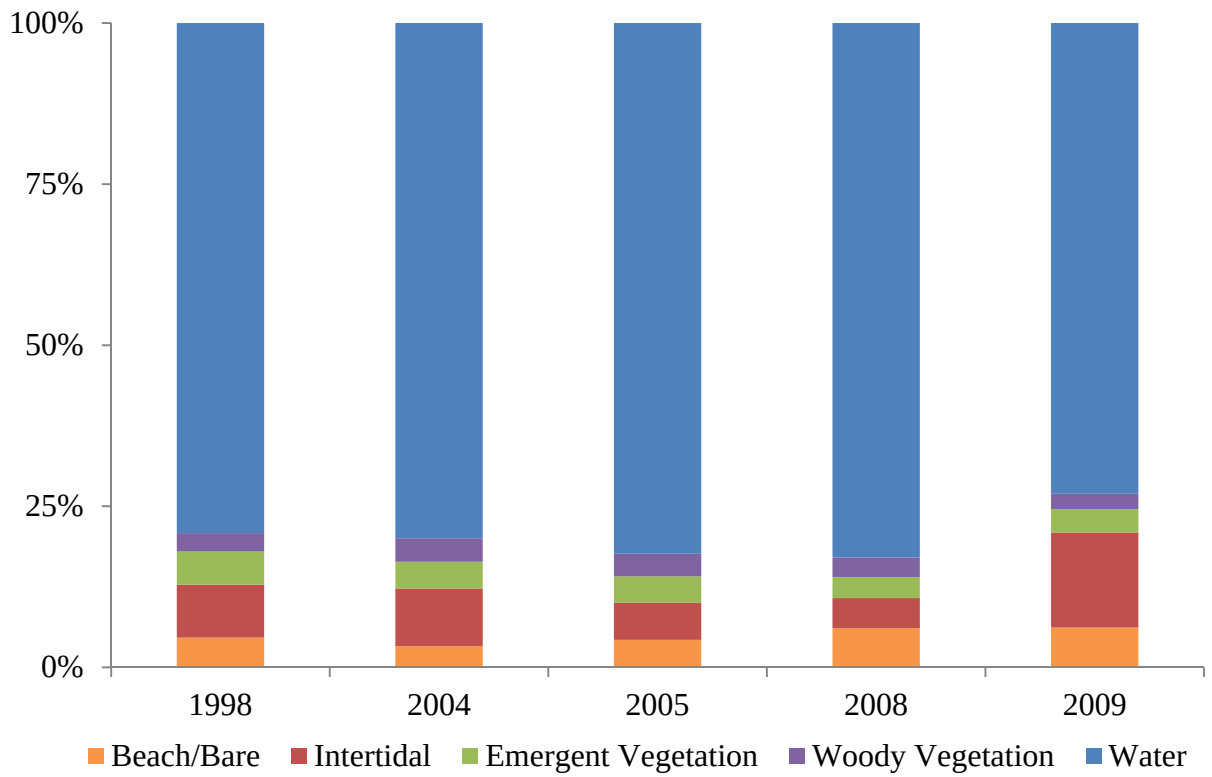

Figure 4.5. Percentage of beach/bare, intertidal, emergent vegetation, woody vegetation, and water habitat types based on the habitat classifications completed for 1998, 2004, 2005, 2008, and 2009.

4.4.2 Post-classification Change Detection

Pixel-by-pixel post-classification change detection was completed to compare imagery from 1998 and 2009, 1998 and 2004, 2004 and 2005, and 2008 and 2009. Table 4.3 shows the results of the change detection procedures. The net vegetation loss in hectares was -32.6 from 1998-2009, -9.1from 1998-2004, -3.5from 2004-2005, and -3.9from 2008-2009. Figure 4.6 shows the combined emergent and woody vegetation change (loss and gain) between 1998 and 2009. Figure 4.7 shows the area of emergent or woody vegetation converted to either beach/bare, intertidal, or water habitat for the time periods for which the change detection procedure was performed, and Figure 4.8 shows the amount of beach/bare, intertidal, or water habitat area converted to either emergent or woody vegetation for the same time periods. Both *Spartina*

alterniflora and *Avicennia germinans* are able to recover from some sand burial due to overwash, but significant sand burial results in plant mortality. Rodrigue *et al*. (2008) documented mangrove mortality resulting from sediment movement into existing mangrove habitat due to overwash.

Additional review of change between 1998 and 2009 shows conversion of over 167 hectares of water to intertidal habitat, and about 62 hectares of intertidal habitat to water – a net gain of approximately 105 hectares of intertidal habitat (Figure 4.9). The majority of the change from water to intertidal is a result of the back barrier marsh platform construction between the west and east lobes of the island as part of the 2009 restoration, but part of the change is also due to differences in the location and extent of ephemeral spits on either side of the island. The documented change from intertidal to water is mainly a result of northerly migration of the island, and as a result, the largest part of this change occurs on the gulf side of the island. An analogous effect is seen when the area of beach/bare habitat is compared to water area between 1998 and 2009. Beach/bare habitat is lost on the gulf side of the island but gained as a result of the newly created marsh and the movement of the west and east spits. Similar to the reported shift from water to intertidal habitat from 1998-2009, over 160 hectares of water area was converted to either intertidal or beach/bare habitat between 2008 and 2009 with the vast majority of this change occurring as a result of the new marsh platform. Change between 2004 and 2005 indicates conversion of 62.4 hectares of intertidal, 8.4 hectares of beach/bare, 2.1 hectares of emergent vegetation, and 2.6 hectares of woody vegetation to open water revealing the alterations that one hurricane season can cause on a barrier island. The area of habitat converted from intertidal habitat to water from 2004-2005 (62.4) is approximately equivalent to the change from intertidal habitat to water (62.2) over the full study period.

Table 4.3. Results of pixel-by-pixel post-classification change detection showing habitat change between 1998 and 2009, 1998 and 2004, 2004 and 2005, and 2008 and 2009 for Whiskey Island. Habitat change of Emergent to Emergent (or similar for other habitat types) is an indication of no change over the time period indicated.

Habitat Change (Hectares)	1998-2009	1998-2004	2004-2005	2008-2009
Beach/Bare to Beach/Bare	6.305	11.438	19.324	51.862
Beach/Bare to Emergent	0.485	0.504	2.017	5.904
Beach/Bare to Intertidal	3.687	24.727	21.947	37.806
Beach/Bare to Mangrove	0.174	0.171	0.016	1.133
Beach/Bare to Water	62.699	36.730	8.358	0.739
Emergent to Beach/Bare	9.207	4.445	5.510	0.954
Emergent to Emergent	35.168	47.327	43.614	43.230
Emergent to Intertidal	14.929	5.912	3.374	4.358
Emergent to Mangrove	16.390	23.291	11.670	1.985
Emergent to Water	7.000	1.359	2.146	0.254
Intertidal to Beach/Bare	22.785	8.124	29.205	15.003
Intertidal to Emergent	5.422	9.377	12.503	2.955
Intertidal to Intertidal	33.489	42.853	36.999	46.081
Intertidal to Mangrove	4.166	3.253	0.205	0.666
Intertidal to Water	62.199	62.882	62.396	8.772
Mangrove to Beach/Bare	4.765	4.070	6.283	0.872
Mangrove to Emergent	0.034	1.790	5.122	6.315
Mangrove to Intertidal	8.653	6.593	1.911	7.996
Mangrove to Mangrove	14.055	36.014	41.795	32.945
Mangrove to Water	15.135	2.088	2.569	0.178
Water to Beach/Bare	56.599	22.396	6.962	30.197
Water to Emergent	15.145	1.433	2.554	0.073
Water to Intertidal	167.586	63.279	25.872	130.161
Water to Mangrove	1.686	0.586	1.028	0.000
Water to Water	1009.353	1160.348	1227.554	1149.317
Area Unchanged	1098.370	1297.980	1369.287	1323.435
Area with Changes	478.746	283.010	211.650	256.322
Area of Vegetation Lost	59.690	24.466	21.793	14.613
Area of Vegetation Gained	27.077	15.325	18.325	10.731
Net Vegetation Change	-32.613	-9.142	-3.468	-3.882

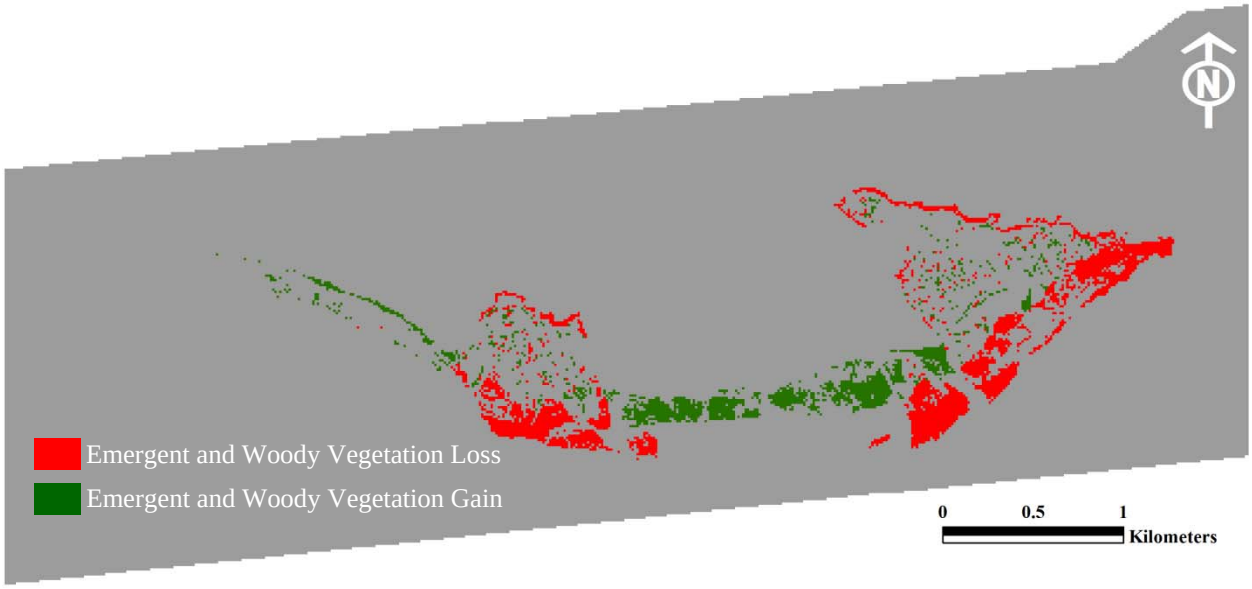

Figure 4.6. Post-classification change detection results showing combined emergent and woody vegetation loss (red) and gain (green) between the 1998 Digital Orthophoto Quarter Quadrangle image and the 2009 aerial photograph.

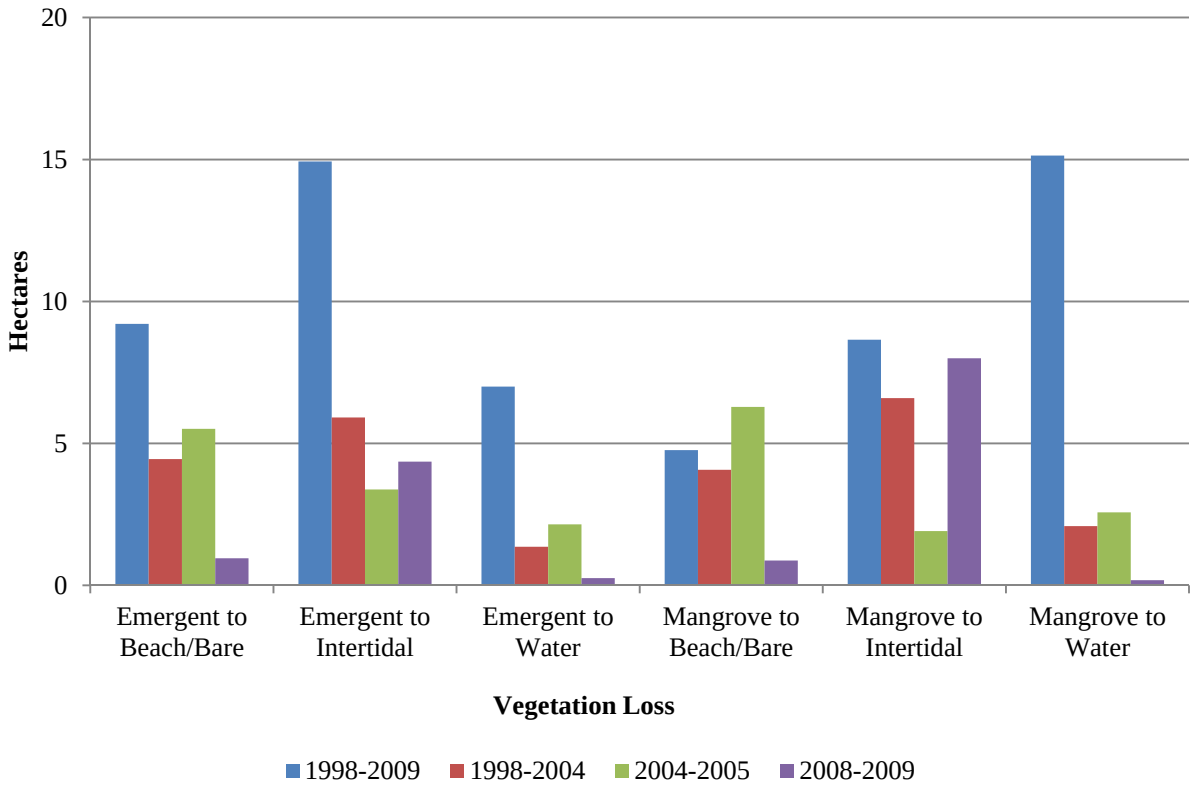

Figure 4.7. Post-classification change detection results showing the amount of area lost for both emergent and woody vegetation and the habitat that each vegetation type changed to for each of the time periods for which the change detection process was performed.

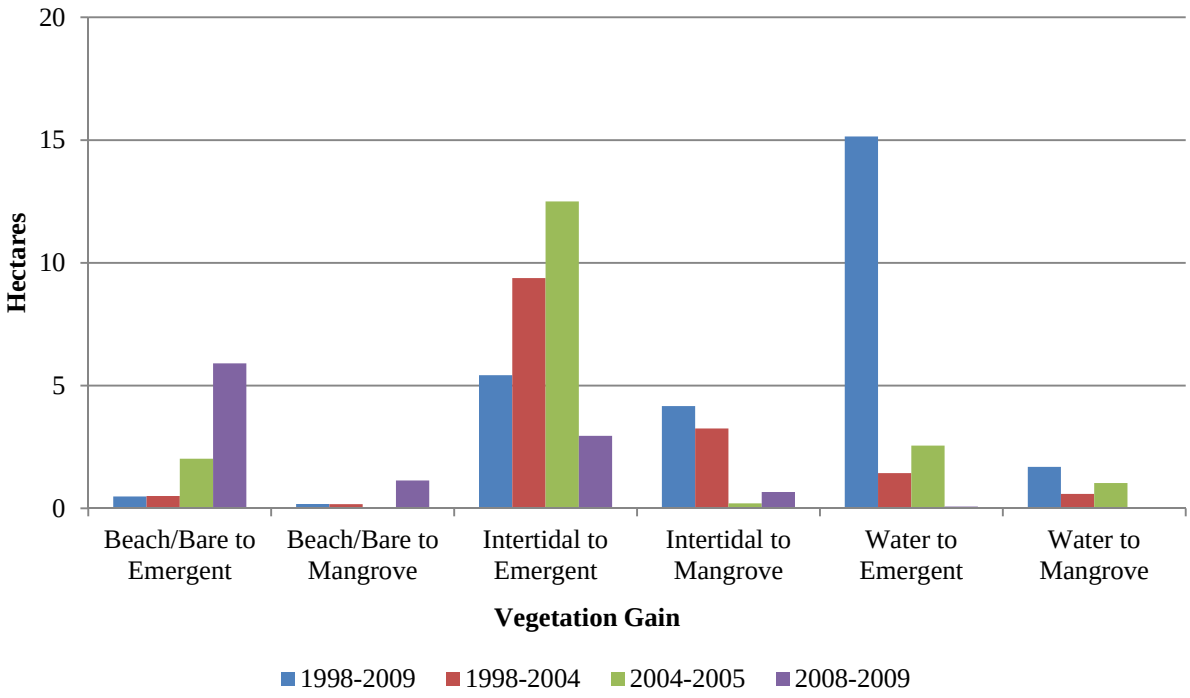

Figure 4.8. Post-classification change detection results showing the amount of area gained for both emergent and woody vegetation and the habitat type that was converted to vegetation for each of the time periods for which the change detection process was performed.

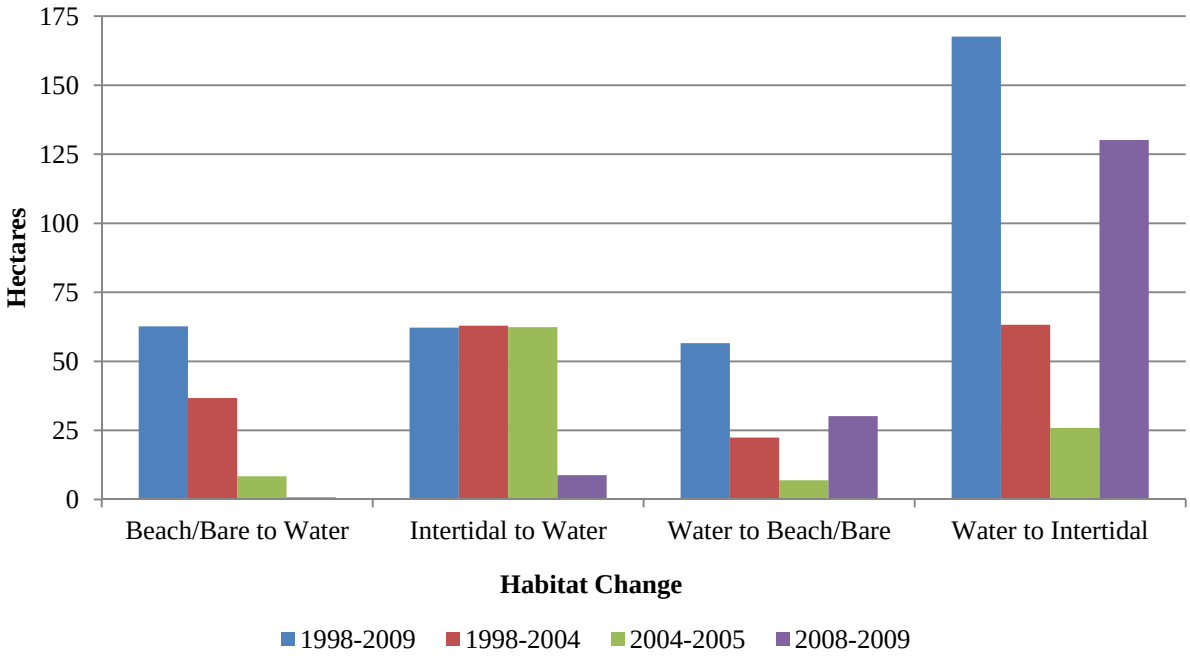

Figure 4.9. Post-classification change detection results showing the amount of area converted from beach/bare or intertidal habitat to water or from water to either beach/bare or intertidal habitat for each of the time periods for which the change detection process was performed.

4.4.3 Elevation Profiles

Elevation profiles were created for each of the transects (Figure 4.2) using the 2001, 2006, and 2011 LiDAR data, and an example profile is shown in Figure 4.10. While the 2001 LiDAR coverage for Whiskey Island is somewhat spotty and represents first return data rather than bare earth, the points along the profile where data are available show retreat of the barrier on its south and east sides. This is consistent with the documented northwest migration of Whiskey Island, particularly the eastern end (Rodrigue *et al*. 2008). The substantial differences between the 2006 and 2011 LiDAR elevations were unexpected, and the scale of the difference is not explainable by the 2009 restoration project alone. LiDAR elevations from the 2011 data set are comparable to elevations from the 2010 DEM as shown in Figures 4.10 and 4.11 below. Additional research into the reason for the elevation differences between the 2006 and 2011 data sets is needed. Cross-island elevation profiles show a maximum dune elevation of 1.6 meters on the east lobe of the island in 2001, 0.99 meters in 2006, and 1.8 meters in 2011. However, the 2006 location of the dune shows a northerly retreat of approximately 100-125 meters, and the 2011 location of the dune shows a northerly retreat of 250-300 meters (depending on transect location) when compared to the 2001 dune location.

Based on the 2005 habitat classification and 2006 LiDAR data, the average elevation of emergent marsh on the west lobe of the island was 0.158 meters, and the average elevation was 0.037 meters on the east lobe. Using the same habitat classification and LiDAR data, the average elevation of woody marsh was 0.202 meters and 0.249 meters on the west and east lobes, respectively. The average 2011 elevation of habitats that were classified as emergent marsh for the 2009 imagery was 0.602 m for the west lobe and 0.621 m for the east lobe. Average elevation of areas classified as woody marsh was generally higher than average elevations of emergent

marsh areas. The 2011 woody marsh (based on 2009 imagery) elevations were 0.603 m for the west lobe and 0.726 m for the east lobe. The 2006 habitat elevations reflect eight years of degradation from the 1998 island restoration, including the effects of hurricanes Katrina and Rita and numerous other tropical events. The 2011 elevation data give an indication of the positive impacts of a restoration project that had not yet been subjected to extensive tropical activity. In addition to the profiles created using the LiDAR data, profiles were also created for the DEMs generated as part of the *Louisiana's Comprehensive Master Plan for a Sustainable Coast* morphology modeling effort (CPRA, 2012b). An example profile is presented in Figure 4.11. The average elevations for areas classified in the 2009 aerial imagery as emergent vegetation and woody vegetation are 0.502 and 0.557, respectively for the west lobe and 0.485 and 0.618, respectively for the east lobe using the 2010 DEM.

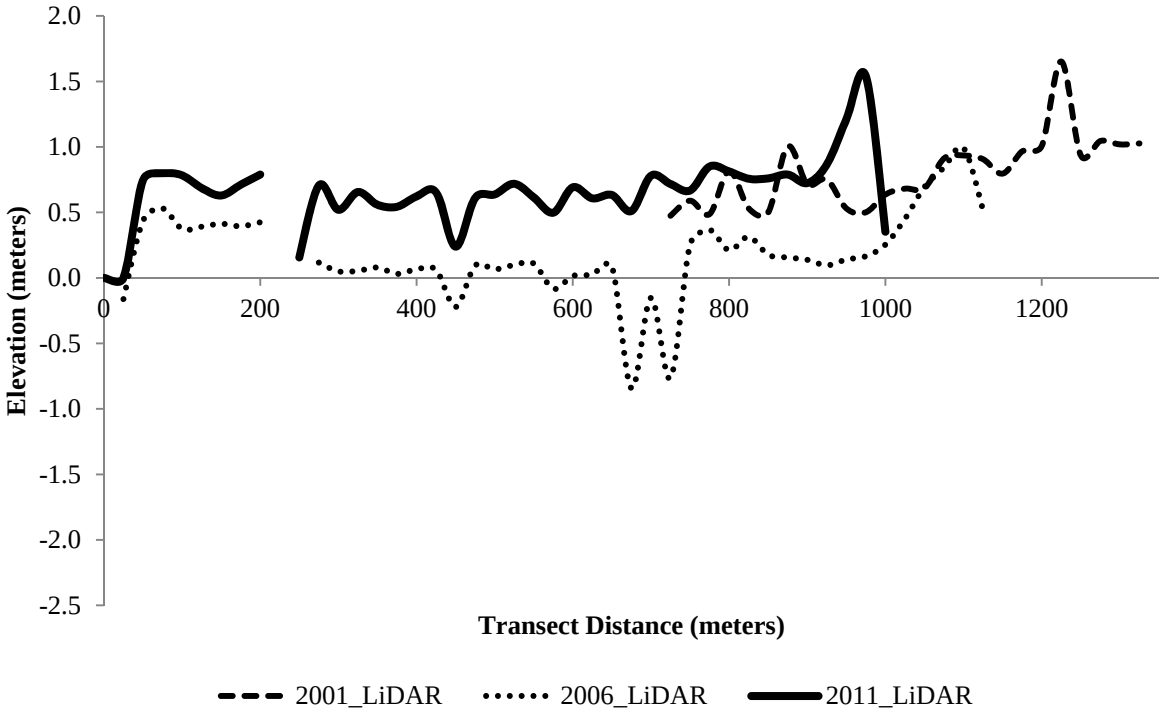

Figure 4.10. Elevation profile across the east lobe of Whiskey Island showing the 2001, 2006, and 2011 LiDAR elevations based upon the westernmost transect identified in Figure 4.2. The transect begins on the bay side of the island (transect distance of 0 meters) and extends to the gulf side of the island (transect distance of greater than 1200 meters).

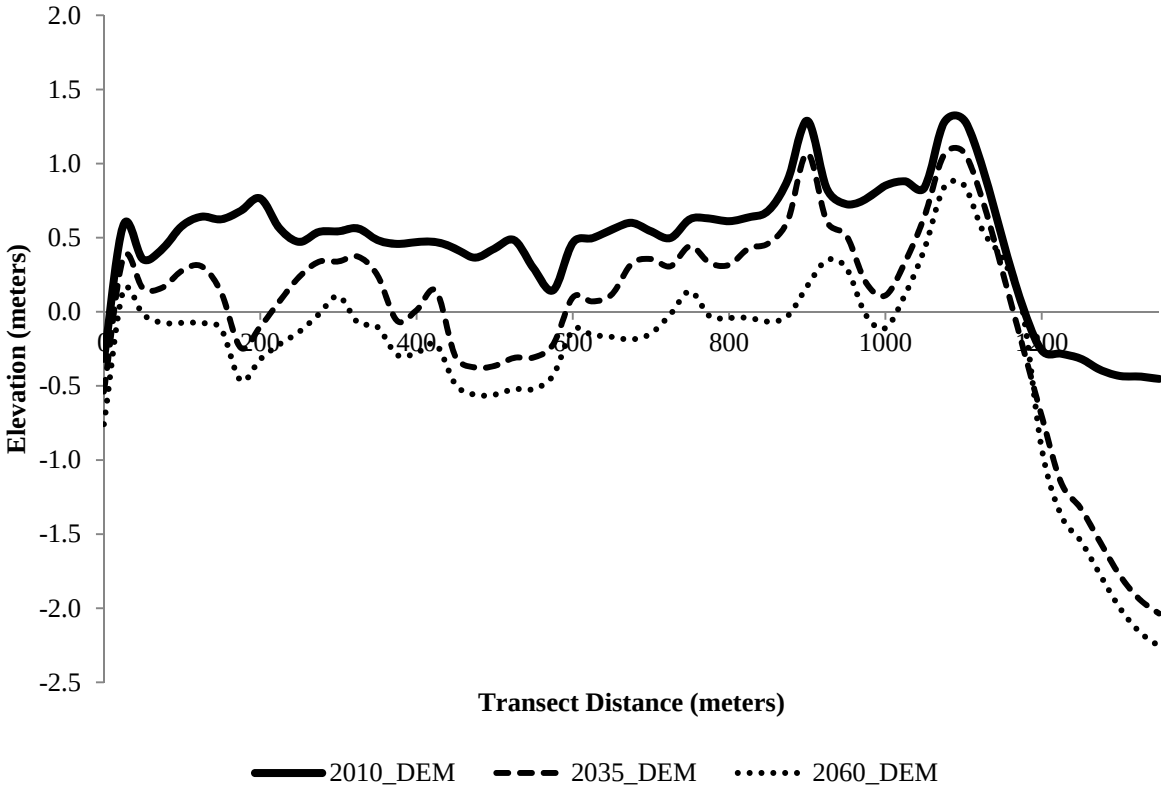

Figure 4.11. Elevation profile across the east lobe of Whiskey Island showing the 2010, 2035, and 2060 DEM elevations based upon the westernmost transect identified in Figure 4.2. The transect begins on the bay side of the island (transect distance of 0 meters) and extends to the gulf side of the island (transect distance of greater than 1200 meters).

4.4.4 Inundation Regime

Gage height data for five year increments (January 2004-December 2008 and October 2007-October 2012) were used to determine the approximate amount of time that emergent vegetation and woody vegetation were inundated over these time periods. Elevations from the 2006 LiDAR data were averaged for emergent and woody marsh habitats identified in the 2005 habitat classification, and elevations from the 2010 DEM and the 2011 LiDAR were averaged separately for emergent and woody marsh habitats identified in the 2009 habitat classification. Elevations from the 2035 and 2060 DEMs were also averaged by habitat type as identified in the 2009 habitat classification to review potential future inundation regimes for current vegetated

habitats. Table 4.4 presents both the elevations and the inundation regime for each habitat based upon the elevation data set it was paired with.

Table 4.4. Elevation (in meters) and inundation regime for emergent and woody vegetation habitats on the west and east lobes of Whiskey Island based upon five different combinations of habitat classifications and elevation datasets.

Habitat Type	2006 LiDAR 2005 Habitat		2010 DEM 2009 Habitat		2011 LiDAR 2009 Habitat	
	Elevation	Inundation	Elevation	Inundation	Elevation	Inundation
West Emergent	0.158	82.5%	0.502	6.8%	0.602	1.8%
West Woody	0.202	71.4%	0.557	3.5%	0.603	1.8%
East Emergent	0.037	95.1%	0.485	7.8%	0.621	1.3%
East Woody	0.249	57.3%	0.618	1.5%	0.726	0.2%

Habitat Type	2035 DEM 2009 Habitat		2060 DEM 2009 Habitat	
	Elevation	Inundation	Elevation	Inundation
West Emergent	0.236	71.2%	-0.091	99.7%
West Woody	0.279	57.7%	-0.095	99.9%
East Emergent	0.123	89.6%	-0.163	100.0%
East Woody	0.291	52.8%	-0.101	99.9%

Based on the 2006 LiDAR data, inundation of emergent and woody vegetation habitats ranged from 82.5%-95.1% and 57.3%-71.4%, respectively (Figure 4.12). Inundation of emergent vegetation ranged from 6.8%-7.8% and woody vegetation from 1.5%-3.5% based on elevations from the 2010 DEM. Elevations from the 2011 LiDAR were slightly higher than those of the 2010 DEM, so inundation was correspondingly less. When the 2035 DEM elevations are used, emergent vegetation is inundated 71.2%-89.6% and woody vegetation is inundated 52.8%-57.7% of the time. These habitat types are inundated over 88.0% of the time when 2060 DEM elevations are used. Table 4.4 highlights the distinct difference between habitat elevations and inundation regimes from 2006 compared to 2010 and 2011. The inundation regimes for the 2005 habitat classification/2006 LiDAR data closely resemble the 2009 habitat classification/2035 DEM data. This points to the important difference that one restoration project can have on the

barrier island landscape. While it is understood that the habitat classified as emergent vegetation and woody vegetation will not remain the same from 2010 to 2035 to 2060 due to sea level rise, subsidence, storm impacts, and other processes, the point here was not to project explicitly how habitats might shift over time on Whiskey Island but rather to understand that without restoration of coastal Louisiana's barriers the majority of the current back barrier marsh could be subaqueous in about fifty years.

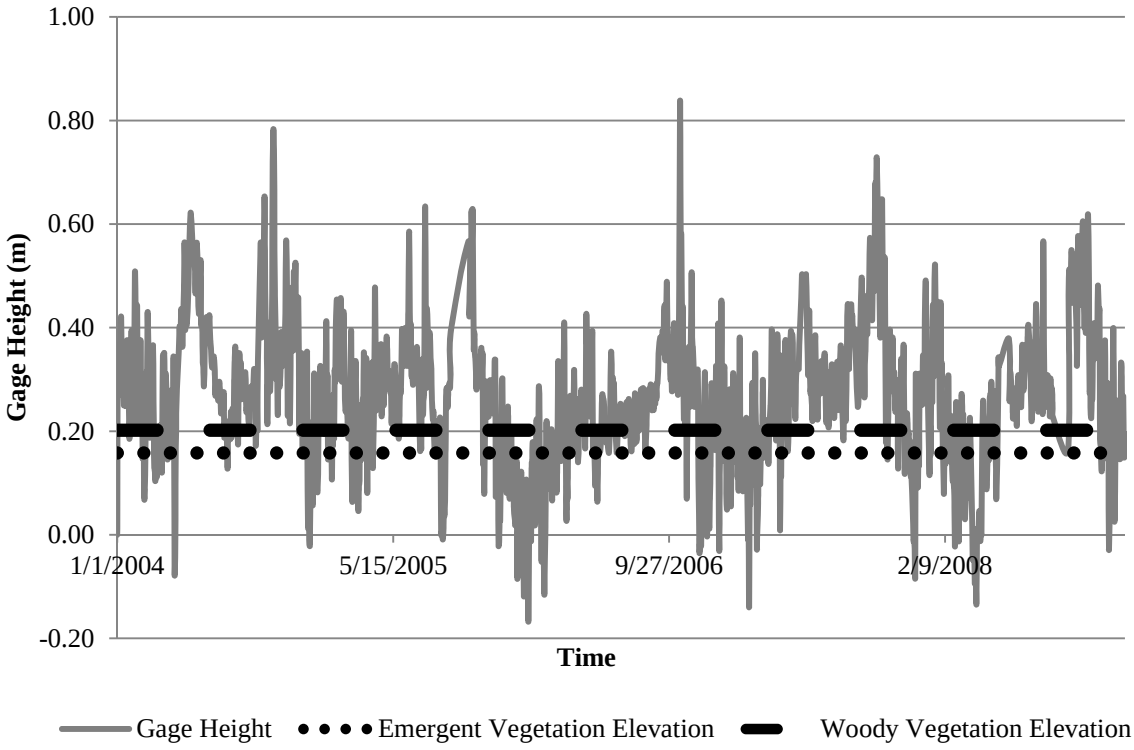

Figure 4.12. Gage height relative to emergent and woody marsh elevations on Whiskey Island. The grey line depicts gage height from January 2004-December 2008 for the USGS Caillou Bay SW of Cocodrie monitoring station. The black dotted line depicts the average elevation of emergent vegetation habitat, and the black dashed line depicts the average elevation of woody marsh habitat. The graph provides a comparison of the inundation regimes for the two habitat types.

4.5 Discussion

There are a wide variety of methods that can be utilized to complete a change detection analysis including post-classification comparison, composite analysis, univariate image

differencing, image ratioing, bi-temporal linear data transformation, change vector analysis, image regression, multi-temporal spectral mixture analysis, and multi-dimensional temporal feature space analysis (Coppin *et al*., 2004; Tuxen *et al*., 2008; Lunetta *et al*., 2002; Jabbar *et al*., 2006). To be consistent with the change detection procedures that were performed as part of the BICM program, pixel-by-pixel post-classification was the method selected for use in this study. In early 2009, the CPRA released a BICM report detailing the change in extent of eight habitat types on Louisiana's barrier islands from 1996-2005 (Fearnley *et al*., 2009). The report provides the change analysis for the marsh vegetation habitat type, but it does not separate the extent of emergent marsh vegetation and woody marsh vegetation nor does it provide for a comparison of how the extent of these separate marsh vegetation types have been altered over time. When the combined area of marsh and barrier vegetation habitat classes from the BICM report are compared to the total area of emergent and woody marsh classes from this study, the numbers are very similar. For example, the reported hectares of vegetation in the BICM report is 118 (based on the 2005 DOQQ), and the hectares of vegetation for the same DOQQ for this study is 120.7. Comparison of 1998 and 2004 results also show minor differences. While the area for these habitat classes is not exact between studies, the similarity in reported acreage for vegetated habitat on Whiskey Island lends credibility to the habitat classification results of this study. As noted, Fearnley *et al*. (2009) completed habitat classification of imagery available from 1996-2005. This study provides habitat classifications for two additional images, 2008 and 2009.

Classification of the high resolution images used in this study required co-registration of the images before they were classified to ensure that the horizontal and vertical positioning between images was as accurate as possible. The registration process may have introduced minor error into the classifications; however, the error would have been greater if the images had not

been co-registered. Additionally, both between images and within images from a single year, visual inspection revealed variation in image color. For example, the mosaic of the 1998 image clearly shows different coloration between the individual images that were mosaicked to provide coverage of the entirety of Whiskey Island. Issues of this nature made classification of the imagery more challenging and may have reduced the accuracy of the classifications. The topographic LiDAR data used in this study was unable to capture the bottom elevation of some tidal creeks and other features within the study area that may have been obscured by turbid (unclear) water when the data was collected. Although this is a known issue with previous LiDAR data collection efforts, land/marine LiDAR systems such as the Experimental Advanced Airborne Research LiDAR (EAARL; http://ngom.usgs.gov/dsp/tech/eaarl/index.php) may be able to collect data for submerged areas such as those on Whiskey Island.

When examining vegetated habitat at a coastwide scale, documenting the extent of emergent and woody marsh habitats may seem insignificant; however, due to the effects of accelerated sea level rise, subsidence, and other processes on Louisiana's barrier islands, the types of vegetation habitats that can persist with increased inundation become more limited. Understanding that mangroves exist with 30% or less inundation, the average 2035 elevations and inundation regime (52.8%-57.7%) of current woody marsh habitat would no longer be suitable black mangrove habitat.

The cost of barrier island restoration projects constructed to date in coastal Louisiana has ranged from $8 to over $40 million (www.lacoast.gov), and plans for additional barrier island restoration reach $1.75 billion (CPRA, 2012a). If an economic cost-benefit analysis were performed for barrier island restoration projects in Louisiana, barrier island projects may not fare well in comparison to projects that can be constructed in more resilient areas of the coast or with

a lower cost per area for construction. The services that barrier islands provide, such as habitat for threatened and endangered avian species, refugia and a source of food for various marine species, commercial and recreational fishing and hunting opportunities, and storm surge protection for the communities and infrastructure that exist landward of the islands, are difficult if not impossible to monetize meaning that they would not be adequately captured with a cost-benefit analysis. Storm surge modeling comparing the current barrier island landscape to the barrier island landscape fifty years in the future with no additional restoration found that migration and degradation of barrier islands resulted in more than a four foot increase in significant wave height (CPRA, 2012c). Cost-benefit analysis is not able to readily capture what the loss of a barrier island would mean for the vast expanse of marsh that would be exposed to open gulf conditions such as increased wave action, increased fetch length, salinity intrusion, sediment redistribution, and increased flooding nor is it able to capture the cultural significance of the loss of a barrier island that has existed in some form for hundreds of years.

4.6 Conclusion

The methods used to perform habitat classifications are well-accepted and utilized in the scientific community, and application of these methods to the Whiskey Island study area provides some insight into habitat dynamics on Louisiana barrier islands, including the elevation at which emergent marsh and woody marsh vegetation occur and the inundation regime for each habitat type.

- Large-scale barrier island restoration can have a positive effect on the extent and composition of vegetative communities. Because restoration increases the aerial extent of the island, vegetation may be able to colonize the new sediments when environmental conditions become appropriate.

- Due to relative sea level rise, lack of sediment supply, hurricane impacts, and other factors, if left to natural deltaic and physical processes operating along the Louisiana coast, neither Whiskey Island nor the entire Isle Dernier barrier island chain is sustainable.
- Without regular maintenance (sediment addition), the island will continue to degrade and will eventually become subaqueous.
- As island elevations continue to subside, the inundation regime that each habitat is subjected to will change. Although this will likely be a gradual shift, within 25 years, locations that are now emergent and woody vegetation habitats will no longer be viable locations for vegetation but may instead be intertidal or open water.
- Because barrier islands serve as Louisiana's first line of defense against hurricane storm surge and provide a diverse array of habitats to support the abundant natural resources of Louisiana, continued investment in the restoration of these features is the only means by which they will remain on the landscape.

4.7 References

Campbell, T.; Benedet, L.; Mann, D.; Resio, D.; Hester, M.W.; and Materne, M., 2004. Restoration Tools for Louisiana's Gulf Shoreline. *In: Louisiana Gulf Shoreline Restoration Report* 04-003, 37p.

Coastal Protection and Restoration Authority (CPRA), 2012a. *Louisiana's Comprehensive Master Plan for a Sustainable Coast*. Baton Rouge, Louisiana: Coastal Protection and Restoration Authority of Louisiana, 188p.

Coastal Protection and Restoration Authority (CPRA), 2012b. *Barrier Shoreline Morphology Model Technical Report*. Baton Rouge, Louisiana: Coastal Protection and Restoration Authority of Louisiana, 43p.

Coastal Protection and Restoration Authority (CPRA), 2012c. *Storm Surge/Wave Model (ADCIRC) Technical Report*. Baton Rouge, Louisiana: Coastal Protection and Restoration Authority of Louisiana, 462p.

Coppin, P.; Jonckheere, I.; Nackaerts, K.; Muys, B.; and Lambin, E., 2004. Review article digital change detection methods in ecosystem monitoring: A review. *International Journal of Remote Sensing,* 25(9), 1565-1596.

Curole, G., 2007. *Project No. TE-50 Whiskey Island Back Barrier Marsh Creation Monitoring Plan*. Baton Rouge, Louisiana: Coastal Protection and Restoration Authority of Louisiana, 19p.

DeLaune, R.D.; Pezeshki, S.R.; and Patrick, W.H., Jr., 1987. Response of coastal plants to increase in submergence and salinity. *Journal of Coastal Research,* 3(4):535-546.

Fearnley, S.; Brien, L.; Martinez, L.; Miner, M.; Kulp, M.; and Penland, S., 2009. *Louisiana Barrier Island Comprehensive Monitoring Program (BICM) Volume 5: Chenier Plain, South-Central Louisiana, and Chandeleur Islands, Habitat Mapping and Change Analysis 1996 to 2005 Part 1: Methods for Habitat Mapping and Change Analysis 1996 to 2005*. New Orleans, Louisiana: University of New Orleans, Pontchartrain Institute for Environmental Sciences, 11p.

Jabbar, M.T.; Zhi-Hua, S.; Tian-Wei, W.; and Chong-Fa, C., 2006. Vegetation change prediction with geo-information techniques in the Three Gorges area of China. *Pedospherem,* 16(4), 457-467.

Khalil, S.M. and Lee, D.M., 2006. Restoration of Isles Dernieres, Louisiana: Some reflections on morphodynamic approaches in the northern Gulf of Mexico to conserve coastal/marine systems. *In:* Klein, A.H.F.; Finkl, C.W.; Sperb, R.M.; Beaumord, A.C.; Diehl, F.L.; Barrreto, A.; Abreu, J.G.; Bellotto, K.N.; Kuroshima, K.N.; Carvalho, J.L.B.; Resgalla, C.; and Fernandes, A.M.R. (eds.), *Proceedings of the 8th International Coastal Symposium (ICS 2004),* Journal of Coastal Research, Special Issue, No. 39. Santa Catarina (Brazil), pp. 65-71.

Lewis, R.R., III., 2005. Ecological engineering for successful management and restoration of mangrove forests. *Ecological Engineering,* 24, 403-418.

Lunetta, R.S.; Ediriwickrema, J.; Johnson, D.M.; Lyon, J.G.; and McKerrow, A., 2002. Impacts of vegetation dynamics on the identification of land-cover change in a biologically complex community in North Carolina, USA. *Remote Sensing of Environment,* 82, 258-270.

Moffatt & Nichol, 2007. *Whiskey Island Back Barrier Marsh Creation (TE-50) Project 95 % Design Report*. New York, New York: Moffatt & Nichol, Inc., 60p.

Natural Resources Conservation Service (NRCS). 2005. *Project Plan and Environmental Assessment Raccoon Island Shoreline Protection/Marsh Creation Project TE-48*. Alexandria, Louisiana, 74p.

Penland, S. and Campbell, T., 2004. Louisiana Gulf Shoreline Restoration. New Orleans, Louisiana: University of New Orleans, Pontchartrain Institute for Environmental Sciences, *Technical Series 04-300.*

Penland, S.; Connor, P.F.; Jr., Beall, A.; Fearnley, S.; and Williams, S.J., 2005. Changes in Louisiana's shoreline: 1855-2002. *In:* Finkl, C.W. and Khalil, S. (eds.), Saving America's Wetlands: Strategies for Restoration of Louisiana's Coastal Wetlands & Barrier Islands, Journal of Coastal Research Special Issue No. 44, pp. 7-39.

Penland, S.; Roberts, H.H.; Williams, S.J.; Sallenger, A.H.; Cahoon, D.R., Jr.; Davis, D.W.; Groat, C.G. 1990a. Coastal land loss in Louisiana. *Transactions – Gulf Coast Association of Geological Societies*, 11, 685-699.

Penland, S.; Connor, P.; Cretini, F.; and Westphal, K., 2004. *CWPPRA Adaptive Management: Assessment of five barrier island restoration projects in Louisiana*. New Orleans, Louisiana: University of New Orleans, Pontchartrain Institute for Environmental Sciences, 15p.

Penland, S.; Suter, J.R.; Ramsey, K.E.; McBride, R.A.; Williams, S.J.; Groat, C.G., 1990b. Offshore sand resources for coastal erosion control in Louisiana. *Transactions – Gulf Coast Association of Geological Societies*, 11, 721-731.

Ritchie, W. and Penland, S., 1988. Rapid dune changes associated with overwash processes on the deltaic coast of south Louisiana. *Marine Geology*, 81, 97-122.

Rodrigue, L.B., Curole, G.P., Lee, D.M., Dearmond, D.A. 2008. *2008 Operations, Maintenance, and Monitoring Report for Whiskey Island Restoration (TE-27) Project*. Thibodaux, Louisiana: Coastal Protection and Restoration Authority of Louisiana, 26p.

Sallenger, A.; Penland, S.; Krabill, W., 2003. Tropical storm Isidore and Hurricane Lili: Louisiana barrier shoreline response, preliminary results. *Gulf Coast Association of Geological Societies* 53, 733-740.

Soille, P., 2002. Morphological image analysis: principles and applications. Berlin: Springer-Verlag, 392p.

Stone, G.W.; Grymes, J.M.; Dingler, R., III, Pepper, D.A., Jr., 1997. Overview and significance of hurricanes on the Louisiana coast, U.S.A. *Journal of Coastal Research* 13(3), 656-669.

Stone, G.W.; Pepper, D.A.; Xu, J.; Zhang, X., 2004. Ship Shoal as a prospective borrow site for barrier island restoration, coastal south-central Louisiana, USA: Numerical wave modeling and field measurements of hydrodynamics and sediment transport. *Journal of Coastal Research*, 21(1), 70-88.

T. Baker Smith, Inc./Moffatt & Nichol, 2007. *Whiskey Island Back Barrier Marsh Creation Project No. TE-50 95% Design Report*. Houma, Louisiana: T.Baker Smith, Inc., 53p.

Tuxen, K.A.; Schile, L.M.; Kelly, M.; Siegel, S.W., 2008. Vegetation colonization in a restoring tidal marsh: A remote sensing approach. *Restoration Ecology*, 16(2), 313-323.

West, J.L. and Dearmond, D., 2004a. *2004 Operations, Maintenance and Monitoring Report for Isles Dernieres Restoration East Island (TE-20)*. Thibodaux, Louisiana: Louisiana Department of Natural Resources, 21p.

West, J.L. and Dearmond, D., 2004b. *2004 Operations, Maintenance and Monitoring Report for Island Dernieres Restoration Trinity Island*. Thibodaux, Louisiana: Louisiana Department of Natural Resources, 21p.

CHAPTER 5: CONCLUSION

The landscape of a dynamic coastal environment, whether glacial or deltaic, tropical storm-dominated or frontal system-dominated, cannot be expected to remain unchanged throughout time. Whether the processes causing the change are related to global (climate change), regional (rainfall), or local (shoreline retreat) events, modifications of the landscape should be anticipated and plans to address these modifications should be pro-active rather than reactive. Whether the cause of landscape change is related to anthropogenic activities such as removal of forests near the Cape Cod seashore or dredging channels for oil and gas production in Louisiana, or natural causes, such as erosion due to normal wave action or compaction and subsidence of deltaic sediments, those charged with maintaining, restoring, or protecting the landscape and the communities and services that it provides should be well informed of the nature of the physical processes and drivers operating in the landscape and the consequences of their management actions as well as costs of inaction.

The intent of this dissertation was to gain a more complete understanding of some of the physical processes and drivers that affect landscapes in coastal Louisiana and Cape Cod, Massachusetts. Chapter 2 focused on analyzing the wind patterns on Cape Cod as they relate to annual, seasonal, ENSO, and storm time periods rather than fully describing the geomorphological evolution that would result from these wind processes. Chapter 3 concentrated on describing wind speed and wave height return periods and magnitudes for three main types of storm events that affect the landscape of coastal Louisiana. Chapter 4 reported on habitat changes that resulted from the combined effects of physical processes impacting Louisiana's barrier islands and actions that have been undertaken to restore and maintain them.

Dune migration on Cape Cod has caused burial of forests and roadways, resulting in loss of habitat as well as the cost to the local communities of sand removal. Analysis of annual, seasonal, and storm behavior of winds in the Cape Cod region shows quite clearly that the dune landscape present within the northern area of the Cape Cod National Seashore is subjected to wind events that are capable of moving vast quantities of sand. Wind direction and magnitude on Cape Cod are seasonal, with winds of the greatest magnitude occurring during the winter months. As a result, resultant drift potential is highest during the winter period; although, RDPs derived for the *Jinx* blowout do not directly take into account the effects of precipitation, temperature, vegetation, or other processes on sand movement.

The mean grain size and resulting threshold velocity must be adjusted from that used in Fryberger and Dean (1979) so that these values are site specific. If the grain size and threshold velocity are not adjusted, the RDP has the potential to be significantly inaccurate. RDPs vary at specific locations within the *Jinx* blowout due to differences in grain size, with the lowest RDP being at the bottom of the deflation basin and the highest on the western rim of the blowout. This corresponds to higher grain size and threshold velocity at the bottom of the deflation basin and lower grain size and threshold velocity along the western rim of the blowout.

The orientation of the relict and modern parabolic dunes near Provincetown appears to be explained by the predominant winter wind direction, as winter winds blow from the northwest and the dunes are migrating toward the southeast. Blowouts on Cape Cod are oriented in nearly every direction; consequently, the orientation of the *Jinx* blowout and other blowouts on Cape Cod cannot be explained by the predominant winter wind direction alone; however, the wind roses for both annual and seasonal time periods clearly show the multidirectional nature of the wind. Winds above the threshold for sediment velocity occur during every season and

topographic alteration and acceleration of winds can drive sand movement in a direction that is distinctly different from the resultant wind direction at a particular time period and location.

Coastal restoration and hurricane protection planning in coastal Louisiana has largely been reactive. Construction of levees along the Mississippi River after the flood of 1927 and the resulting termination of sediment movement into the wetlands have resulted in tremendous loss of wetlands in southeastern Louisiana. Continued subsidence, sea level rise, and hurricane strikes exacerbate the issue. Recent coastal restoration and hurricane protection planning efforts in coastal Louisiana have focused on determining which projects build/maintain land or protect lives and properties over a fifty year period of analysis. For projects that will be built directly along the coast, it is of critical importance that the effects of winds and waves from both storm and day-to-day events be calculated. Based on examination of wind speed and wave height quantile estimates derived from the Gumbel and Beta-P probability distributions and the Huff Angel and SRCC regression distributions, it was determined that the Huff Angel distribution produced the best fit for the majority of the data sets analyzed and as such should be considered for use by engineers designing coastal restoration and protection projects for Louisiana.

This study provides a first attempt at estimating the magnitude and return period of wind speed and wave heights resulting from tropical, frontal, and airmass thunderstorm events across coastal Louisiana. Estimated wind speeds for AT events range from 18.0-22.0 m/s for the twenty-five year return period to 19.0-23.0 m/s for the fifty year return period. Wind speed estimates for these return periods are similar for FR events, with a range of 18.6-24.0 m/s for the twenty-five year return period and 19.5-25.0 m/s for the fifty year return period. Estimated wind speeds for TR events are much greater than those for AT and FR events, with a wind speed range of 30.0-50.0 m/s for the twenty-five year return period and a range of 32.5-60.5 m/s for the fifty

year return period. For the twenty-five year return period, wave heights ranged from 1.4-5.5 m for AT events to 2.0-6.9 m for FR events to 3.7-16.0 m for TR events. By contrast, wave height estimates for the fifty year return period ranged from 1.5-5.9 m for AT events to 2.2-7.8 m for FR events to 4.1-23.0 m for TR events.

Future research for deriving quantile estimates for restoration project planning and design might consider the following: analysis of wave height and wind speed data should include use of other methods besides the Gumbel and Beta-P distributions for deriving quantile estimates; although the Huff Angel regression method produced the best fit for the majority of the data sets analyzed for coastal Louisiana, to apply this same methodology to other areas in the United States or the world, it may be best to examine multiple types of distributions for the specific application before deciding on which to use for a project in a particular location; quantile estimates derived from tropical events (not airmass thunderstorm or frontal events) should be considered for use in determining the optimal design of a restoration project built along the Louisiana coastline, as the effects of winds and waves (generated by tropical events) on coastal landscapes should be accounted for in the design of restoration projects; because wind speed and wave height quantile estimates are shown to vary based on location within coastal Louisiana as well as the length of the data record, care should be taken in selecting the data from which quantile estimates are derived.

Large-scale barrier island restoration can have an effect on the extent and composition of vegetative communities. Because restoration increases the aerial extent of the island, vegetation may be able to colonize the new sediments. Although there may an initial increase in the extent of vegetation following restoration, the extent of vegetation coverage will likely decline as the island goes through the process of degradation. Due to relative sea level rise, lack of sediment

supply, hurricane impacts, and other factors, if left to natural deltaic and physical processes operating along the Louisiana coast, Whiskey Island and other Louisiana barrier islands are not sustainable. Without regular maintenance (sediment addition), the island will continue to degrade. As island elevations continue to subside, the inundation regime that each habitat is subjected to will change. Within twenty-five years, locations that are now emergent and woody vegetation habitats will no longer be viable locations for vegetation but may instead be intertidal or open water. Because barrier islands serve as Louisiana's first line of defense against hurricane storm surge and provide a diverse array of habitats to support the abundant natural resources of Louisiana, continued investment in the restoration of these features is the only means by which they will remain on the landscape.

VITA

Mandy Green was born in Lafayette, Louisiana. In 2002, she received her Bachelor of Science degree in sustainable agriculture from the University of Louisiana at Lafayette. She received her Master of Science degree in environmental sciences from Louisiana State University in 2004. After completion of her Master's degree, she began work at the Coastal Protection and Restoration Authority of Louisiana. She is expected to receive her Doctor of Philosophy degree in geography from Louisiana State University in 2012.